

Methodical developments for hyphenation of electrochemistry and mass spectrometry coupled to different separation techniques



Dissertation

Zur Erlangung des Doktorgrades der Naturwissenschaften (Dr. rer. nat.)

der Fakultät für Chemie und Pharmazie

der Universität Regensburg

vorgelegt von

Thomas Herl

aus Oberviechtach

im Mai 2020

Die vorgelegte Arbeit entstand in der Zeit von Januar 2017 bis Mai 2020 am Institut für Analytische Chemie, Chemo- und Biosensorik der naturwissenschaftlichen Fakultät IV Chemie und Pharmazie der Universität Regensburg.

Die Arbeit wurde angeleitet durch Prof. Dr. Frank-Michael Matysik.

Promotionsgesuch wurde eingereicht am 19. Mai 2020.

Das Kolloquium fand statt am 24. Juli 2020.

Der Prüfungsausschuss setzte sich zusammen aus:

Vorsitzender: Prof. Dr. Alkwin Slenczka

Erstgutachter: Prof. Dr. Frank-Michael Matysik

Zweitgutachter: Prof. Dr. Christian Neusüß

Drittprüfer: Prof. Dr. Rainer Müller

Danksagung

Die vorliegende Arbeit wäre ohne Unterstützung nicht möglich gewesen, weshalb mein Dank insbesondere den im Folgenden genannten Personen gilt:

Meinem Betreuer Prof. Dr. Frank-Michael Matysik für die vielen ergebnisreichen Diskussionen und die Förderung während der gesamten Promotionszeit.

Dem weiteren Prüfungsausschuss bestehend aus Prof. Dr. Alkwin Slenczka, Prof. Dr. Christian Neusüß und Prof. Dr. Rainer Müller, die sich dankenswerterweise dazu bereit erklärt haben, zur Begutachtung der Dissertation und zur Durchführung des Promotionskolloquiums zur Verfügung zu stehen.

Allen meinen Kollegen und Freunden im AK Matysik, insbesondere meinem langjährigen Büropartner Andreas Schmidberger und meinen Kommilitonen Timo Raith und Bernhard Durner, für das unvergleichlich kollegiale Arbeitsklima, die gute Zusammenarbeit sowie die äußerst unterhaltsamen Mittagspausen.

Den Werkstätten der Universität Regensburg, stellvertretend Herbert Tischhöfer, Andreas Graf, Peter Fuchs und Andreas Gruber, ohne deren tatkräftige Hilfe der Forschungsalltag kaum möglich gewesen wäre.

Josef Kiermaier und Wolfgang Söllner aus der MS Abteilung der Zentralen Analytik der Universität Regensburg für die aufschlussreichen Messsessionen und die tatkräftige Teilnahme an sozialen Veranstaltungen des Arbeitskreises.

Meiner gesamten Familie, ohne deren Unterstützung ein derart herausforderndes Studium wie das der Chemie nicht möglich gewesen wäre.

Table of content

Table of content.....	I
List of oral presentations	IV
List of poster presentations.....	VI
List of peer-reviewed publications	VII
Declaration of collaboration.....	XII
1. Introduction	1
2. Background and theory.....	2
2.1 Introduction to voltammetry.....	2
2.2 Fundamentals of time-of-flight mass spectrometry.....	4
2.3 Fundamentals of capillary zone electrophoresis.....	7
3. Recent developments in electrochemistry-mass spectrometry.....	14
3.1 Introduction	15
3.1.1 Historical developments.....	15
3.1.2 Terminology	18
3.1.3 Instrumental setups.....	19
3.2 Latest developments and applications.....	21
3.2.1 DEMS.....	22
3.2.2 EC-MS.....	23
3.2.3 EC-HPLC-MS	30
3.2.4 EC-CE-MS	33
3.2.5 Further studies	35
3.3 Summary and outlook.....	36
4. Experimental.....	45
4.1 Materials and instruments.....	45
4.1.1 Chemicals	45
4.1.2 Consumables.....	46
4.1.3 Instruments	46

4.1.4 Software.....	47
4.1.5 Handling of capillaries	47
4.1.6 Handling of electrodes.....	48
4.1.7 Mass spectrometer configuration	48
4.2 Instrumentation and methods	49
4.2.1 Instrumental setup for EC-MS.....	49
4.2.2 Instrumental setup for EC-CE-MS	50
5. Results and discussion.....	53
5.1 Development of a miniaturized injection cell for online electrochemistry-capillary electrophoresis-mass spectrometry.....	53
5.1.1 Introduction	54
5.1.2 Experimental.....	56
5.1.3 Results and discussion.....	58
5.1.4 Conclusion.....	62
5.2 Bile acids: Electrochemical oxidation on bare electrodes after acid-induced dehydration	65
5.2.1 Introduction	66
5.2.2 Experimental.....	66
5.2.3 Results and discussion.....	67
5.2.4 Conclusion.....	71
5.3 Electrooxidation of cytosine on bare screen-printed carbon electrodes studied by online electrochemistry-capillary electrophoresis-mass spectrometry.....	75
5.3.1 Introduction	76
5.3.2 Experimental.....	77
5.3.3 Results and discussion.....	77
5.3.4 Conclusion.....	82
5.4 Investigation of the electrooxidation of thymine on screen-printed carbon electrodes by hyphenation of electrochemistry and mass spectrometry.....	85
5.4.1 Introduction	86
5.4.2 Experimental.....	87
5.4.3 Results and discussion.....	89

5.4.4 Conclusion.....	97
5.4.5 Supporting information	102
6. Summary.....	105
7. Zusammenfassung in deutscher Sprache.....	107
8. Appendix	109
List of abbreviations	109
Eidesstattliche Erklärung.....	110

List of oral presentations

2017

13th International Students Conference Modern Analytical Chemistry, Prague (CZ), Title: *Development and characterization of a miniaturized injection cell for the hyphenation of electrochemistry-capillary electrophoresis-mass spectrometry*, September 21-22, 2017.

1st JOINT CE- and FFE-Forum, Karlsruhe-Berghausen (DE), Title: *Hyphenation of electrochemistry-capillary electrophoresis-mass spectrometry for bioanalytical applications*, October 5-6, 2017.

2018

1st Cross-Border Seminar on Electroanalytical Chemistry (ELACH), Furth im Wald (DE), Title: *Online electrochemistry-mass spectrometry based on disposable electrodes*, April 4-6, 2018.

17th International Conference on Electroanalysis ESEAC 2018, Rhodes (GR), Title: *Hyphenation of electrochemistry and mass spectrometry based on disposable electrodes*, June 3-7, 2018.

Electrochemistry 2018, Ulm (DE), Title: *Investigation of electrochemical reactions by online electrochemistry-capillary electrophoresis-mass spectrometry*, September 24-26, 2018.

2nd JOINT CE- and FFE-Forum, Karlsruhe-Berghausen (DE), Title: *Investigation of cytosine oxidation on screen-printed carbon electrodes by means of EC-CE-MS*, October 10-11, 2018.

2019

ANAKON 2019, Münster (DE), Title: *Investigation of cytosine and thymine oxidation by electrochemistry-capillary electrophoresis-mass spectrometry*, March 25-28, 2019.

2nd Cross-Border Seminar on Electroanalytical Chemistry (CBSEC), České Budějovice (CZ), Title: *Hyphenation of electrochemistry-capillary electrophoresis-mass spectrometry and its application to the investigation of nucleobase oxidation*, April 10-12, 2019.

RSE-SEE 7 & 8th Kurt Schwabe Symposium, Split (HR), Title: *Electrooxidation of nucleobases on disposable electrodes investigated by electrochemistry-capillary electrophoresis-mass spectrometry*, May 27-30, 2019.

5th International Workshop on Electrochemistry/Mass Spectrometry 2019, Münster (DE), Title: *Hyphenation of electrochemistry and mass spectrometry based on disposable electrode materials*, June 11-12, 2019.

CE-Forum 2019, Waldbronn (DE), Title: *Investigation of the electrooxidation of thymine on screen-printed carbon electrodes*, December 11-12, 2019.

2020

30. Doktorandenseminar des AK Separation Science der GDCh, Hohenroda (DE), Title: *Hyphenation of electrochemistry and mass spectrometry and its application to nucleobase oxidation*, January 11-14, 2020.

List of poster presentations

2016

7. Kurt-Schwabe-Symposium, Mittweida (DE), Title: *Characterization and application of various flow cell configurations for the hyphenation of electrochemistry with mass spectrometry*, September 4-7, 2016.

Electrochemistry 2016, Goslar (DE), Title: *Hyphenation of electrochemistry-capillary electrophoresis-mass spectrometry*, September 26-28, 2016.

CE-Forum 2016, Regensburg (DE), Title: *Hyphenation of electrochemistry and mass spectrometry by electrochemical flow cells*, October 4-5, 2016.

2017

11. Interdisziplinäres Doktorandenseminar, Berlin (DE), Title: *Hyphenation of electrochemistry and mass spectrometry by electrochemical flow cells with integrated disposable electrodes*, March 12-14, 2017.

ANAKON 2017, Tübingen (DE), Title: *Development and characterization of electrochemical flow cells for the hyphenation of electrochemistry and mass spectrometry*, April 3-6, 2017.

2018

1st International Conference on Ion Analysis, Berlin (DE), Title: *Electrochemical generation and identification of charged species by a miniaturized EC-CE-MS setup based on disposable thin-film electrodes*, September 9-13, 2018.

2019

ANAKON 2019, Münster (DE), Title: *Investigation of electrochemical oxidation processes by EC-CE-MS based on disposable thin-film electrodes*, March 25-28, 2019.

List of peer-reviewed publications

2017

Characterization of electrochemical flow cell configurations with implemented disposable electrodes for the direct coupling to mass spectrometry

T. Herl, F.-M. Matysik, *Tech. Mess.* **2017**, *84*, 672-682.

Abstract

The characterization of the redox behavior of analytes is a very important aspect for many applications. Pure electrochemical approaches can provide useful information on electroactive species, but are of limited use regarding the identification of generated species. The hyphenation of electrochemistry and mass spectrometry (EC-MS) is a powerful method to investigate redox systems. In the present work, we show a simple approach to online EC-MS based on the application of electrochemical flow cells with implemented disposable electrodes. They are connected to electrospray ionization mass spectrometry (ESI-MS) via fused silica capillary tubing. The modularity of the flow cells offers a high flexibility of experimental setup and settings, so that a fast detection of oxidation or reduction products can be achieved. The usage of disposable electrodes guarantees a high level of quality assurance for EC-MS measurements.

2018

Development of a miniaturized injection cell for online electrochemistry-capillary electrophoresis-mass spectrometry

T. Herl, N. Heigl, F.-M. Matysik, *Monatsh. Chem.* **2018**, *149*, 1685-1691.

Abstract

The elucidation of oxidation or reduction pathways is important for the electrochemical characterization of compounds of interest. In this context, hyphenation of electrochemistry and mass spectrometry is frequently applied to identify products of electrochemical reactions. In this contribution, the development of a novel miniaturized injection cell for online electrochemistry capillary electrophoresis-mass spectrometry (EC-CE-MS) is presented. It is based on disposable thin-film electrodes, which allow for high flexibility and fast replacement of electrode materials. Thus, high costs and time-consuming maintenance procedures can be avoided, which makes this approach interesting for routine

applications. The cell was designed to be suitable for investigations in aqueous and particularly non-aqueous solutions making it a universal tool for a broad range of analytical problems. EC–CE–MS measurements of different ferrocene derivatives in non-aqueous solutions were carried out to characterize the cell. Oxidation products of ferrocene and ferrocenemethanol were electrochemically generated and could be separated from the decamethylferricenium cation. The importance of fast CE–MS analysis of instable oxidation products was demonstrated by evaluating the signal of the ferriceniummethanol cation depending on the time gap between electrochemical generation and detection.

Bile acids: Electrochemical oxidation on bare electrodes after acid-induced dehydration

J. Klouda, J. Barek, P. Kočovský, T. Herl, F.-M. Matysik, K. Nesměrák, K. Schwarzová-Pecková, *Electrochem. Commun.* **2018**, *86*, 99-103.

Abstract

Bile acids and sterols in general have long been considered practically inactive for direct redox processes. Herein, a novel way of electrochemical oxidation of primary bile acids is reported, involving an initial acid-induced dehydration step, as confirmed by capillary electrophoresis–mass spectrometry, thereby extending the electrochemical activity of the steroid core. Oxidation potentials were found to be ca +1.2 V vs. Ag/AgNO₃ in acetonitrile on boron doped diamond, glassy carbon, and platinum electrodes in a mixed acetonitrile–aqueous medium employing perchloric acid as a chemical reagent, and as a supporting electrolyte for the voltammetric measurements. The chemical step proved to be effective only for primary bile acids, possessing an axial 7 α -hydroxyl group, which is a prerequisite for providing a well-developed voltammetric signal. Preliminary results show that other steroids, e.g., cholesterol, can also be oxidized by employing a similar approach.

New electrochemical flow-cell configuration integrated into a three-dimensional microfluidic platform: improving analytical application in the presence of air bubbles

M. A. G. Trindade, C. A. Martins, L. Angnes, T. Herl, T. Raith, F.-M. Matysik, *Anal. Chem.* **2018**, *90*, 10917-10926.

Abstract

A newly configured electrochemical flow cell to be used for (end-channel) amperometric detection in a microfluidic device is presented. The design was assembled to place the reference electrode in a separated compartment, isolated from the flow in the microchannel, while the working and counter

electrodes remain in direct contact with both compartments. Moreover, a three-dimensional coil-shaped microfluidic device was fabricated using a nonconventional protocol. Both devices working in association enabled us to solve the drawback caused by the discrete injection when the automatic micropipette was used. The high performance of the proposed electrochemical flow cell was demonstrated after in situ modifying the surface of the platinum working electrode with surfactant (e.g., using Tween 20 at 0.10%). As the reference electrode remained out of contact with the flowing solution, there was no trouble by air bubble formation (generated by accidental insertion or by presence of surfactants) throughout the measurements. This device was characterized regarding its analytical performance by evaluating the amperometric detection of acetaminophen, enabling determination from 6.60 to 66.0 $\mu\text{mol L}^{-1}$. This issue is important since at high concentration (e.g., as assessed in clinical analysis) the acetaminophen is known to passivate the working electrode surfaces by electrogenerated products, impairing the accuracy of the electrochemical measurements.

2019

Selectivity enhancement in capillary electrophoresis by means of two-dimensional separation or dual detection concepts

A. Beutner, T. Herl, F.-M. Matysik, *Anal. Chim. Acta* **2019**, 1057, 18-35.

Abstract

For the identification and quantification of analytes in complex samples, highly selective analytical strategies are required. The selectivity of single separation techniques such as gas chromatography (GC), liquid chromatography (LC), or capillary electrophoresis (CE) with common detection principles can be enhanced by hyphenating orthogonal separation techniques but also by using complementary detection systems. In this review, two-dimensional systems containing CE in at least one dimension are reviewed, namely LC-CE or 2D CE systems. Particular attention is paid to the aspect of selectivity enhancement due to the orthogonality of the different separation mechanisms. As an alternative concept, dual detection approaches are reviewed using the common detectors of CE such as UV/VIS, laser-induced fluorescence, capacitively coupled contactless conductivity (C^4D), electrochemical detection, and mass spectrometry. Special emphasis is given to dual detection systems implementing the highly flexible C^4D as one detection component. Selectivity enhancement can be achieved in case of complementarity of the different detection techniques.

Electrooxidation of cytosine on bare screen-printed carbon electrodes studied by online electrochemistry-capillary electrophoresis-mass spectrometry

T. Herl, L. Taraba, D. Böhm, F.-M. Matysik, *Electrochem. Commun.* **2019**, *99*, 41-45.

Abstract

The electrooxidation of cytosine on common commercially available screen-printed carbon electrodes was investigated. To characterize the processes on the electrode surface, the oxidation products were analyzed by online electrochemistry-capillary electrophoresis-mass spectrometry. Capillary electrophoresis was the ideal separation technique as all occurring species were positively charged at acidic separation conditions. Comparing the results to literature data on cytosine oxidation by one electron oxidants, the compound 6-hydroxy-5-hydroperoxy-5,6-dihydrocytosine was identified as the main oxidation product that could be detected on the screen-printed carbon electrode material. This product species was found to be quite stable over an investigated period of 60 min under the conditions present in our experiments. A small amount of cytosine glycol was detected, probably formed as a decomposition product. During oxidation in acetate electrolyte, a side reaction with the electrolyte took place forming an artificial product, which was not the case in hydrogencarbonate electrolyte. This showed that products have to be investigated carefully in the context of the background electrolyte to avoid misinterpretations.

2020

Investigation of the electrooxidation of thymine on screen-printed carbon electrodes by hyphenation of electrochemistry and mass spectrometry

T. Herl, F.-M. Matysik, *Anal. Chem.* **2020**, *92*, 6374-6381.

Abstract

The electrooxidation of thymine on screen-printed carbon electrodes was investigated utilizing different complementary instrumental approaches. The potential-dependent product profile was obtained by recording real-time mass voltammograms. Electrochemical flow cells with integrated disposable electrodes were directly coupled with mass spectrometry to facilitate a very fast detection of electrogenerated species. Thymine dimers were found at a potential of about 1.1 V in ammonium acetate (pH 7.0) and 1.25 V in ammonium hydrogen carbonate electrolyte (pH 8.0). Electrochemistry-capillary electrophoresis-mass spectrometry measurements revealed that two isobaric isomers of a dimeric oxidation product were formed. Separations at different time intervals between end of oxidation and start of separation showed that these were hydrated over time. An investigation of the pK_a values by

changing the separation conditions in electrochemistry-capillary electrophoresis-ultraviolet-visible spectroscopy measurements allowed for further characterization of the primary oxidation products. The results showed that both isomers exhibited two deprotonation steps. The oxidation products were further characterized by high-performance liquid chromatography-tandem mass spectrometry. Based on the obtained data, the main oxidation products of thymine in aqueous solution could most likely be identified as N(1)-C(5') and N(1)-C(6') linked dimer species evolving into the corresponding dimer hydrates over time. The presented methods for online characterization of electrochemically pretreated samples showed that not only mass spectrometric data can be obtained by electrochemistry-mass spectrometry but also further characterizations such as the investigation of product stability and the pH-dependent protonation or deprotonation behavior are possible. This is valid not only for stable oxidation products but also for intermediates, as analysis can be carried out within a short time scale. Thus, a vast amount of valuable experimental data can be acquired, which can help in understanding electrooxidation processes.

Recent developments in electrochemistry-mass spectrometry

T. Herl, F.-M. Matysik, *ChemElectroChem* **2020**, 7, 2498-2512.

Abstract

Hyphenation of electrochemistry and mass spectrometry is an attractive method to investigate oxidation and reduction processes. By using mass spectrometry electrochemically generated products can be identified. In this Review, different approaches to electrochemistry-mass spectrometry will be summarized including hyphenation of electrochemical flow cells to mass spectrometry as well as integration of separation steps between electrochemical reactions and detection of products. Fields of application range from bioanalytical studies to studies regarding corrosion, electrosynthesis and energy carriers. Important historical developments will be highlighted, followed by an overview of terminology and instrumental setups and discussion of developments within recent years (2017-2020).

Declaration of collaboration

The research presented within this thesis was partly obtained in cooperation with other scientists. In accordance with § 8 Abs. 1 Satz 2 Punkt 7 of the *Ordnung zum Erwerb des akademischen Grades eines Doktors der Naturwissenschaften (Dr. rer. nat.) an der Universität Regensburg vom 18. Juni 2009*, these collaborations are described within this section.

3. Recent developments in electrochemistry-mass spectrometry

The manuscript was written by the author. The project was supervised by Prof. Dr. Frank-Michael Matysik.

5.1 Development of a miniaturized injection cell for online electrochemistry-capillary electrophoresis-mass spectrometry

The electrochemical cell was designed by the author. Measurements were planned by the author and done by the author and Nicole Heigl under supervision of the author in the frame of a research internship. The manuscript for publication was written by the author. The project was supervised by Prof. Dr. Frank-Michael Matysik.

5.2 Bile acids: Electrochemical oxidation on bare electrodes after acid-induced dehydration

Measurements on the voltammetric response of bile acids and effects of solvent, supporting electrolyte and water on voltammetric signals were done by Jan Klouda. CE-MS measurements were done by the author and Jan Klouda in the frame of a research internship of Jan Klouda at the University of Regensburg. All authors contributed to writing and revising the manuscript. The project was supervised by Prof. Dr. Frank-Michael Matysik, Assoc. Prof. Dr. Karel Nesměrák and Assoc. Prof. Dr. Karolina Schwarzová-Pecková.

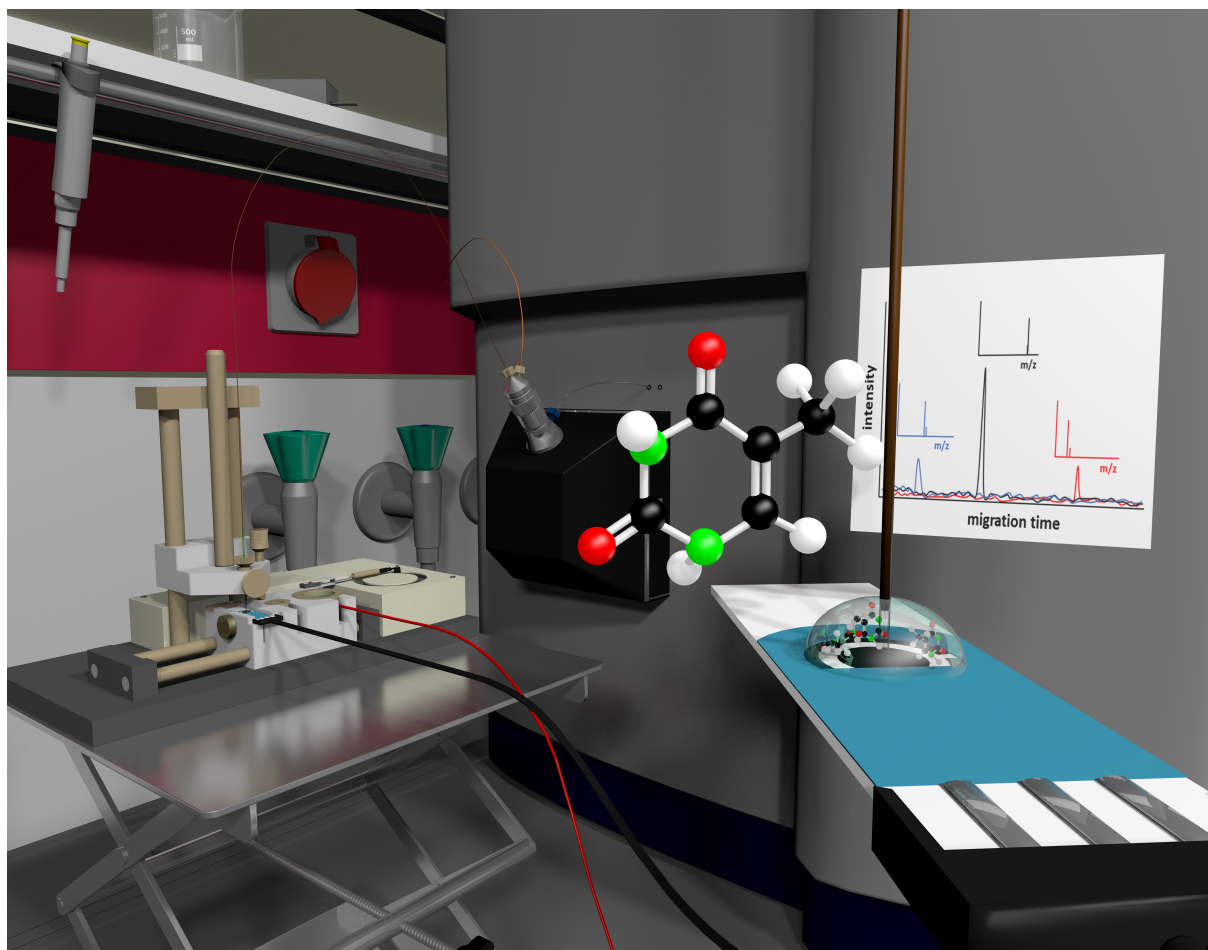
5.3 Electrooxidation of cytosine on bare screen-printed carbon electrodes studied by online electrochemistry-capillary electrophoresis-mass spectrometry

Preliminary electrochemical measurements were done by Lukas Taraba in the frame of a research internship at the University of Regensburg. EC-CE-MS measurements were planned by the author and done by the author and Daniel Böhm under the supervision of the author in the frame of a research internship. Tandem MS measurements were carried out in the central analytical department of the University of Regensburg under technical support of Josef Kiermaier. The manuscript was written by the author. The project was supervised by Prof. Frank-Michael Matysik.

5.4 Investigation of the electrooxidation of thymine on screen-printed carbon electrodes by hyphenation of electrochemistry and mass spectrometry

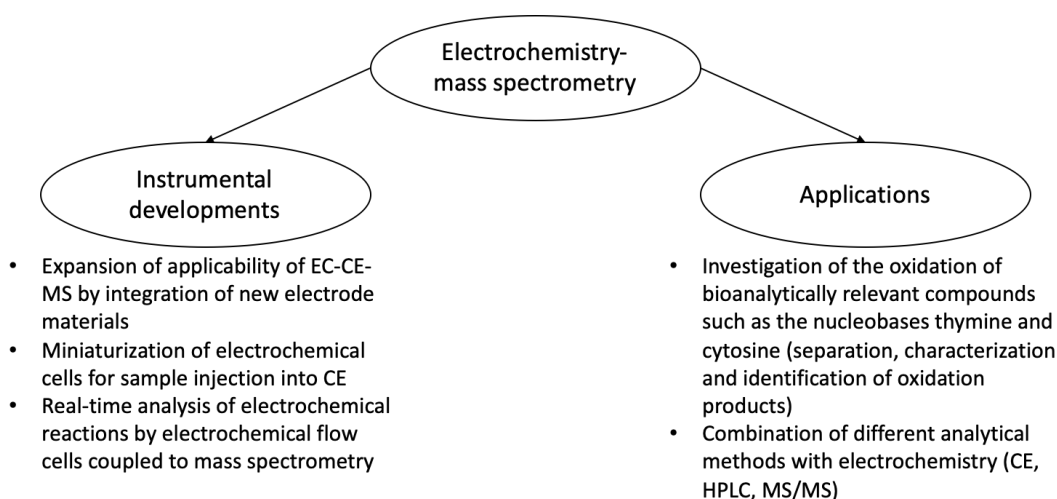
Experimental work was planned and carried out solely by the author. EC-HPLC-MS and tandem MS measurements were carried out in the central analytical department of the University of Regensburg under technical support of Josef Kiermaier. The manuscript was written by the author. The project was supervised by Prof. Dr. Frank-Michael Matysik.

Methodical developments for hyphenation of electrochemistry and mass spectrometry coupled to different separation techniques



1. Introduction

Electroanalytical methods can be found in the context of various types of samples in environmental, pharmaceutical and bioanalytical applications, as a number of recent reviews shows [1–11]. The electrochemical determination of analytes has the potential to be an attractive alternative to expensive instrumental methods like gas chromatography-mass spectrometry (GC-MS) or high-performance liquid chromatography-mass spectrometry (HPLC-MS), as the compound-specific oxidation or reduction potentials are obtained as qualitative information while the current delivers quantitative information [12]. However, the reliability of pure electrochemical data may be limited in some cases due to limited selectivity and the missing possibility to identify products. To increase the understanding of electrochemical processes and reveal mechanistic details of oxidation or reduction pathways, hyphenation to advanced detection techniques is in demand. Since the first beginnings by Thomson [13,14], mass spectrometry (MS) evolved into a very important technique that is well suited for this purpose as it offers high sensitivity and the possibility to identify products of electrochemical reactions by their mass to charge ratios and fragmentation patterns. There are different approaches to hyphenate electrochemistry and mass spectrometry such as direct coupling of electrochemical flow cells to mass spectrometry (EC-MS) as well as electrochemistry coupled with capillary electrophoresis-mass spectrometry (EC-CE-MS) or high-performance liquid chromatography-mass spectrometry (EC-HPLC-MS) as for example reviewed by Faber et al [15], Cindric and Matysik [16], and Portychová and Schug [17]. Since the first idea of electrochemical online sample preparation combined with injection to capillary electrophoresis by a concept called electrochemically assisted injection was proposed by Matysik in 2003 [18], different approaches to online EC-MS and EC-CE-MS based on disposable electrodes have been developed and applied in the Matysik research group [19–22]. In this thesis, the focus was put on further developments and applications of these methods. In Scheme 1.1, the main topics addressed in the research are summarized:



Scheme 1.1 Summary of the main aspects addressed in this thesis.

2. Background and theory

2.1 Introduction to voltammetry

Working with macroscopic electrodes (dimension in the scale of millimeters to centimeters), electrochemical measurements are usually carried out in a three-electrode configuration consisting of a working electrode (WE), an auxiliary or counter electrode (AE or CE), and a reference electrode (RE) [23]. Electrode potentials are externally controlled by a potentiostat. As shown in equation (1) the potential at the WE-solution interface E_{app} is applied as the potential difference between the WE (E_{WE} , variable) and the RE (E_{RE} , fixed). Both are connected in a high-resistance circuit [24].

$$E_{app} = E_{WE} - E_{RE} - iR \quad (1)$$

As almost no current flow i occurs between WE and RE, the applied potential is not affected by the electrical resistance of the bulk solution R in form of the Ohmic drop iR and electrolytic change within the reference electrode [23]. The current of the electrochemical reaction flows between WE and AE [24]. A supporting electrolyte is added to the solution to minimize mass transport by migration effects and to reduce the solution resistance [25]. If the current response upon the application of a fixed potential is recorded over time, the experiment is called chronoamperometry [24]. Without convection, as shown in equation (2), the current i decreases over time t according to the Cottrell equation [26]:

$$i(t) \propto \frac{1}{\sqrt{t}} \quad (2)$$

This is due to diffusion limited mass transport towards the electrode surface and increasing diffusion layer thickness if the potential is set to a value where the surface concentration of the consumed species equals zero [26]. Typical potential-time and current-time curves are depicted in Figure 2.1. Analytical information obtained from chronoamperometry are for example diffusion coefficients of electroactive species and the surface areas of working electrodes [24].

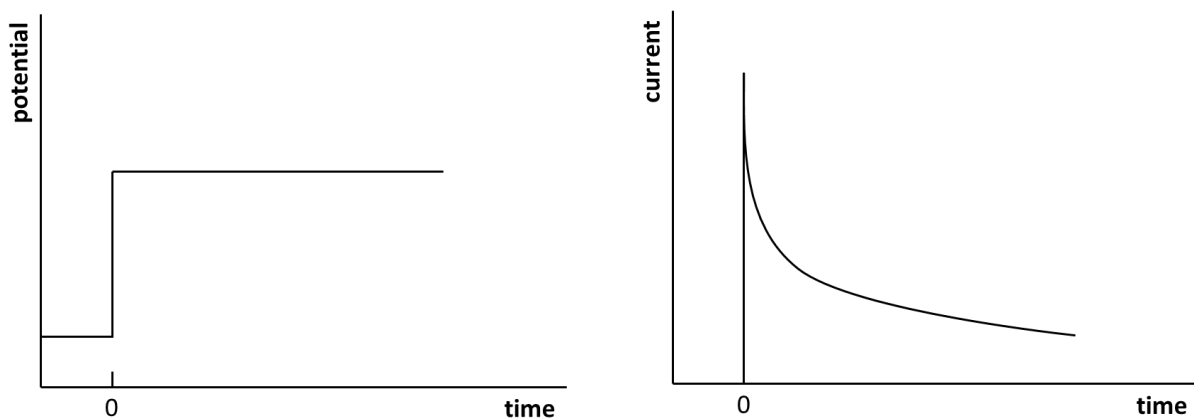


Figure 2.1 Potential (left) and current as a function of time (right) in a chronoamperometric experiment at a macroscopic electrode in quiescent solution. Adapted from [24].

Linear sweep voltammetry (LSV) and cyclic voltammetry (CV) are potential sweep methods where the current response is measured with respect to the change in the WE potential [25]. At the beginning of a potential sweep the potential is set to a value at which no electrochemical conversion takes place. Only nonfaradaic currents, also called capacitive or charging currents, flow. These are caused by charging of the electrical double layer at the electrode-solution interface. At some point a potential is reached where, depending on the scan direction, oxidation or reduction of the species of interest begins [25]. With increasing anodic (i.e. oxidative) or cathodic (i.e. reductive) potential the surface concentration of the available species drops and the faradaic current increases due to increased electrochemical conversion. At a certain potential all species close to the surface is consumed and the current decreases due to the formation of a growing diffusion layer with flattening concentration gradient. This results in a peak-shaped current response [25]. In LSV the potential is only scanned in one direction while in CV the scan direction is reversed at the vertex potential. A plot of the current as a function of the applied potential is called voltammogram [23]. An exemplary cyclic voltammogram obtained for a reversible diffusion controlled redox reaction exhibiting a one electron transfer is depicted in Figure 2.2.

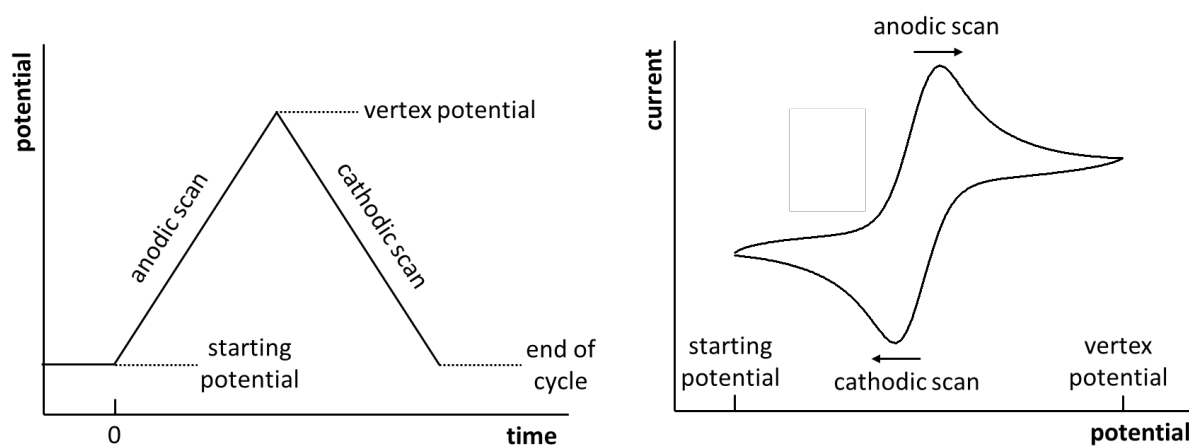


Figure 2.2 Potential as a function of time (left) and current as a function of potential (right) in cyclic voltammetry at a macroscopic electrode in quiescent solution. Adapted from [25].

Typical results obtained in CV are the ratio of anodic and cathodic peak currents and the separation of anodic and cathodic peak potentials which give information on electrode kinetics (reversible/Nernstian, quasireversible, or totally irreversible) [25]. CV is perfectly suited to give a qualitative overview on the redox activity of analytes (position of redox potentials, effects of electrolyte composition) but has some drawbacks for quantitative evaluations as the faradaic current is overlapping with charging currents that have to be corrected [24,25]. Cyclic voltammetry was used for preliminary electrochemical characterization of analytes during this thesis (investigation of redox properties of analytes, comparison of electrolytes, optimization of oxidation potentials for electrochemical sample preparation prior to CE-MS or HPLC-MS). Chronoamperometry was used for oxidation of samples prior to mass spectrometric investigation of electrogenerated products by EC-CE-MS or EC-HPLC-MS.

2.2 Fundamentals of time-of-flight mass spectrometry

A mass spectrometer consists of a sample inlet, an ion source, a mass analyzer, and a detector [27]. There are different kinds of mass analyzers such as quadrupole [28] or time-of-flight instruments [29]. Time-of-flight mass spectrometry (TOF-MS) was first proposed in 1946 by Stephens [29] and is characterized by its practically unlimited mass range and high spectra acquisition rates [30]. Combined with electrospray ionization (ESI) [31–33], a so-called soft ionization method characterized by low fragmentation [34], it is a powerful tool to identify analytes out of liquid samples [30]. In ESI, schematically shown in Figure 2.3, an ionization voltage of usually 1 to 5 kV is applied between ESI sprayer and spray shield resulting in a liquid filament called Taylor cone [30]. During evaporation of the solvent, the charge density at the surface of the liquid increases until the Rayleigh limit is reached and highly charged droplets are detached. Upon further evaporation of the solvent, so-called Coulomb explosions into small and highly charged droplets take place that repetitively undergo the same process, until gas phase ions are formed [30]. These ions are then transferred to the mass analyzer.

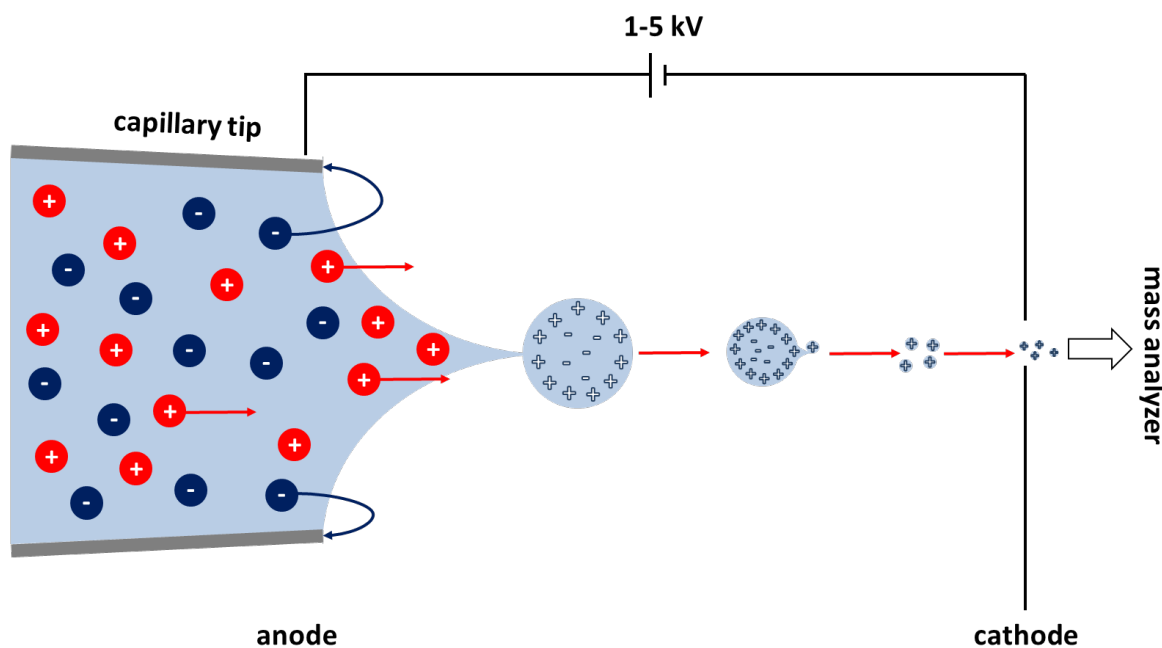


Figure 2.3 Schematic illustration of the ESI process. Adapted from [30].

The working principle of a time-of-flight mass analyzer is illustrated in Figure 2.4. After passing the ionization source and several vacuum stages, the ions carrying the charge $z \cdot e$ are accelerated to the same kinetic energy E_{kin} by an acceleration voltage E_a . The velocity v is depending on the mass m according to equation (3) (adapted from [34]):

$$E_{kin} = \frac{1}{2} \cdot m \cdot v^2 = z \cdot e \cdot E_a \quad (3)$$

Based on equation (3), the time of flight t_{TOF} , which is resulting from v and the length of the flight tube, can be expressed depending on the mass-to-charge ratio m/z as shown in equations (4) and (5) (adapted from [30,34]):

$$v = \sqrt{\frac{z}{m} \cdot 2 \cdot e \cdot E_A} \quad (4)$$

$$t_{TOF} \propto \sqrt{\frac{m}{z}} \quad (5)$$

The higher m/z , the longer is the drift time to cross the field-free drift zone under high vacuum conditions. If a TOF analyzer is operated in reflectron mode as illustrated in Figure 2.4, the flight direction of ions is reversed at the end of the field-free drift zone and mass resolution is increased by compensation of energy distributions and elongation of the flight path [34].

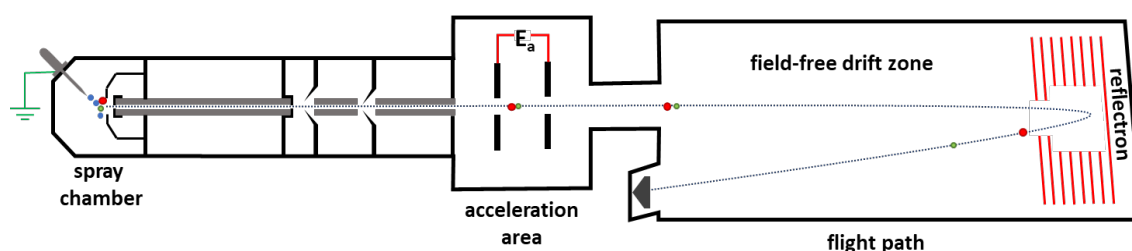


Figure 2.4 Simplified scheme of an ESI-TOF mass analyzer. After ionization in the spray chamber the ions are transferred to the mass analyzer, where they are accelerated to the same kinetic energy by an acceleration voltage E_a . The time needed to transfer a field-free drift zone is depending on the velocity, which is depending on the mass-to-charge ratio of the ions. Adapted from [30,34].

An important operating mode of modern MS systems is tandem mass spectrometry. Triple quadrupole or quadrupole-TOF instruments are often used for this purpose. Typically, three steps are carried out: (i) selection of a target m/z , (ii) fragmentation (by collision-induced dissociation CID, electron capture dissociation ECD, photodissociation PD, or electron transfer dissociation ETD), and (iii) detection of fragments. The evaluation of the fragmentation pattern can be helpful for identification of structural features of target ions while the selection of target precursors and target fragments can lead to enhanced sensitivity due to separation from background ions (single- or multiple-reaction monitoring) [30].

Another technique capturing increasing attention is ion mobility mass spectrometry (IM-MS), especially in form of ion mobility time-of-flight mass spectrometry (IM-TOF-MS) [35–37]. As reviewed by Kanu et al [38] four methods of ion mobility spectrometry (IMS) exist, namely drift-time ion mobility spectrometry (application of continuous low electrical field in drift cell), aspiration ion mobility spectrometry, differential-mobility spectrometry (or field-asymmetric waveform ion mobility spectrometry; based on alternating electrical field), and traveling-wave ion mobility spectrometry (high electrical field swept sequentially through IMS cell). The most common type is drift-time ion mobility spectrometry, which is mostly just called ion mobility spectrometry (IMS) [38]. For IM-MS the drift cell is included between ionization source and mass analyzer [37]. Gas phase ions are migrating through

a buffer gas in the presence of an electrical field [38]. By ion mobility spectrometry gas phase ions can be separated based on their size and shape and their interaction with buffer gases so that additional information on isobaric compounds with the same m/z can be obtained (e.g. rotationally averaged cross-sectional area) [38,39]. Isomers, isobars and conformers can be separated, chemical noise can be reduced, and the size of ions can be measured which is very powerful in combination with mass spectrometric identification [38].

2.3 Fundamentals of capillary zone electrophoresis

Capillary electrophoresis (CE) is a separation method based on the migration of charged species in an electrical high voltage field (usually up to 30 kV) [27]. It can be carried out in fused silica capillaries but also in glass and polymer capillaries with typical inner diameters of 50-100 μm and lengths of 10-50 cm [27]. But also inner diameters as small as 5 μm can be used [40]. CE is characterized by low consumption of samples and solvent, fast separation, high resolution, and a comparably simple experimental setup [41]. There are different modes of CE such as capillary zone electrophoresis (CZE), isotachopheresis, capillary electrokinetic chromatography, capillary gel electrophoresis, and isoelectric focusing [42]. In the following, the basics of CZE will be further described. CZE using capillaries with small inner diameters and high separation voltages was introduced by Jorgenson and Lukacs [43] in 1981 who used a borosilicate glass tube with an inner diameter of 80 μm and a length of 1 m at a separation voltage of 30 kV. A scheme of a CZE setup is depicted in Figure 2.5 (A).

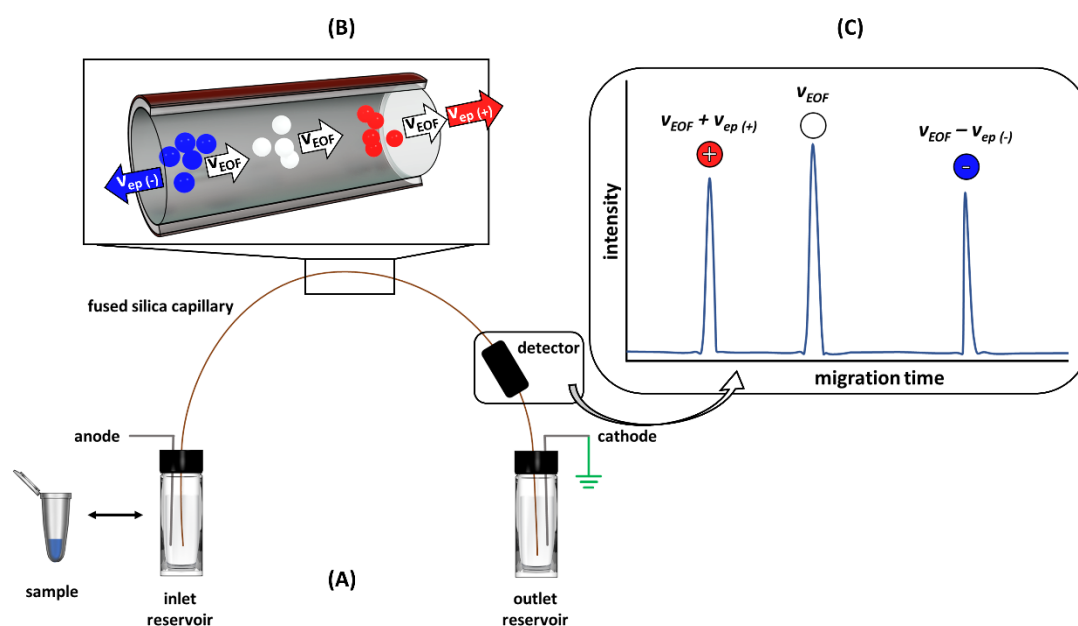


Figure 2.5 (A) Schematic setup for capillary zone electrophoresis with on-column detection at the cathode side. (B) Illustration of the relative migration velocities in CZE. (C) Migration order in a corresponding electropherogram. Cationic species migrate with the sum of their electrophoretic velocity and the velocity of the EOF and are detected first. Neutral species are transported by the EOF and anionic species are migrating against the EOF and are detected last. Adapted from [41].

The capillary is immersed into two buffer reservoirs equipped with high voltage electrodes. The detector can be placed on the cathode or the anode side [41]. Typical on-column detectors are UV, fluorescence or capacitively-coupled contactless conductivity detectors (C^4D) [44]. At one electrode the separation voltage is applied while the other electrode is at ground potential. The inlet end of the capillary can be immersed into a sample solution for injection. There are two injection modes: hydrodynamic injection (injection by pressure at inlet, vacuum at outlet or gravity flow) and electrokinetic injection (injection by application of high voltage) [41]. The migration behavior is, depending on the CE separation mode, based on the polarity and magnitude of the charge, the size, and the shape of the analytes [41]. In CZE a buffer with constant composition and pH is used as separation medium [27]. Applying the electrical

high voltage E_{el} , the electrophoretic migration velocity v_{ep} depending on the charge q and the friction coefficient f_c can be expressed by equation (6) [41]:

$$v_{ep} = \frac{q \cdot E_{el}}{f_c} = u \cdot E_{el} \quad (6)$$

According to equation (6), the electrophoretic mobility u can be described by the migration velocity depending on the separation voltage and thus can be experimentally determined by evaluating the migration time at a known length of the capillary. An important phenomenon in CE is the electroosmotic flow (EOF). At a pH higher than 4, the inner wall of fused silica capillaries starts to become negatively charged due to deprotonation of the silanol groups at its surface [45]. By interaction with positively charged buffer components, an electrical double layer is formed [27]. When a separation voltage is applied, the cations at the inner wall of the capillary move towards the cathode, resulting in a suction effect causing the EOF [45]. The EOF is characterized by a flat flow profile in contrast to the parabolic flow profile present in pressure driven systems (Figure 2.6) leading to low band broadening and narrow peaks [41].

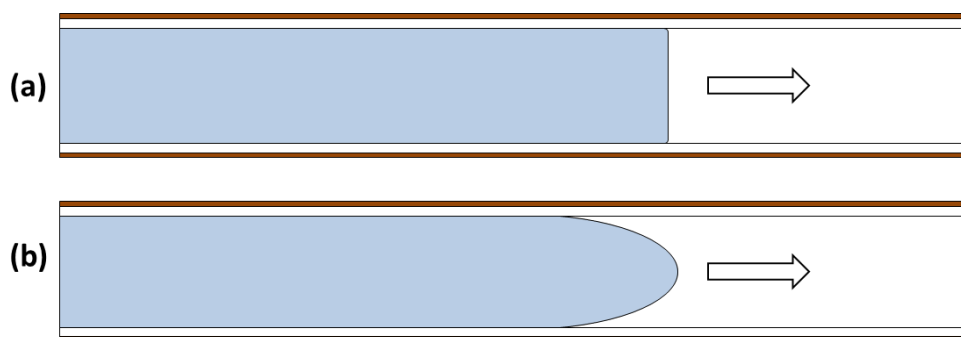


Figure 2.6 (a) Flat flow profile of electroosmotic flow and (b) parabolic flow profile of laminar flow. Adapted from [41].

The velocity of the EOF v_{EOF} is depending on the zeta-potential ζ of the double layer, the dielectric constant ε , the viscosity η and the potential E_{el} according to equation (7) [41]:

$$v_{EOF} = \frac{\varepsilon \cdot \zeta \cdot E_{el}}{4 \cdot \pi \cdot \eta} \quad (7)$$

Neutral molecules that are not influenced by the electrical field are transported to the cathode with the EOF at v_{EOF} . Cationic species are migrating towards the cathode with the sum of the velocity of the EOF and their electrophoretic velocity $v_{EOF} + v_{ep(+)}$, while anionic species are migrating with $v_{EOF} - v_{ep(-)}$ as they migrate against the direction of the EOF. Figure 2.5 (B) illustrates the migration behavior of differently charged species in CZE. If the detector is placed on the cathode side and v_{EOF} is larger than $v_{ep(-)}$, all species present in the solution can be detected on the cathode side in one run [45]. The resulting migration order is illustrated in Figure 2.5 (C). The coupling of capillary electrophoresis with mass spectrometry was introduced in 1987 by Olivares et al [46]. It is commonly established by electrospray ionization [27,41,45], an ionization technique suitable for the investigation of biological

macromolecules as well as small polar molecules and metal complexes [30,34]. The outlet buffer reservoir present in the case of on-column detection is replaced by the ionization interface of the MS system. There are different types of interfaces, including sheath flow (or liquid-supported; high voltage applied via sheath liquid) and sheathless (or nonliquid-supported; high voltage applied directly to CE buffer) interfaces [41,47]. In a coaxial sheath flow interface as it was used during this thesis, a sheath flow with a flow rate of commonly between $2\text{-}10\ \mu\text{L min}^{-1}$ is surrounding the capillary. It has the function of increasing the flow rate to stabilize the electrospray as the CE flow rate is very low [27,41]. Additionally, the electrical contact between CE effluent and the sprayer is established [41]. A nebulizer gas is supporting spray formation and solvent evaporation [30]. A typical sprayer configuration of a so-called triple-tube sprayer is depicted in Figure 2.7.

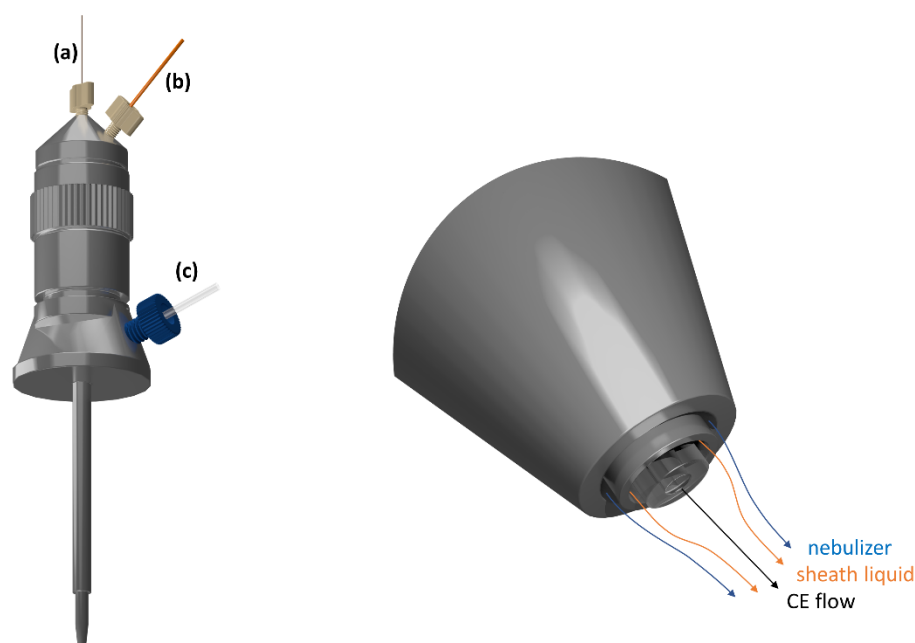


Figure 2.7 Illustration of a triple-tube ESI sprayer (left) and enlarged view of the sprayer tip (right). The fused silica capillary (a) is installed in the center and coaxially surrounded by a sheath liquid flow (b) and a nebulizer gas (c). Own drawing based on the ESI sprayer by Agilent Technologies (Waldbronn, Germany).

As demonstrated by Grundmann and Matysik [40], the flow rate of the sheath liquid does not lead to significant dilution effects of the ionized CE effluent in a sheath flow range between $2\text{-}10\ \mu\text{L min}^{-1}$. A schematic illustration of a CE-ESI-MS setup is shown in Figure 2.8. The grounded stainless-steel sprayer acts as shared electrode between the CE high voltage circuit and the ESI ionization circuit. Selectivity of capillary electrophoresis can be significantly enhanced by applying two-dimensional separation (coupling of CE to HPLC or coupling of two orthogonal CE modes) or dual detection concepts (combining different detectors) [44].

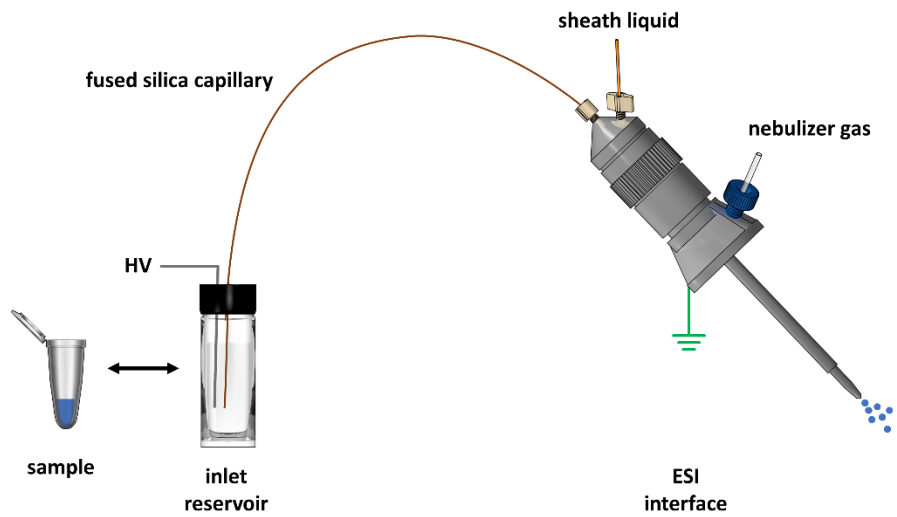


Figure 2.8 Scheme of a CE-ESI-MS setup with a coaxial sheath liquid sprayer. The ESI interface replaces the outlet reservoir of the CE setup. Adapted from [41].

References

- [1] D. Omanović, C. Garnier, K. Gibbon–Walsh, I. Pižeta, *Electroanalysis in environmental monitoring: Tracking trace metals—A mini review*, *Electrochem. Commun.* 61 (2015) 78–83.
- [2] S. Baluchová, A. Daňhel, H. Dejmková, V. Ostatná, M. Fojta, K. Schwarzová-Pecková, *Recent progress in the applications of boron doped diamond electrodes in electroanalysis of organic compounds and biomolecules – A review*, *Anal. Chim. Acta.* 1077 (2019) 30–66.
- [3] A. Brotons, F.J. Vidal-Iglesias, J. Solla-Gullón, J. Iniesta, *Carbon materials for the electrooxidation of nucleobases, nucleosides and nucleotides toward cytosine methylation detection: A review*, *Anal. Methods* 8 (2016) 702–715.
- [4] N. Thapliyal, R. V. Karpoormath, R.N. Goyal, *Electroanalysis of antitubercular drugs in pharmaceutical dosage forms and biological fluids: A review*, *Anal. Chim. Acta* 853 (2015) 59–76.
- [5] A. Rana, N. Baig, T.A. Saleh, *Electrochemically pretreated carbon electrodes and their electroanalytical applications – A review*, *J. Electroanal. Chem.* 833 (2019) 313–332.
- [6] J. Klouda, J. Barek, K. Nesměrák, K. Schwarzová-Pecková, *Non-Enzymatic Electrochemistry in Characterization and Analysis of Steroid Compounds*, *Crit. Rev. Anal. Chem.* 47 (2017) 384–404.
- [7] B. Bansod, T. Kumar, R. Thakur, S. Rana, I. Singh, *A review on various electrochemical techniques for heavy metal ions detection with different sensing platforms*, *Biosens. Bioelectron.* 94 (2017) 443–455.
- [8] J. Barton, M.B.G. García, D.H. Santos, P. Fanjul-Bolado, A. Ribotti, M. McCaul, D. Diamond, P. Magni, *Screen-printed electrodes for environmental monitoring of heavy metal ions: a review*, *Microchim. Acta* 183 (2016) 503–517.
- [9] B. Brunetti, *Recent Advances in Electroanalysis of Vitamins*, *Electroanalysis* 28 (2016) 1930–1942.
- [10] J. Gajdar, E. Horakova, J. Barek, J. Fischer, V. Vyskocil, *Recent Applications of Mercury Electrodes for Monitoring of Pesticides: A Critical Review*, *Electroanalysis* 28 (2016) 2659–2671.
- [11] V. Sharma, F. Jelen, L. Trnkova, *Functionalized Solid Electrodes for Electrochemical Biosensing of Purine Nucleobases and Their Analogues: A Review*, *Sensors* 15 (2015) 1564–1600.
- [12] M. Brycht, A. Nosal-Wiercińska, K. Sipa, K. Rudnicki, S. Skrzypek, *Electrochemical determination of closantel in the commercial formulation by square-wave adsorptive stripping voltammetry*, *Monatsh. Chem. - Chem. Mon.* 148 (2017) 463–472.
- [13] J.J. Thomson, XIX. *Further experiments on positive rays*, *London, Edinburgh, Dublin Philos. Mag. J. Sci.* 24 (1912) 209–253.
- [14] J.J. Thomson, *Bakerian Lecture: Rays of Positive Electricity*, *Proc. R. Soc. A Math. Phys. Eng. Sci.* 89 (1913) 1–20.
- [15] H. Faber, M. Vogel, U. Karst, *Electrochemistry/mass spectrometry as a tool in metabolism studies—A review*, *Anal. Chim. Acta* 834 (2014) 9–21.
- [16] M. Cindric, F.-M. Matysik, *Coupling electrochemistry to capillary electrophoresis-mass spectrometry*, *TrAC Trends Anal. Chem.* 70 (2015) 122–127.
- [17] L. Portychová, K.A. Schug, *Instrumentation and applications of electrochemistry coupled to mass spectrometry for studying xenobiotic metabolism: A review*, *Anal. Chim. Acta* 993 (2017) 1–21.
- [18] F. Matysik, *Electrochemically assisted injection – a new approach for hyphenation of electrochemistry with capillary-based separation systems*, *Electrochem. Commun.* 5 (2003) 1021–1024.
- [19] T. Herl, F.-M. Matysik, *Characterization of electrochemical flow cell configurations with implemented disposable electrodes for the direct coupling to mass spectrometry*, *Tech. Mess.* 84 (2017) 672–682.

- [20] P. Palatzky, A. Zöpfl, T. Hirsch, F.-M. Matysik, Electrochemically Assisted Injection in Combination with Capillary Electrophoresis-Mass Spectrometry (EAI-CE-MS) - Mechanistic and Quantitative Studies of the Reduction of 4-Nitrotoluene at Various Carbon-Based Screen-Printed Electrodes, *Electroanalysis* 25 (2013) 117–122.
- [21] R. Scholz, P. Palatzky, F.-M. Matysik, Simulation of oxidative stress of guanosine and 8-oxo-7,8-dihydroguanosine by electrochemically assisted injection–capillary electrophoresis–mass spectrometry, *Anal. Bioanal. Chem.* 406 (2014) 687–694.
- [22] M. Cindric, M. Vojs, F.-M. Matysik, Characterization of the Oxidative Behavior of Cyclic Nucleotides Using Electrochemistry-Mass Spectrometry, *Electroanalysis* 27 (2015) 234–241.
- [23] R.G. Compton, C.E. Banks, *Understanding Voltammetry*, 2nd ed., Imperial College Press, London, 2010.
- [24] J. Wang, *Analytical Electrochemistry*, John Wiley & Sons, Inc., Hoboken, NJ, USA, 2006.
- [25] A.J. Bard, L.R. Faulkner, *Electrochemical Methods: Fundamentals and Applications*, 2nd ed., Wiley & Sons, Hoboken, NJ, 2001.
- [26] C.G. Zoski, *Handbook of Electrochemistry*, Elsevier, 2007.
- [27] M.H. Gey, *Instrumentelle Analytik und Bioanalytik*, 2nd ed., Springer, Berlin, Heidelberg, 2008.
- [28] W. Paul, H. Steinwedel, Notizen: Ein neues Massenspektrometer ohne Magnetfeld, *Zeitschrift Für Naturforsch. A* 8 (1953).
- [29] W.E. Stephens, A Pulsed Mass Spectrometer with Time Dispersion, *Phys. Rev.* 69 (1946) 691.
- [30] M. Hesse, H. Meier, B. Zeeh, *Spektroskopische Methoden in der organischen Chemie*, 8th ed., Georg Thieme Verlag, Stuttgart, 2012.
- [31] M. Yamashita, J.B. Fenn, Electrospray ion source. Another variation on the free-jet theme, *J. Phys. Chem.* 88 (1984) 4451–4459.
- [32] J.B. Fenn, M. Mann, C.K. Meng, S.F. Wong, C.M. Whitehouse, Electrospray ionization-principles and practice, *Mass Spectrom. Rev.* 9 (1990) 37–70.
- [33] J. Fenn, Electrospray ionization mass spectrometry: How it all began, *J. Biomol. Tech. JBT* 13 (2002) 101–118.
- [34] J.H. Gross, *Massenspektrometrie*, Springer Berlin Heidelberg, Berlin, Heidelberg, 2013.
- [35] E.W. McDaniel, D.W. Martin, W.S. Barnes, Drift Tube-Mass Spectrometer for Studies of Low-Energy Ion-Molecule Reactions, *Rev. Sci. Instrum.* 33 (1962) 2–7.
- [36] K.B. McAfee, D. Edelson, Identification and Mobility of Ions in a Townsend Discharge by Time-resolved Mass Spectrometry, *Proc. Phys. Soc.* 81 (1963) 382–384.
- [37] C.S. Hoaglund, S.J. Valentine, C.R. Spordeder, J.P. Reilly, D.E. Clemmer, Three-Dimensional Ion Mobility/TOFMS Analysis of Electrosprayed Biomolecules, *Anal. Chem.* 70 (1998) 2236–2242.
- [38] A.B. Kanu, P. Dwivedi, M. Tam, L. Matz, H.H. Hill, Ion mobility-mass spectrometry, *J. Mass Spectrom.* 43 (2008) 1–22.
- [39] F. Lanucara, S.W. Holman, C.J. Gray, C.E. Eyers, The power of ion mobility-mass spectrometry for structural characterization and the study of conformational dynamics, *Nat. Chem.* 6 (2014) 281–294.
- [40] M. Grundmann, F.-M. Matysik, Fast capillary electrophoresis–time-of-flight mass spectrometry using capillaries with inner diameters ranging from 75 to 5 μm , *Anal. Bioanal. Chem.* 400 (2011) 269–278.
- [41] F. Lottspeich, J.W. Engels, *Bioanalytik*, 3rd ed., Springer, Berlin, Heidelberg, 2012.
- [42] A.G. Ewing, R.A. Wallingford, T.M. Olefirowicz, Capillary electrophoresis, *Anal. Chem.* 61 (1989) 292A-303A.

- [43] J.W. Jorgenson, K. DeArman Lukacs, Zone electrophoresis in open-tubular glass capillaries: Preliminary data on performance, *J. High Resolut. Chromatogr.* 4 (1981) 230–231.
- [44] A. Beutner, T. Herl, F.-M. Matysik, Selectivity enhancement in capillary electrophoresis by means of two-dimensional separation or dual detection concepts, *Anal. Chim. Acta* 1057 (2019) 18–35.
- [45] H. Whatley, *Clinical and Forensic Applications of Capillary Electrophoresis*, Humana Press, Totowa, NJ, 2001.
- [46] J.A. Olivares, N.T. Nguyen, C.R. Yonker, R.D. Smith, On-line mass spectrometric detection for capillary zone electrophoresis, *Anal. Chem.* 59 (1987) 1230–1232.
- [47] P. Schmitt-Kopplin, M. Frommberger, Capillary electrophoresis–mass spectrometry: 15 years of developments and applications, *Electrophoresis* 24 (2003) 3837–3867.

3. Recent developments in electrochemistry-mass spectrometry

This chapter was published in the journal *ChemElectroChem*. The layout specifications of the journal were changed for uniformity. Copyright 2020 The Authors. Published by Wiley-VCH.

T. Herl, F.-M. Matysik, *ChemElectroChem* **2020**, 7, 2498-2512.

Abstract

Hyphenation of electrochemistry and mass spectrometry is an attractive method to investigate oxidation and reduction processes. By using mass spectrometry electrochemically generated products can be identified. In this Review, different approaches to electrochemistry-mass spectrometry will be summarized including hyphenation of electrochemical flow cells to mass spectrometry as well as integration of separation steps between electrochemical reactions and detection of products. Fields of application range from bioanalytical studies to studies regarding corrosion, electrosynthesis and energy carriers. Important historical developments will be highlighted, followed by an overview of terminology and instrumental setups and discussion of developments within recent years (2017-2020).



3.1 Introduction

Detailed characterization of electrochemical reactions demands coupling of electrochemical systems to advanced detection techniques so that it is possible to identify oxidation or reduction products and elucidate reaction pathways. Mass spectrometry (MS) is ideally suited for this purpose as it can be used in combination with electrochemical flow cells as well as separation methods like high-performance liquid chromatography (HPLC) and capillary electrophoresis (CE). Furthermore, it offers valuable information for the identification of substances in terms of molecular ion masses, mass fragments, and isotopic patterns. Recent reviews covered different aspects of this topic such as bioanalytical and metabolic studies [1–4] as well as instrumental aspects [5–11], organic electrosynthesis under flow conditions [12], and electrocatalysis research [13]. Herein, the most important developments of electrochemistry-mass spectrometry (EC-MS) since its beginnings will be shortly summarized. Aspects of terminology and instrumentation will be highlighted followed by the latest developments in this topic from 2017 to early 2020. Main focus will be put on online approaches (i.e. electrochemical cells with two- or three-electrode setups and externally controlled potential are directly coupled to separation systems or MS). In-source electrochemistry (i.e. part of the ion source of MS system serves as electrochemical cell) will not be covered in detail.

3.1.1 Historical developments

One of the main challenges of the investigation of electrochemical reactions is the rather small amount of products generated by electrochemistry compared to solution chemistry [14], so that the transfer of analytes from electrode to detection system plays an important role. Mass spectrometric characterization of electrochemically generated species started in 1971 when Bruckenstein and Gadde [15] collected gaseous reaction products in a vacuum system before they were transferred to electron ionization mass spectrometry (EI-MS). Wolter and Heitbaum [16] improved the setup to the first online EC-MS approach and named it differential electrochemistry mass spectrometry (DEMS) to distinguish from offline sampling methods. Reaction products formed at a porous electrode were directly transferred to MS via a porous membrane. Due to the direct transfer, so-called mass spectrometric cyclic voltammetry (MSCV) could be accomplished as the MS response could be directly correlated with faradaic current. Thus, typical information gained in DEMS experiments is the MS signal development during potential sweeps. However, this approach for fast and direct analysis of electrogenerated products was limited to volatile compounds that could be transferred through the membrane [16]. After progress in interfacing technologies, Hambitzer and Heitbaum [17] were the first to analyze non-volatile oxidation products by online EC-MS using thermospray ionization. A scheme of the corresponding instrumental setup is depicted in Figure 3.1.

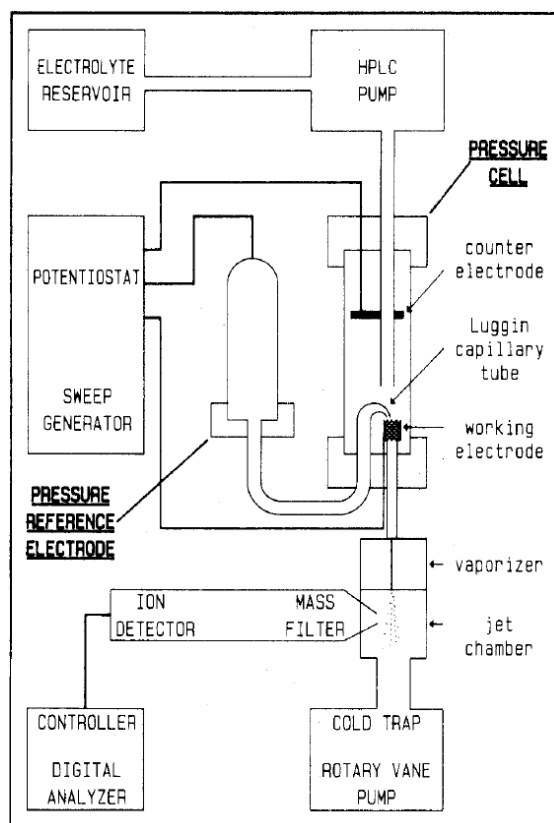


Figure 3.1 Schematic setup of an online EC-MS setup with thermospray ionization. Reprinted with permission from G. Hambitzer, J. Heitbaum, *Anal. Chem.* 1986, 58, 1067–1070. Copyright 1986 American Chemical Society.

The electrooxidation of *N,N*-dimethylaniline was investigated by recording MSCVs. The dead time of this flow cell approach was 9 s and was proposed to be reduced to 1 s, which was supposed to allow for kinetic studies if the transfer time was varied [17]. This shows that the idea of real-time EC-MS which is of high interest nowadays arose already quite early. Rotating disk electrodes were also successfully coupled to mass spectrometry [18]. In 1988 Volk et al [19] applied the methodology in bioanalytical context. The oxidation of uric acid and 6-thioxanthine was investigated and the usefulness for characterizing redox reactivity of drugs and xenobiotics was proposed. One year later, in 1989, further studies on uric acid oxidation were published by the same group and reaction intermediates and products were described together with proposed reaction pathways [20]. In the same year, the first online coupling of electrochemistry and high-performance liquid chromatography to separate stable products was described [21] (Figure 3.2).

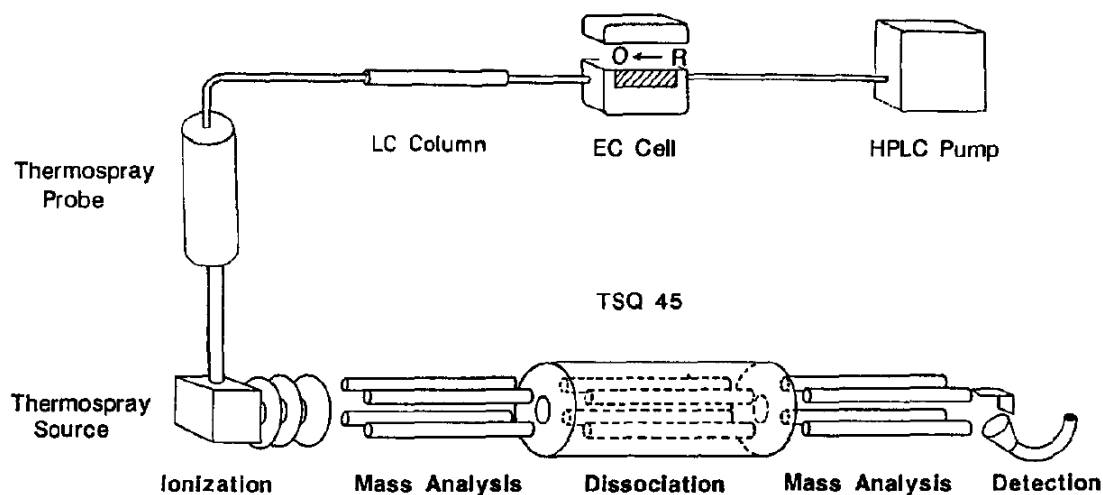


Figure 3.2 Illustration of an online EC-LC-thermospray-MS system. Reprinted with permission from K. J. Volk, R. A. Yost, A. Brajter-Toth, *J. Chromatogr. A* 1989, 474, 231–243. Copyright 1989 Elsevier.

Further studies were concerned with the application of online-EC-HPLC-MS to study the oxidation of thiopurines [22,23]. A significant drawback of thermospray ionization is the risk of thermal decomposition of labile analytes in the ion source [24]. Electrospray ionization (ESI) represents an alternative ionization method facilitating the investigation of such thermally labile compounds [25]. After some studies on the inherent electrochemistry of ESI were published [26–30], Dupont et al [31] were the first to use electrochemistry to allow for the ESI-MS detection of neutral compounds by generation of stable oxidation or reduction products, however, in an offline approach. Fullerenes were used as model compounds. The applicability of in-source electrochemistry and offline electrochemistry to detect neutral species in ESI was compared. Zhou and Van Berkel [32] first described online coupling of different types of electrochemical flow cells (thin-layer electrode flow-by cell, tubular electrode flow-through cell, and porous electrode flow-through cell) to ESI-MS and addressed challenges and applications of this approach. First attempts to online electrochemical oxidation after HPLC separation were carried out by Karst and coworkers [33] with the goal of detecting ferrocenecarboxylic acid esters of different alcohols and phenols (Figure 3.3). Coulometric oxidation allowed for detection of these non-polar species in ESI-MS by generation of charged oxidation products. Next to HPLC, capillary electrophoresis (CE) is an alternative separation method suitable to be coupled with EC-MS. In 2003, Esaka et al [34] and Matysik [35] independently described first electrophoretic separations of online electrogenerated species. Esaka et al focused on the characterization of electrochemically generated anion radicals of phenanthrenequinone and anthraquinone while Matysik proposed so-called electrochemically assisted injection as an online sample preparation method for enhanced separation performance in CE and detectability of non-polar analytes in ESI-MS. The latter was demonstrated by online EC-CE-MS measurements of Scholz and Matysik [36] in 2011, when different ferrocene derivatives were analyzed by EC-CE-ESI-MS. Since then, the different methodologies of online EC-MS, EC-HPLC-MS, HPLC-EC-MS and EC-CE-MS have been widely applied, as several reviews show [1-11,37–39].

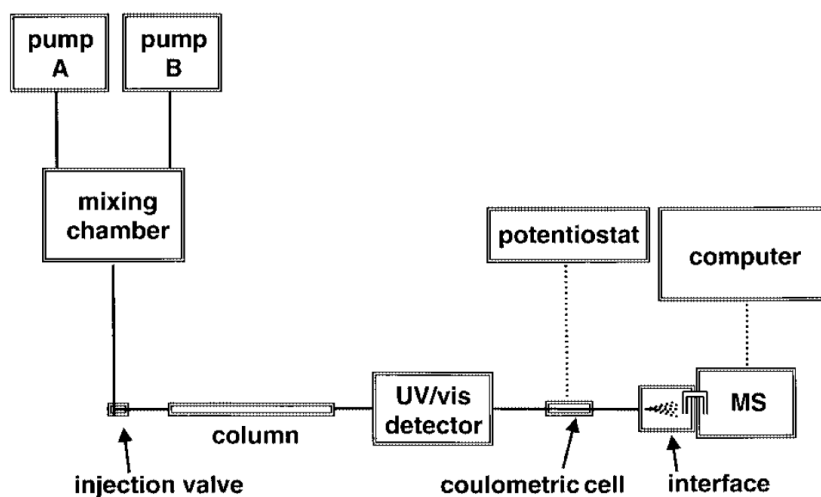


Figure 3.3 Scheme of an HPLC-EC-MS setup. Reprinted with permission from G. Diehl, A. Liesener, U. Karst, *Analyst* 2001, 126, 288–290. Copyright 2001 Royal Society of Chemistry.

3.1.2 Terminology

Different kinds of data can be derived from EC-MS depending on the measurement mode and the denotation of the data is not uniform. By online EC-MS, so-called mass spectrometric cyclic voltammograms [16,17,40], mass spectrometric hydrodynamic voltammograms [20,21], on-line linear sweep voltammetry-electrospray mass voltammetry measurements [41], extracted ion voltammograms [42] or mass voltammograms [43–48] have been described. The potential-dependent mass intensity was measured and correlated to the potential. This method is perfectly suited to assign formed product species to the respective potential regions. Prerequisite for this is a fast transfer from the electrochemical cell to MS in order to directly correlate potential and mass intensity to each other. An alternative method is the application of constant potential steps [17,20], which is the method of choice to characterize the instrumental setups regarding time-delays between generation and detection of products. Constant current and anodic stripping modes have also been applied [32].

Considering mass voltammograms, two different modes of data acquisition have to be taken into account: (i) the potential is swept at a certain scan rate and the MS response is recorded in real time and correlated to the faradaic current [17,40,41] and (ii) the potential is increased step wise and the corresponding MS response is recorded. The discrete data points are collected to a mass voltammogram [20,21,24,32]. The first approach demands short dead times (below 1 s [17]). Already in the first online EC-MS studies a quantitative correlation between faradaic current and mass intensity was proposed as a source of information on current efficiency and number of transferred electrons [17]. However, in many cases, the current response of the electrode is not considered in data evaluation and only the mass intensity versus potential is presented. Considering the term voltammetry, which was introduced by Laitinen and Kolthoff [49] in 1941 as a description for determination and interpretation of current-voltage curves, a complete mass voltammogram should include both mass and current intensity to give comprehensive information and fully fit the term mass voltammogram. Due to time-resolution of the

separation step, EC-HPLC-MS and EC-CE-MS experiments are usually carried out after constant-potential electrolysis as potential sweeps can not be directly transferred to the separation system. Figure 3.4 shows an example of how a comprehensive mass voltammogram could be presented. The oxidation of ferrocenemethanol (FcMeOH) in a thin-layer flow cell equipped with a thin-film gold electrode is depicted and the current response as well as the mass intensity are drawn in dependence of the applied potential.

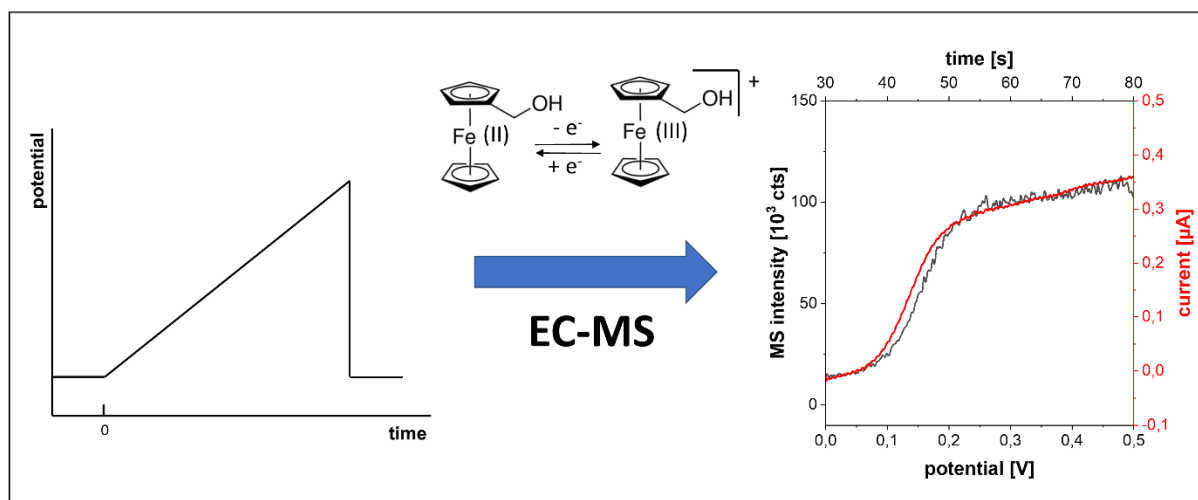


Figure 3.4 Example of a mass voltammogram for the oxidation of FcMeOH to FcMeOH⁺. Hydrodynamic linear sweep voltammogram of 1 mM FcMeOH in ACN/1 mM HOAc/10 mM NH₄OAc (red, 10 mV s⁻¹, Micrux ED-SE1-Au electrode, 16 μL min⁻¹) recorded parallel to MS signal of FcMeOH⁺ (black, m/z 216.06) with a PEEK thin-layer flow cell equipped with a thin-film electrode. The cell was coupled to ESI-TOF-MS via a fused silica capillary (50 μm x 21 cm). Experimental setup based on [50]. Unpublished work.

3.1.3 Instrumental setups

In this section, a rough overview of different instrumental approaches to EC-MS will be presented. A straightforward method for EC-MS characterization of electrogenerated species is offline electrolysis followed by HPLC-MS or CE-MS [45,51]. However, it is combined with a loss of time resolution and experimental effort in sample preparation. Thus, online approaches are preferred when fast analysis is required. DEMS as the most traditional method is still relevant today. Gaseous products of electrochemical reactions can be detected after passing a porous membrane, usually consisting of polytetrafluoroethylene (PTFE), which separates the electrochemical cell from the MS system [52]. Different electrochemical cell configurations such as thin-layer flow cells or cells based on coated PTFE membranes exist as reviewed by Abd-El-Latif et al [52]. DEMS is characterized by very fast response times but is limited to gaseous reaction products [52]. In direct EC-MS of liquid solutions, mostly coulometric flow-through cells and amperometric thin-layer flow cells are used as previously described [1]. Different configurations are available on the market. ESA analytical cells [42,53,54], electrochemical guard cells [55,56] and conditioning cells [48,55] as well as Antec ReactorCells [44,45,47,57] and μ-prepCells [51] equipped with different electrode materials have been quite popular in the last years. HPLC pumps (typically applied flow rates up to 50 μL min⁻¹) [42,53,55] or syringe pumps (typically applied flow rates 5-20 μL min⁻¹) [44-47,51,54] are used for transport of solutions.

EC-HPLC-MS measurements are achieved by coupling the aforementioned flow cells to HPLC-MS by direct infusion into injection loops of the HPLC system [46,48,57] so that samples can be electrochemically pretreated on-line. Online EC-CE-MS measurements have been carried out either by injection from electrolytical batch cells [36] or disposable electrodes [58,59] with the advantage that no valve-based systems are needed as a direct injection into the separation capillary is possible. Especially in bioanalytical context EC-MS and EC-CE-MS offer the advantages that physiological conditions can be simulated by using the corresponding (MS compatible) aqueous electrolytes. This is not valid for HPLC separation, where typical separation conditions are very different from the electrolytes so that ongoing reactions during separation might not be representative for the behavior in close-to physiological solutions. However, if electrochemistry is coupled to CE systems, care has to be taken to decouple the electrochemical cells from the separation high voltage to avoid interferences and damage of the potentiostat. Miniaturization of electrochemical systems also plays an important role in instrumental developments. As reviewed by van den Brink et al [8], miniaturization offers the advantages of high conversion efficiencies at low sample consumption based on rapid diffusive mass transport in microvolumes, reduced transfer times to MS, and compatibility to nano-LC and nano-electrospray conditions due to the low flow rates. Experiments that would be associated with critical conditions in conventional cells with larger amount of sample such as reactions of highly reactive compounds or reactions under high pressure can be carried out at low risk [8]. Micro and nanoscale cells of different materials such as ceramics, glass, or plastics with volumes ranging from low μL to even pL have been reported using flow rates in the range of several hundred $\mu\text{L min}^{-1}$ down to low nL min^{-1} [8]. However, not all cells have been coupled to MS and many configurations are in the prototype status [8]. A further aspect of miniaturization is the combination of electrochemistry and electrospray ionization in one device [8]. Next to the methods mentioned above, a lot of innovative concepts are in development as will be shown in the following sections. Interfacing electrochemistry and mass spectrometry is another important issue. While membrane-based interfaces and electron ionization (EI) are used for analysis of volatile compounds in DEMS [6], mostly electrospray ionization (ESI) [4,6] and inductively coupled plasma (ICP) [13] are used as interfacing strategies for liquid samples. ESI is a soft ionization method characterized by low fragmentation and is especially suited for analysis of bioanalytically relevant compounds of all sizes such as drugs, peptides and proteins, as covered in different reviews [1,4,6]. However, the electrochemical cell has to be decoupled from the ionization voltage of several kV, and the inherent electrochemistry of the ESI source has to be kept in mind [6]. As reviewed by Kasian et al [13], ICP-MS is characterized by high sensitivity and the possibility of multielement analysis, particularly of trace metals. Therefore, it was widely applied for stability studies of electrode materials in the context of electrocatalysis in fuel cells and water electrolyzers and the authors pointed out that it is also promising for stability studies in other fields of research [13]. As a drawback, however, it is not possible to determine the oxidation state of the respective dissolved species by ICP-MS alone [13].

3.2 Latest developments and applications

In this section, developments and applications of mainly the last three years (2017-2020) will be shortly summarized. Table 3.1 shows the reported methods and fields of application. However, the different methods are often used in combination and a large variety of different topics are addressed so that the given classification is just intended to present a rough overview.

Table 3.1 Reported methods and fields of application

Method, advantages and disadvantages	Fields of application	Ref.
DEMS*		
Pro:	CO ₂ reduction	[60,61]
Fast response, separation of products from electrolyte	Lithium-ion batteries	[62]
Contra:	Methanol oxidation	[63]
Limited to volatile products	Carbon corrosion	[64]
	Hydroxylamine oxidation	[65]
EC-MS*		
Pro:	Energy carriers	[66–70]
Fast, rather simple setup, high instrumental flexibility and diversity of setups	Alloy corrosion	[71,72]
	Electrode corrosion	[73–77]
Contra:	Interfacing	[78–80]
Suppression effects by electrolyte salts or product mixtures possible, compatibility of EC and MS conditions prerequisite (e.g. electrolyte salts and concentrations)	Electrosynthesis	[81–85]
	Simulation of metabolism	[86–94]
	Protein cleavage	[95]
	Detection of complexes	[50]
	Reduction of quinones	[96]
	Disulfide bond mapping	[97]
	Location of double bonds	[98]
	Antibiotics degradation	[99]
EC-HPLC-MS*		
Pro:	Simulation of metabolism	[100–103]
Separation, retention time as additional information, identification via analytical standards	Quantification in MS	[104–106]
	Coupling reactions	[107]
Contra:	Protein digestion	[108]
Instrumentally complex, loss of time resolution, analytical standards often not available		
EC-CE-MS		
Pro:	Separation of complexes	[109]
Separation, migration time as additional information, suited for small charged compounds (orthogonal to HPLC)	Nucleobase oxidation	[110,111]
Contra:		
Instrumentally complex, limited sensitivity due to small injected volume, decoupling of EC and CE voltage necessary		
*Commercial setups available		

3.2.1 DEMS

DEMS is an important method for research in the context of energy carriers as recent publications show. Figure 3.5 illustrates a DEMS cell that was developed by Bell and coworkers [60]. It enabled the real time quantification of electrochemically generated products of CO₂ reduction, which was taking several hours with conventional methods. For the first time, DEMS could be used to quantify most of the major products of the CO₂ reduction reaction on polycrystalline copper within one hour. The cell was intended to be used for screening of the potential-dependent activity and selectivity of novel electrocatalysts and to characterize the activity and sensitivity over time. The same group investigated the concentration of carbon dioxide and reaction products in the immediate vicinity of the cathode surface [61]. The electrocatalyst was directly coated onto the pervaporation membrane and volatile species were directly sampled from the electrode-electrolyte interface. Thus, the reaction conditions close to the electrode surface could be characterized. Ag and Cu were used as electrode materials.

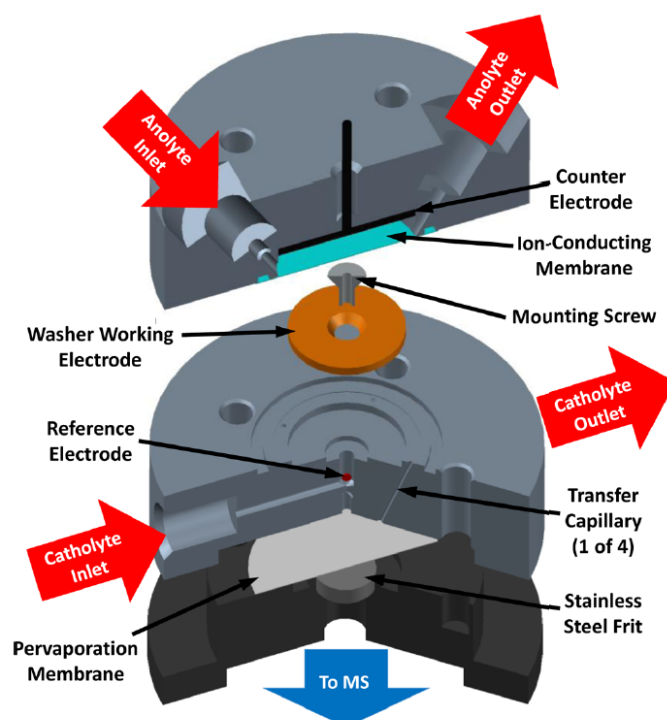


Figure 3.5 Exploded view of a DEMS cell applied for the investigation of CO₂ reduction. Reprinted with permission from E. L. Clark, M. R. Singh, Y. Kwon, A. T. Bell, *Anal. Chem.* 2015, 87, 8013–8020. Copyright 2015 American Chemical Society.

Shen et al [62] used online continuous flow differential electrochemical mass spectrometry and in situ X-ray diffraction to investigate Li-rich layered oxide materials. The structure transformation during charge and discharge processes was characterized. High-energy nickel-manganese-cobalt cathode materials with different Co/Ni ratios showed different initial medium discharge voltages and voltage decays upon cycling. DEMS was used to detect gaseous products (CO₂, O₂) released from the electrodes during the initial cycle. Mateos-Santiago et al [63] investigated the anodic oxidation of methanol on nanostructured Pt/C and Pt/WO₃-C electrode materials under acidic conditions. Methanol oxidation was different on both electrodes. The addition of WO₃ to the electrode support matrix led to an increased

direct oxidation of methanol to CO_2 and the formation of formic acid. The electrochemical corrosion of carbon electrode materials at high anodic potentials in alkaline electrolytes was investigated by Möller et al [64] by DEMS for the first time. By a modified DEMS system, the initially generated CO_3^{2-} could be detected as corrosion marker in form of CO_2 by in situ acidification in front of the DEMS membrane (Figure 3.6). Using highly active oxygen evolution reaction (OER) catalysts, carbon oxidation could be reduced.

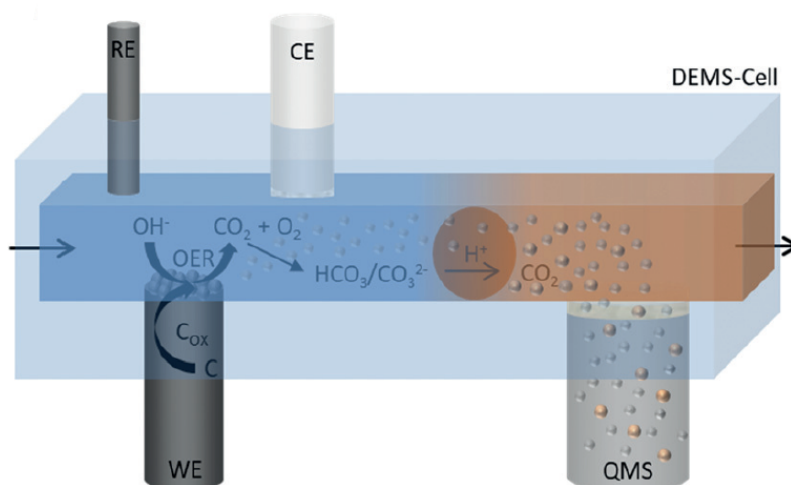


Figure 3.6 Setup for the investigation of carbon corrosion at high anodic potentials in alkaline electrolytes by DEMS. CO_2 was detected as corrosion marker after conversion to CO_3^{2-} due to the alkaline pH and release as CO_2 by in situ acidification. Adapted under the terms of the Creative Commons Attribution Licence (CC BY) from S. Möller, S. Barwe, J. Masa, D. Wintrich, S. Seisel, H. Baltruschat, W. Schuhmann, *Angew. Chemie Int. Ed.* 2020, 59, 1585–1589. Copyright 2020 The Authors.

DEMS under forced convection was used by Pozniak et al [65] to determine absolute faradaic efficiencies for the generation of nitrogen by oxidation of hydroxylamine on polycrystalline gold electrodes. N_2 and N_2O were found as main products in acidic and neutral media and NO as well as N_2O in alkaline media.

3.2.2 EC-MS

3.2.2.1 Energy carriers and corrosion

Cheng et al [66] investigated the generation of formaldehyde by oxidation of methanol in the context of fuel cell research. Online EC-desorption electrospray ionization (DESI)-MS was used as method. The oxidation at Pt, Au, and Pt/C electrodes was characterized in acidic and alkaline solution. Formaldehyde was detected after online derivatization with phenylhydrazine. Liu et al [67] developed a Y-shaped dual-channel microchip to investigate the reduction of oxygen by decamethylferrocene or tetrathiafulvalene under catalysis of tetraphenylporphyrin at a water/oil interface by EC-ESI-MS, which is important for electrochemical energy conversion. The electrochemical reaction steps were either induced by applying an external potential to glass microchips with integrated electroplated platinum line electrodes or by lithium tetrakis(pentafluorophenyl) borate in a polyimide-based microchip. The same topic was

addressed by Gu et al [68], who investigated the oxygen reduction reaction by ferrocene under catalysis of cobalt tetraphenylporphine. Gel hybrid ultramicroelectrodes were developed that worked as electrochemical cells and nanospray emitters. Spray formation was achieved via a piezoelectric pistol. The agar-gel and PVC-gel components worked as liquid/liquid interface between aqueous and organic phase (agar-gel/dichloroethane, water/PVC-gel). Real time analysis of the oxygen reduction reaction was possible. Other investigations were concerned with the development of methods for the evaluation of water splitting catalysts. Electrolysis was coupled with mass spectrometry to measure the faradaic efficiency of water splitting at planar metal electrodes, metal-foam-based electrodes and porous electrodes with carbon additive under real time conditions [69]. Gaseous products were transferred to MS during electrolysis by a nitrogen carrier gas. In contrast to DEMS, transfer to MS was not achieved via a gas permeable membrane but an exhaust system. The anode and cathode chambers were separated by an ion exchange membrane. During slow potential scans the produced gases were quantified by MS while accumulation in the cell was minimized. Xu et al [71] reported the investigation of alloys by so-called electrochemical ionization mass spectrometry (ECI-MS). A microelectrolytic cell equipped with platinum wire working and auxiliary electrode and a silver/silverchloride reference electrode was used for the investigations and the metal of interest was either connected to the anode or operated as bipolar electrode. By applying suitable potentials, the alloy components were selectively dissolved to the corresponding metal ions, which were complexed by ligands in the electrolyte and detected by mass spectrometry. The method was suggested to investigate organic compounds and alloys for example in the context of engine abrasion and engine oil analysis or cast post analysis in the context of dental treatment. The same method was applied to the analysis of metal impurities on the surface of objects with irregular shape such as necklaces and rings. Non-destructive sampling with sample consumption in the nanogram range was achieved by potential-dependent formation of metal ions from the sample followed by mass spectrometric detection [72]. Jovanović et al [73] investigated the corrosion of gold materials by measuring the potential-resolved dissolution of gold from a gold disc electrode and a carbon disc electrode coated with gold nanoparticles by EC-ICP-MS based on an electrochemical flow cell which has been previously applied for characterization of platinum electrocatalysts [74]. Online dissolution profiles of gold were obtained during cyclic voltammetry depending on the amount of simulated chloride impurities (Figure 3.7). Nanostructured gold on carbon supports was more stable against corrosion as less dissolution was observed. Another study was concerned with the investigation of platinum and gold dissolution in an organic methanol-based electrolyte. A modified EC-ICP-MS setup was used [75]. Ledendecker et al [76] investigated the optimization of the iridium utilization during the acidic oxygen evolution reaction while reducing the noble metal content, which is important for future large scale applications. The stability of iridium oxide layers on tin oxide based support materials was investigated by dissolution experiments utilizing a flow cell coupled online to ICP-MS. Kasian et al [77] used a scanning flow cell coupled to ICP-MS and online electrochemical mass spectrometry to investigate the oxygen evolution reaction on iridium and iridium oxide electrodes and

the associated electrode degradation pathways. Three different dissolution mechanisms were identified. The reported measurements described above showed a trend towards miniaturization of electrochemical cells and interfacing systems. In many cases, two-electrode setups are used. However, no commercial standard systems have been established yet. As demonstrated in several studies, EC-MS is an attractive method to investigate and optimize the corrosion stability of coatings and electrocatalysts especially if electrochemistry is coupled to ICP-MS.

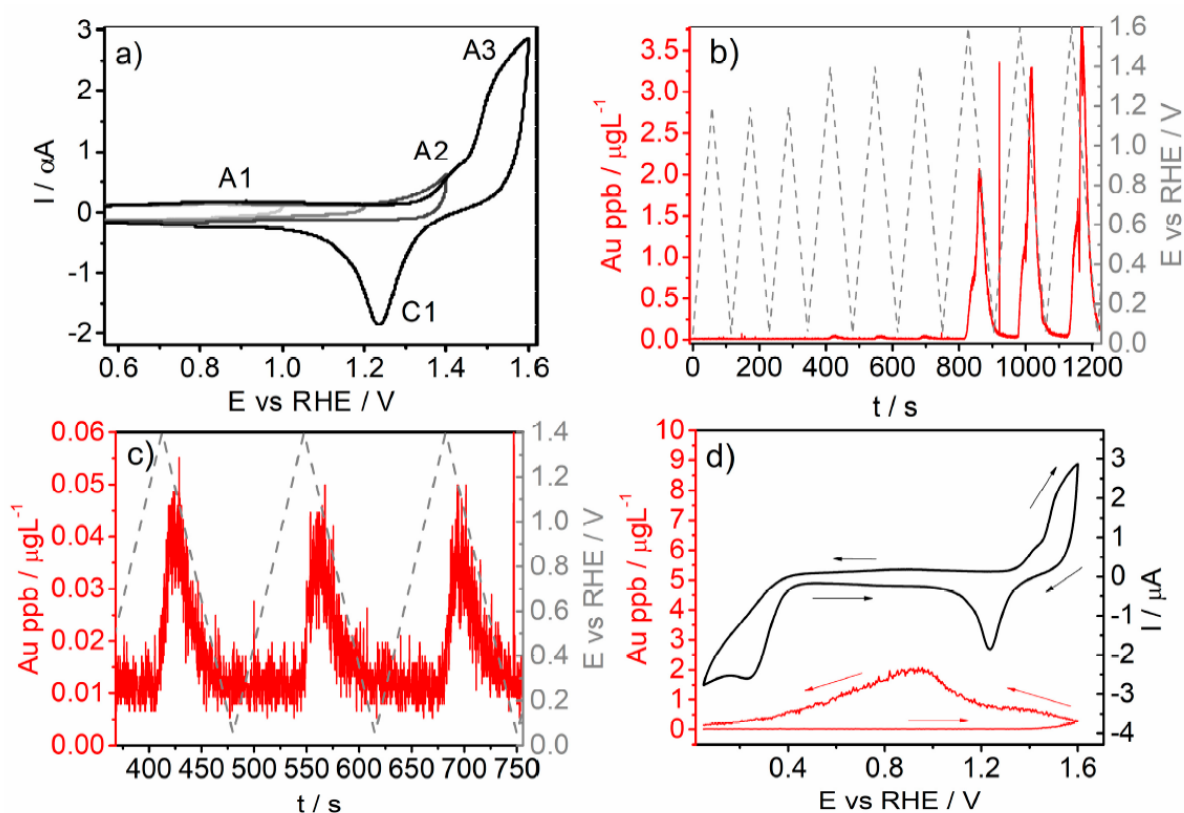


Figure 3.7 (a) Cyclic voltammograms of 0.05 M H_2SO_4 on a polycrystalline Au electrode with increasing anodic potential limits (scan rate 20 mV s^{-1}). (b+c) EC-ICP-MS measurements of Au dissolution during potentiodynamic cycling at 20 mV s^{-1} . (d) Au dissolution profile (red) and current signal (black) during potentiodynamic cycle (20 mV s^{-1}). Reprinted under the terms of the Creative Commons Attribution Licence (CC BY) from P. Jovanovič, M. Može, E. Gričar, M. Šala, F. Ruiz-Zepeda, M. Bele, G. Marolt, N. Hodnik, *Coatings* 2019, 9, 10. Copyright 2018 The Authors.

3.2.2.2 Electrosynthesis and metabolism studies

Brajter-Toth and coworkers [78] investigated the ionization process in liquid sample (LS)-DESI and characterized an in-line LS-DESI configuration in comparison to common angled LS-DESI-MS systems, electrosonic spray ionization (ESSI) and ESI. As main advantage of the in-line LS-DESI-MS approach, a higher tolerance of the interface towards electrolyte solutions was described, avoiding contamination or clogging of the sprayer as it can occur in regular ESI. The MS intensity was found to be lower in LS-DESI-MS compared to ESI-MS but the ion signal stability was higher in LS-DESI-MS. The compatibility of the used electrolytes to the MS system is an important aspect as volatile electrolytes have to be used. However, in electrochemistry often high concentrations of electrolytes are preferred while low concentrations are better for MS to avoid suppression effects in the ionization process [32].

Miniaturization of electrochemical systems plays an important role for electrosynthesis processes. Folgueiras-Amador et al [81] developed an electrochemical flow microreactor for organic electrosynthesis as improved version of their previous design [82–84]. Due to the small dimensions, the addition of high amounts of supporting electrolytes can be avoided. Among other studies, the cyclization of amides to isoindolinones was investigated and the number of electrons for a complete conversion was determined by inline mass spectrometry. This approach is interesting as minimizing the amount of supporting electrolyte avoids time consuming clean-up procedures and facilitates high-efficiency electrosynthesis of product solutions that can directly be investigated by further techniques such as NMR without interferences by electrolyte salts. Next to Fenton-like oxidation and UV irradiation, online as well as offline EC-ESI-MS was used to investigate the phase I metabolism of the mycotoxins citrinin and dihydroergocristine and results were compared to *in vitro* metabolites by Koch and coworkers [86]. Even if the Fenton-like reaction was the better suited method to predict phase I metabolites, the products generated by EC were suggested to be potentially interesting for future research. The same group investigated transition products of monensin by EC-MS and compared the results with microsomal metabolism and hydrolysis experiments of monensin [87]. Subsequent HPLC-MS/MS studies were used for further investigations. Decarboxylation, O-demethylation and acid catalyzed ring-opening reactions were found to be the main processes. By electrochemistry, some products formed in the microsomal assay could be reproduced but also additional products could be found. Colombo et al [88] used online EC-ESI-MS to simulate oxidative injury of three phosphatidylethanolamines with a boron-doped diamond (BDD) working electrode and suggested an oxidation mechanism mediated by hydroxyl radicals. EC-ESI-MS was demonstrated to be able to reproduce oxidative metabolism by reactive oxygen species. Rohn and coworkers [89] analyzed the redox properties of various phenolic compounds such as chlorogenic acid or caffeic acid on a boron-doped diamond electrode and used EC-MS for investigation of adduct formation of oxidized phenolic compounds to food proteins by reaction of oxidized chlorogenic acid with peptides of alpha-lactalbumin. The same group reported the electrochemical simulation of phase-I and phase-II metabolism of cholecalciferol and ergocalciferol in the context of vitamin D metabolism [90]. Electrochemical investigations as well as binding studies to glucuronic acid were carried out and products of *in vivo* studies could be simulated. Additionally, EC-MS was suggested as a promising method for generating reference compounds. Oxidative metabolism of the antimicrobial agent triclosan was investigated by Zhu et al [91]. An electrochemical flow cell with a boron-doped diamond electrode was coupled to MS to identify possible metabolites. Additionally, the toxicity of triclosan and the simulated metabolites was investigated with modelling tools and bioassays on zebrafish embryos. The results demonstrated potential harmfulness of triclosan and its metabolites. Though far less frequently applied, investigations of reductive processes are also carried out. Pietruk et al [92] investigated the reduction reactions of the azo-dyes Sudan I-IV and 4-nitroaniline at a glassy carbon electrode. Possible metabolites were identified by a flow cell approach. For further confirmation of the products, LC-MS/MS measurements were carried out after offline electrolysis. A

novel paper based electrochemical cell was developed by Narayanan et al [80]. A filter paper coated with carbon nanotubes and equipped with printed silver paste electrodes was used to convert thiols to disulfides, to functionalize polycyclic aromatic hydrocarbons, detect radical cations of metallocenes and polycyclic aromatic hydrocarbons and to investigate the oxidation of glucose. van den Brink et al [95] developed a glass-based microfluidic electrochemical cell with an integrated boron-doped diamond electrode for specific electrochemical protein cleavage. The cell volume was 160 nL. The potential-dependent cleavage was investigated by recording mass voltammograms and selectivity was proposed to be tunable by the selection of the potential. Cleavage of bovine insulin and chicken egg white lysozyme was demonstrated. The microfluidic cell was suggested as a purely instrumental approach to protein analysis and proteomics studies by high electrochemical conversion efficiency and mass spectrometric detection. The timescale of investigations can be reduced and reactions can be carried out under conditions not suitable for enzymatic cleavage [95]. Figure 3.8 illustrates the chip design. The reported studies show that instead of pure electrochemical investigations more and more additional experiments are carried out such as toxicity studies of electrogenerated compounds or conjugation studies of electrogenerated intermediates.

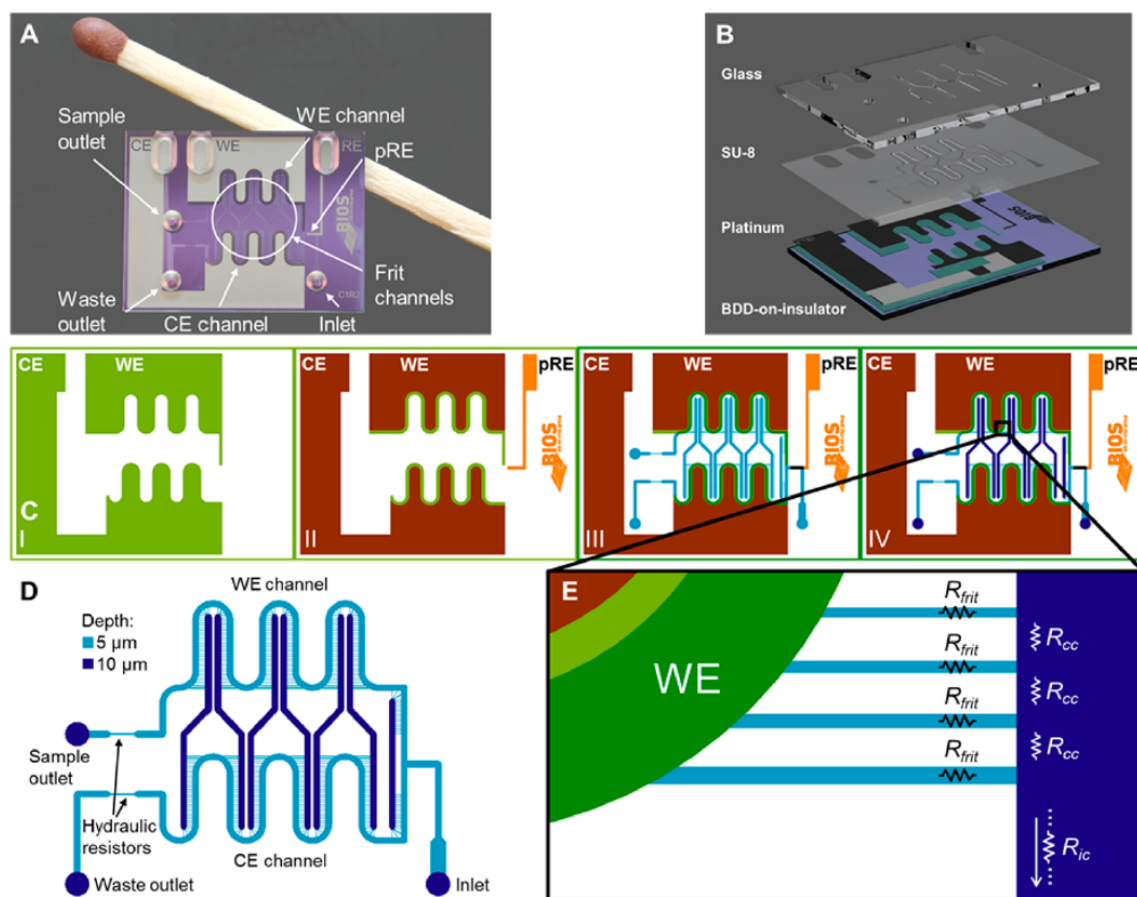


Figure 3.8 Microfluidic electrochemical cell used for electrochemical protein digestion. (A) Photograph of assembled chip. (B) Exploded view of the different chip layers. (C) Structures of BDD working electrode and counter electrode (I), Pt pseudo reference electrode and contact pads (II), SU-8 layers (III), and microfluidic structures and access holes (IV). (D) Scheme of fluidic structures. (E) Expanded view of a part of the working electrode and frit channel network. Reprinted with permission from F. T. G. van den Brink, T. Zhang, L. Ma, J. Bomer, M. Odijk, W. Olthuis, H. P. Permentier, R. Bischoff, A. van den Berg, *Anal. Chem.* 2016, 88, 9190–9198. Copyright 2016 American Chemical Society.

3.2.2.3 Real time EC-MS

The idea of fast real time analysis of electrochemical reactions was already present in the beginnings of EC-MS. However, in the last years this idea was reactivated and several developments towards real time detection of electrogenerated species were described by different working groups. Matysik and coworkers [50] used amperometric thin layer flow cells with integrated disposable electrodes for direct coupling to ESI-TOF-MS. The dead volume for the transfer to MS was minimized by using short fused silica capillaries with low inner diameters and an ESI interface commonly used in CE-MS. By appropriate flow rates, short transfer times in the range of 1 s could be achieved. However, this approach is limited to ESI compatible electrolytes. Wang et al [79] described the real time investigation of ascorbic acid oxidation by the previously developed so-called in situ liquid secondary ion mass spectrometry (in situ liquid SIMS [112,113]). A radical intermediate could be detected and dynamic double layer processes at the electrode-electrolyte interface could be investigated by coupling a vacuum compatible microfluidic electrochemical cell with integrated gold film working electrode to TOF-SIMS. Secondary ions were directly sampled from the electrode-electrolyte interface by a primary Bi^{3+} ion beam that was penetrating a silicon nitride membrane as illustrated in Figure 3.9.

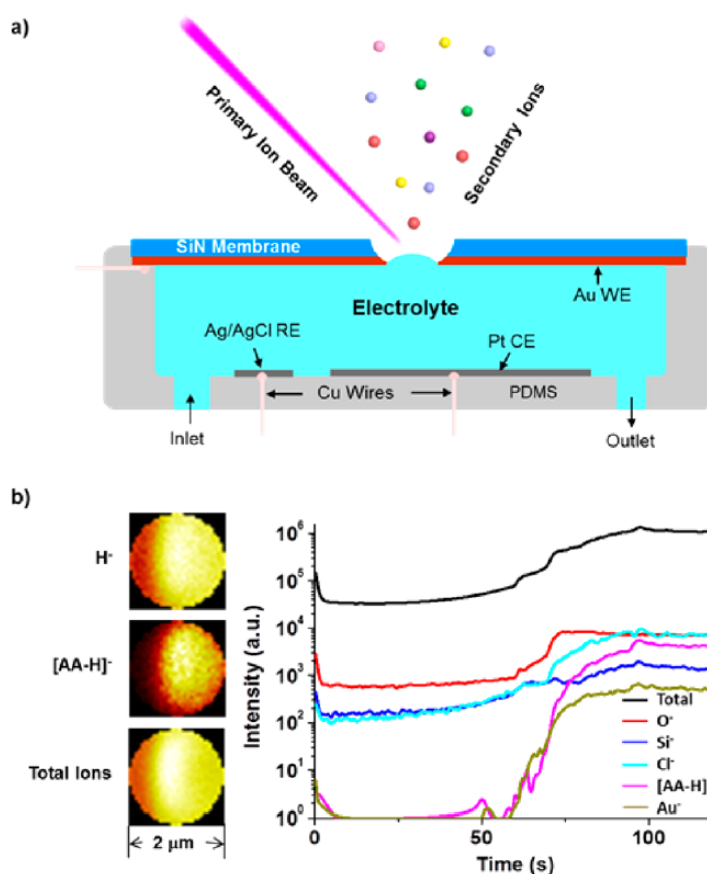


Figure 3.9 (a) Illustration of an electrochemical cell for in situ liquid SIMS. (b) Depth profiles of different ions obtained during drilling a hole through a SiN membrane and a Au film electrode in a solution of 0.5 mM ascorbic acid (AA) in 10 mM HCl. Reprinted with permission from Z. Wang, Y. Zhang, B. Liu, K. Wu, S. Thevuthasan, D. R. Baer, Z. Zhu, X.-Y. Yu, F. Wang, *Anal. Chem.* 2017, 89, 960–965. Copyright 2016 American Chemical Society.

Khanipour et al [70] presented a method for time- and potential-resolved investigation of liquid and gaseous products of electrochemical reactions by electrochemical real time mass spectrometry (EC-RTMS). The CO_2 reduction reaction on pristine and anodized copper was investigated. A scanning electrochemical flow cell with extraction capillary was coupled to mass spectrometry. Though instrumentally quite complex because of the parallel use of two MS systems, this method allowed for highest flexibility as volatile and non-volatile species could be investigated. The first was achieved by gas extraction through a hydrophobic membrane and detection by electron ionization quadrupole MS while the latter was realized by nebulizing the electrolyte solution and coupling to direct analysis in real time (DART) TOF-MS (Figure 3.10). Using DART ionization this approach was more robust towards electrolyte salts than regular EC-ESI-MS techniques.

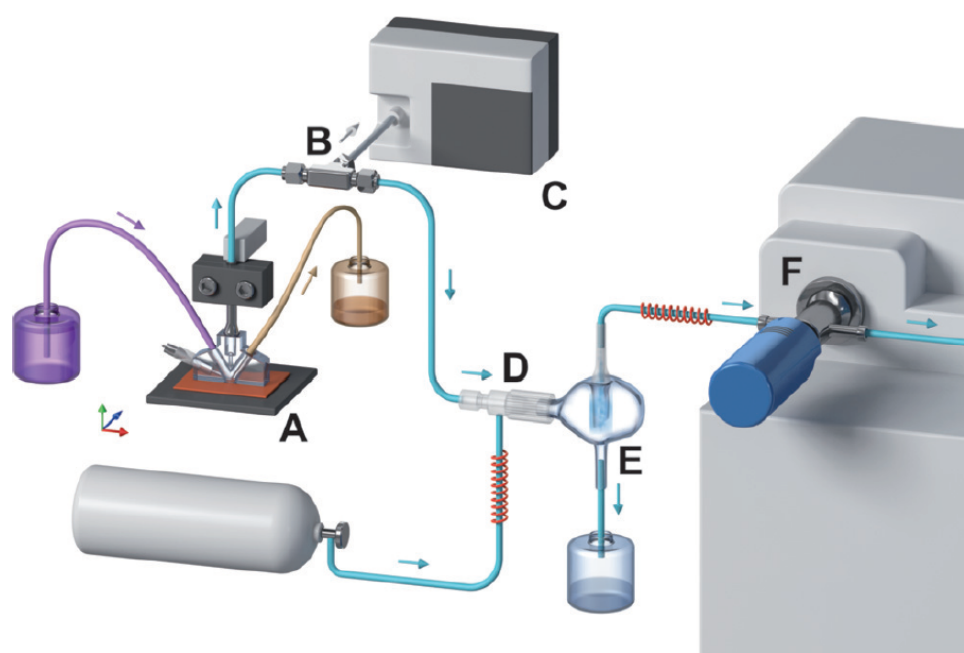


Figure 3.10 Setup for real time EC-MS consisting of a scanning flow cell (A), a degasser with hydrophobic tubing for gas-liquid separation (B), an electron-ionization quadrupole MS for gas analysis (C), a nebulizer (D), a spray chamber (E), and a direct analysis in real-time-TOF-MS for liquid analysis (F). Reprinted with permission from P. Khanipour, M. Löffler, A. M. Reichert, F. T. Haase, K. J. J. Mayrhofer, I. Katsounaros, *Angew. Chemie Int. Ed.* 2019, 58, 7273–7277. Copyright 2019 Wiley-VCH.

Though it is contentious in some cases [114], in-source electrochemistry or electrochemical systems combining electrochemistry and spray formation controlled by the ionization high voltage represent other variants of real-time EC-MS. However, in most cases the thermodynamic redox potentials can not be investigated as no classical electrochemical cells with three-electrode system are used. Precise control of electrochemical potentials may be difficult in such systems and mechanistic findings have to be transferred to regular electrochemical cells carefully. Because of that only a few applications will be mentioned and not discussed in detail. Pei et al [96] investigated corona discharge-induced reduction of various quinones by negative mode ESI-MS. Cramer et al [97] used in-source reduction for disulfide bond mapping. Wan et al [85] developed a real-time electrochemical reaction platform to monitor

picomole-scale electrosynthetic reactions by nano-ESI-MS. Tang et al [98] used electro-epoxidation in nano-ESI-MS controlled by the spray voltage. By fragmentation in tandem MS the capability to locate double bonds in lipids was demonstrated. He et al [99] investigated the real-time monitoring of electrochemical degradation of ciprofloxacin by electrochemical mass spectrometry. Oxidation and spray formation by high voltage based on a platinum slice electrode placed on an ITO glass chip was used. Another application was demonstrated for dopamine [93] as well as DOPA and adrenaline [94]. Oxidation was either carried out by the ESI spray high voltage of 3 kV or by an integrated electrochemical cell using the stainless-steel electrospray emitter as working electrode and a second stainless-steel capillary as counter electrode that was connected by PTFE tubing. The voltage of the electrochemical cell was supplied by a battery and a variable resistor and the cell voltage was floated on the ESI high voltage [94]. Intermediates were detected in real time with a specified response time of about 3 ms [93,94].

3.2.3 EC-HPLC-MS

Offline and online HPLC-MS and HPLC-MS/MS are often applied to support findings of EC-MS studies. On the other hand, EC-MS is regularly used to optimize oxidation conditions to get the highest possible yields of the products that should be analyzed by consecutive HPLC-MS so that both instrumental approaches are mostly applied in combination. By evaluation of the retention behavior, additional information on the polarities of analytes can be obtained and suppression effects in the ionization source can be avoided. In the following, recent online studies with focus on hyphenation of electrochemistry to chromatographic methods and mass spectrometry are summarized. Karst and coworkers [100] analyzed the oxidative transformation of roxarsone by EC-MS and EC-hydrophilic interaction liquid chromatography (HILIC)-MS using an electrochemical thin-layer cell with boron-doped diamond electrode. ESI and ICP were used as ionization methods. Adduct formation experiments were also carried out. By HILIC polar analytes could be separated using liquid chromatography, which shows the flexibility and universality of modern HPLC techniques. Using ICP-MS additionally to ESI-MS not only identification of organic substances but also speciation and quantification of inorganic constituents is possible. Another study was concerned with reduction of prodrugs based on Pt(IV) in the context of anticancer agents (Figure 3.11) [101]. Electrochemistry was presented as alternative to chemical reducing agents where in some cases the reduction kinetics are very slow. Different platinum complexes were reduced and analyzed by EC-MS, EC-HPLC-ESI-MS and EC-HPLC-ICP-MS.

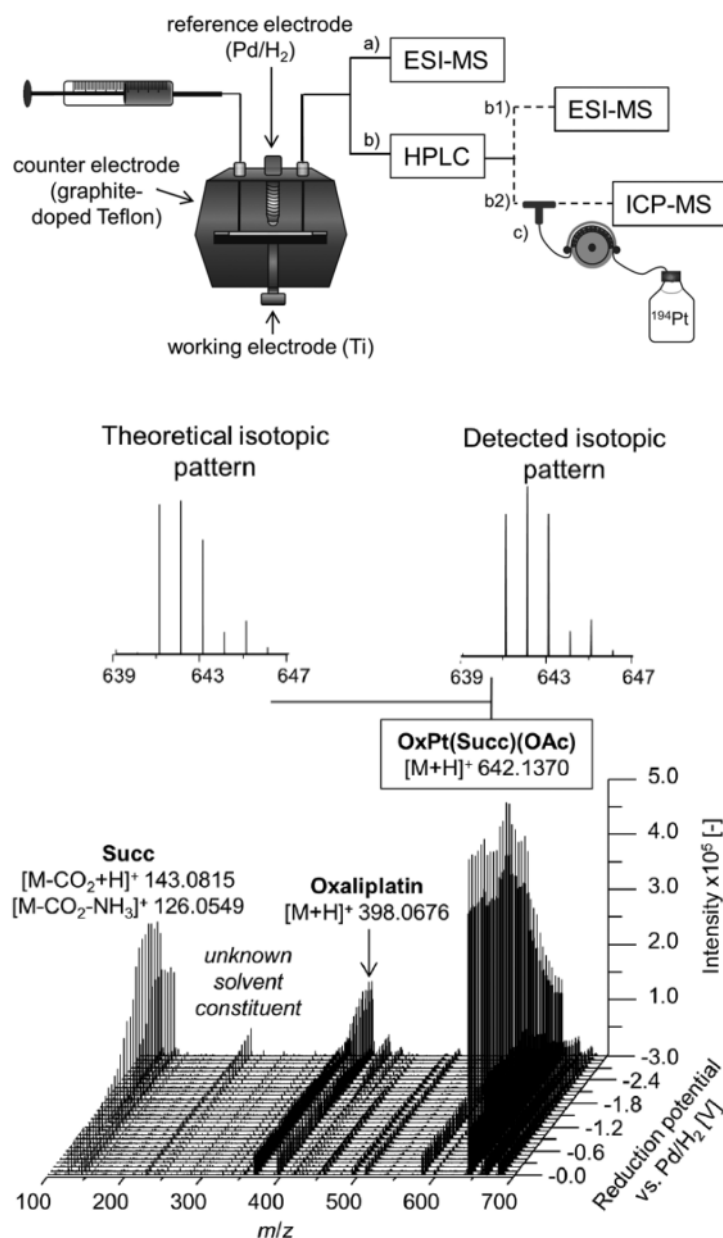


Figure 3.11 Top: Experimental setup used for reduction of Pt(IV) compounds either by EC-ESI-MS (a) or EC-HPLC-ESI-MS (b1)/EC-HPLC-ICP-MS (b2). Bottom: Mass voltammogram obtained for the reduction of OxPt(Succ)(OAc) on a Ti cathode during a potential ramp at a scan rate of 10 mV s⁻¹. Adapted under the terms of the Creative Commons Attribution 3.0 Unported License from L. M. Frensemeier, J. Mayr, G. Koellensperger, B. K. Keppler, C. R. Kowol, U. Karst, *Analyst* 2018, 143, 1997–2001. Copyright 2018 The Authors.

Mekonnen et al [102] developed an automated EC-HPLC-MS method for electrochemical simulation of biotransformation products of the insecticide chlorpyrifos and compared the electrogenerated products with in vitro generated metabolites of rat and human liver microsomes. Six products could be identified with both methods while the authors emphasized the time that could be saved by the instrumental approach due to the missing sample preparation steps (matrix removal). Oxidations were carried out on boron-doped diamond and glassy carbon electrodes and the oxidation potential was optimized by EC-MS. The same group reported the investigation of biotransformation of the fungicide fluopyram [103]. Several known phase I metabolites could be simulated by electrochemical oxidation on a boron-doped diamond electrode, but also new metabolites were predicted by electrochemistry and studies based on

human and rat liver microsomes. Additionally, mechanistic reaction steps were proposed. Xu et al [104] used electrochemical oxidation for quantification in HPLC-MS without the need of standard compounds or calibration curves (electrochemical mass spectrometry) in a dual detection-like method. By evaluating the faradaic current in an LC-EC-MS approach the amount of oxidized analyte could be calculated, and the yield of oxidation was determined by comparing the MS signal before and after electrolysis. No quantitative electrolysis was needed as it would have been the case for coulometric quantification. Applications were demonstrated for determination of dopamine, norepinephrine, rutin, and glutathione as well as uric acid in urine. The same method was used for quantification of tyrosine containing peptides [105]. However, in both cases it is mandatory to know the oxidation mechanism and the number of transferred electrons as well as the number of oxidizable groups of each target molecule. The method was also applied to purified samples where no separation was needed and the sample could directly be analyzed and quantified without separation step [106]. A novel approach to online dual electrochemistry coupled to LC-MS was presented by Karst and coworkers [107]. Two liquid streams were combined for online derivatization of a disulfide reduced to a thiol and a phenol oxidized to a benzoquinone. The coupling products were evaluated by HPLC separation and mass spectrometry. In future studies the concept is intended to be used for online protein labelling. Bischoff and coworkers [108] developed a method for electrochemical digestion of proteins. Next to digestion, chemical labeling of the cleavage products by introduction of reactive spirolactone groups was addressed. Cu(II) ions were used to stabilize spirolactone containing peptides which were subsequently labeled with biotin and enriched by avidin affinity chromatography. Identification was carried out by mass spectrometry. LC-MS measurements after the different reaction steps are shown in Figure 3.12. The method was applied to the analysis of chicken egg white lysozyme. The results show that electrochemical reaction steps can be effectively included into sample preparation and derivatization procedures. Overall it can be stated that various applications of rising complexity are reported. Usually different techniques are combined. The general redox behavior of analytes is often investigated and optimized by EC-MS while HPLC-MS is used for characterization based on the retention behavior and mass of products. Different ionization methods are applied for characterization of organic and inorganic constituents. In most cases methods based on electrochemistry are not used independently but are still compared to conventional methods leading to the conclusion that this field is still not fully established. A vast amount of applications is concerned with metabolic and biomimetic studies and the biggest advantage of electrochemistry is the rather simple setup and well controllable reaction conditions. Compared to regular assays the effort of sample preparation is significantly reduced and timescales of analysis are much shorter.

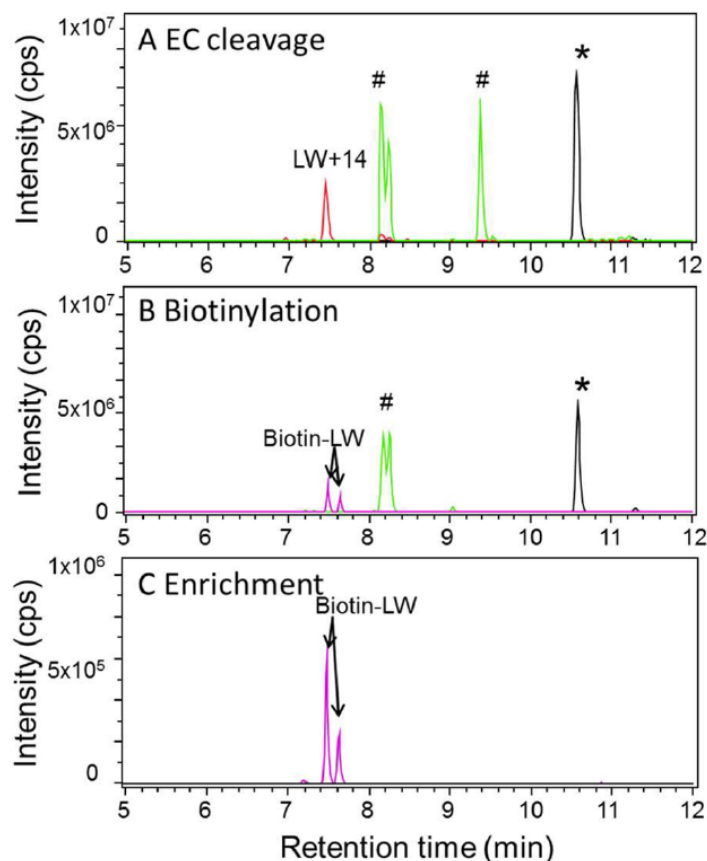


Figure 3.12 (A) LC-MS of the electrochemically digested tripeptide LWL, (B) measurement of the reaction mixture after biotinylation and solid-phase extraction, and (C) measurement of the biotinylated LW+14 fragment after enrichment on monomeric avidin agarose. Extracted ion chromatograms of unoxidized LWL (*, m/z 431.26), uncleaved isomeric oxidation products LWL+32 (#, m/z 463.26), LW+14 (m/z 332.16), and biotinylated LW+14 (m/z 706.37). Reprinted with permission from T. Zhang, M. P. de Vries, H. P. Permentier, R. Bischoff, *Anal. Chem.* 2017, 89, 7123–7129. Copyright 2017 American Chemical Society.

3.2.4 EC-CE-MS

Capillary electrophoresis is a complementary separation method that can be used as an alternative to HPLC. However, it is much less frequently applied. Matysik and coworkers established an online EC-CE-MS system based on direct injection into the CE system from screen-printed electrodes. The capillary tip was directly placed on the working electrode surface for hydrodynamic injection [58,59]. This allows for a fast and efficient transfer of electrochemically pretreated solutions to the separation step without the need of quantitative oxidation or reduction. The approach was limited to aqueous electrolytes due to the screen-printed electrode materials that are not resistant against organic solvents. To extend the applicability to non-aqueous solutions, a miniaturized electrochemical injection cell based on disposable thin-film electrodes was developed and characterized. The instrumental setup is illustrated in Figure 3.13 [109]. Very low amounts of sample (below 10 μL) could be oxidized and characterized online by CE-MS as demonstrated for different ferrocene derivatives [109]. Next to guanosine and 8-oxo-7,8-dihydroguanosine [115] and cyclic nucleotides [116], cytosine [110] and thymine [111] oxidation was investigated by online EC-CE-MS based on screen-printed carbon electrodes. Contrary to HPLC, the same electrolyte can be used for oxidation and separation in the case of CE. This has the

advantage that the migration behavior in CE is representative for the state of charge of the analyte in the electrolyte as no solvent exchange takes place. Physiological conditions can be simulated also in the separation step, which is not possible in reversed-phase HPLC.

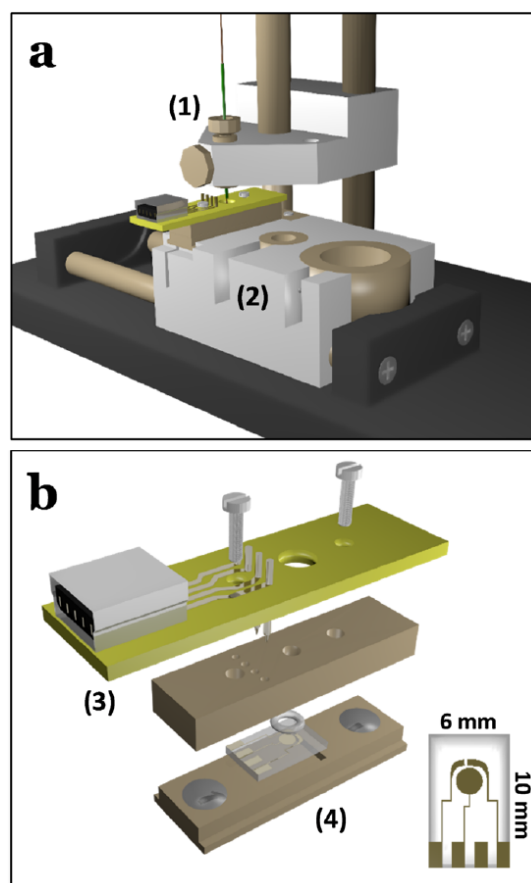


Figure 3.13 EC-CE-MS setup based on an injection cell equipped with disposable thin-film electrodes. (a) Injection device at injection position. The separation capillary (1) is moveable vertically and the base unit with integrated electrochemical injection cell and electrolyte reservoirs (2) is moveable horizontally. (b) Exploded view of the electrochemical injection cell consisting of a cover with electrical contacts (3) and base with electrode slot (4). Reprinted with permission from T. Herl, N. Heigl, F.-M. Matysik, *Monatsh. Chem. - Chem. Mon.* 2018, 149, 1685–1691. Copyright 2018 Springer Nature.

3.2.5 Further studies

In Table 3.2, further recent studies from 2017-2020 are shortly summarized.

Table 3.2 Further EC-MS studies from 2017-2020.

Category	Method	Content	Ref.
Metabolism	EC-MS, EC-HPLC-MS	-Simulation of oxidative metabolism of antitumor-active compounds	[117,118]
Metabolism	EC-MS	-Simulation of oxidative metabolism of nucleosides and nucleotides by EC-ESI-MS	[119]
Metabolism	EC-MS, EC-HPLC-MS	-Simulation of the oxidative metabolism of cardiovascular drugs -Conjugation to glutathione -Comparison to in-vivo experiments	[120,121]
Protein analysis, interfacing	EC-MS	-Disulfide bond electroreduction and tagging by electrochemical-mass spectrometry	[122]
Protein analysis	EC-MS, EC-HPLC-MS	-Disulfide linkage assignment of disulfide-rich peptides by electrochemical reduction on a lead electrode -Alkylation of peptides followed by alkylated peptide sequencing	[123]
Metabolism, degradation, remediation	EC-MS, EC-HPLC-MS	-Simulation of metabolism and degradation of polycyclic aromatic hydrocarbons -Comparison to UV irradiation and microsomal incubation	[124]
Metabolism	EC-MS	-Simulation of enzyme-mediated metabolism processes of phosphatidylethanolamines	[125]
Energy carriers	EC-MS	-Screening of CO ₂ reduction electrocatalysts by scanning flow cell and pervaporator	[126]
Metabolism	EC-HPLC-MS	-Aromatic hydroxylation of lidocaine to 3-hydroxylidocaine at a Pt electrode -Identification of oxygen source by experiments with ¹⁸ O labelled water	[127]

3.3 Summary and outlook

EC-MS is an attractive method for characterization of redox processes and identification of oxidation and reduction products. A vast amount of the EC-MS investigations is concerned with the electrochemical simulation of oxidative metabolism, oxidative stress, or degradation processes. But also, electrochemical sample preparation, for example in the context of corrosion studies, plays an important role. While instrumental setups for EC-MS and EC-HPLC-MS are already established and commercially available, new developments in recent years dealt with interfacing strategies and development of real time analytical systems and electrochemical interfaces combining electrochemistry and ionization for MS. However, potential control and evaluation of thermodynamic redox information is barely possible with such systems, as often two-electrode setups are applied and the potential drop within the ionization system is used for the electrochemical conversion. One crucial part of EC-MS is the identification of oxidation products. Evaluation of the masses and molecular formulas by MS is straightforward but deriving structural features is difficult. EC-MS systems are therefore often combined with separation techniques to obtain additional information on the retention or migration behavior. Tandem MS experiments can be applied to identify structural features by characteristic fragments. However, a lot of valuable data can be obtained this way but in many cases structures can still only be proposed because there is often a lack of analytical standards for comparison. Another difficulty is the low amount of product species generated by EC. Thus, producing enough sample for preparative separation and offline analysis, for example by NMR, is difficult. Especially if long electrolysis times are applied, one significant advantage of EC-MS, the short timescale of analysis, is lost. A lot of follow up reactions of primary oxidation products will take place and the composition of the reaction mixture will change significantly over time, which makes analysis quite complex. This may be a problem especially in studies with biological context as there is often interest in reactive intermediates. In the future, additional techniques for structural identification will be in demand for more detailed characterization of oxidation and reduction products.

In one of the main fields of application, investigations in bioanalytical context, metabolism studies showed that some characteristic processes can be simulated by electrochemistry. Different electrode materials can simulate different mechanisms like direct electron transfer or radical mediated processes. A current trend is that not only oxidation or reduction products are identified to simulate phase I metabolism but also conjugation studies for simulation of phase II metabolism are carried out. Applications of rising complexity are reported, and even dual electrochemical approaches are already established. In more and more investigations, microsomal experiments and toxicity studies of electrochemically generated metabolites are carried out additionally to electrochemical studies so that EC-MS slowly develops from pure proof-of-concept studies to an applied technique in this field. EC-MS is an attractive approach for preliminary screening procedures that can be carried out on a reduced time scale compared to *in vitro* assays and animal studies might be reduced. However, a lot of electrogenerated products are artificial and probably won't be present in *in vivo* metabolism so that

conclusions have to be drawn carefully. One important issue especially for routine and high-throughput analysis is electrode maintenance. Electrodes need to be cleaned and polished properly to avoid artifacts and electrode fouling. This is time-consuming and demands experienced users. The application of disposable electrodes can be attractive in this case as electrodes can in principle be replaced by new ones after each measurement so that a constant performance can be ensured.

While in the past many instrumental developments in electrochemical cells and hyphenation to separation techniques have been established, future developments should deal with more powerful methods for online structural identification such as NMR [128]. Additionally, final steps from proof-of-concept to standardized applications should be done.

References

- [1] H. Faber, M. Vogel, U. Karst, Electrochemistry/mass spectrometry as a tool in metabolism studies—A review, *Anal. Chim. Acta* 834 (2014) 9–21.
- [2] U. Bussy, M. Boujtita, Advances in the Electrochemical Simulation of Oxidation Reactions Mediated by Cytochrome P450, *Chem. Res. Toxicol.* 27 (2014) 1652–1668.
- [3] H. Oberacher, R. Erb, S. Plattner, J.-P. Chervet, Mechanistic aspects of nucleic-acid oxidation studied with electrochemistry-mass spectrometry, *TrAC Trends Anal. Chem.* 70 (2015) 100–111.
- [4] L. Portychová, K.A. Schug, Instrumentation and applications of electrochemistry coupled to mass spectrometry for studying xenobiotic metabolism: A review, *Anal. Chim. Acta* 993 (2017) 1–21.
- [5] P. Liu, M. Lu, Q. Zheng, Y. Zhang, H.D. Dewald, H. Chen, Recent advances of electrochemical mass spectrometry, *Analyst* 138 (2013) 5519.
- [6] H. Oberacher, F. Pitterl, R. Erb, S. Plattner, Mass spectrometric methods for monitoring redox processes in electrochemical cells, *Mass Spectrom. Rev.* 34 (2015) 64–92.
- [7] M. Cindric, F.-M. Matysik, Coupling electrochemistry to capillary electrophoresis-mass spectrometry, *TrAC Trends Anal. Chem.* 70 (2015) 122–127.
- [8] F.T.G. van den Brink, W. Olthuis, A. van den Berg, M. Odijk, Miniaturization of electrochemical cells for mass spectrometry, *TrAC Trends Anal. Chem.* 70 (2015) 40–49.
- [9] A.P. Bruins, An overview of electrochemistry combined with mass spectrometry, *TrAC Trends Anal. Chem.* 70 (2015) 14–19.
- [10] J. Lu, X. Hua, Y.-T. Long, Recent advances in real-time and in situ analysis of an electrode–electrolyte interface by mass spectrometry, *Analyst* 142 (2017) 691–699.
- [11] E.M. Yuill, L.A. Baker, Electrochemical Aspects of Mass Spectrometry: Atmospheric Pressure Ionization and Ambient Ionization for Bioanalysis, *ChemElectroChem* 4 (2017) 806–821.
- [12] M. Elsherbini, T. Wirth, Electroorganic Synthesis under Flow Conditions, *Acc. Chem. Res.* 52 (2019) 3287–3296.
- [13] O. Kasian, S. Geiger, K.J.J. Mayrhofer, S. Cherevko, Electrochemical On-line ICP-MS in Electrocatalysis Research, *Chem. Rec.* 19 (2019) 2130–2142.
- [14] H. Baltruschat, Differential electrochemical mass spectrometry, *J. Am. Soc. Mass Spectrom.* 15 (2004) 1693–1706.
- [15] S. Bruckenstein, R.R. Gadde, Use of a porous electrode for in situ mass spectrometric determination of volatile electrode reaction products, *J. Am. Chem. Soc.* 93 (1971) 793–794.
- [16] O. Wolter, J. Heitbaum, Differential Electrochemical Mass Spectroscopy (DEMS) - a New Method for the Study of Electrode Processes, *Berichte Der Bunsengesellschaft Für Phys. Chemie* 88 (1984) 2–6.
- [17] G. Hambitzer, J. Heitbaum, Electrochemical thermospray mass spectrometry, *Anal. Chem.* 58 (1986) 1067–1070.
- [18] D. Tegtmeier, J. Heitbaum, A. Heindrichs, Electrochemical on line mass spectrometry on a rotating electrode inlet system, *Berichte Der Bunsengesellschaft Für Phys. Chemie* 93 (1989) 201–206.
- [19] K.J. Volk, M.S. Lee, R.A. Yost, A. Brajter-Toth, Electrochemistry/thermospray/tandem mass spectrometry in the study of biooxidation of purines, *Anal. Chem.* 60 (1988) 720–722.
- [20] K.J. Volk, R.A. Yost, A. Brajter-Toth, On-line electrochemistry/thermospray/tandem mass spectrometry as a new approach to the study of redox reactions: the oxidation of uric acid, *Anal. Chem.* 61 (1989) 1709–1717.

- [21] K.J. Volk, R.A. Yost, A. Brajter-Toth, Characterization of solution-phase and gas-phase reactions in on-line electrochemistry—thermospray tandem mass spectrometry, *J. Chromatogr. A* 474 (1989) 231–243.
- [22] K.J. Volk, On-Line Mass Spectrometric Insights Into Electrochemical Reactions: Oxidation of Thiopurines, *J. Electrochem. Soc.* 137 (1990) 1764.
- [23] S.-M. Zhu, A. Brajter-Toth, Liquid chromatographic determination of 6-thiopurine metabolites formed in vitro in electrochemical and enzymatic oxidative activation, *Anal. Chim. Acta* 237 (1990) 305–310.
- [24] K.J. Volk, R.A. Yost, A. Brajter-Toth, Electrochemistry on line with mass spectrometry, *Anal. Chem.* 64 (1992) 21A.
- [25] M. Yamashita, J.B. Fenn, Electrospray ion source. Another variation on the free-jet theme, *J. Phys. Chem.* 88 (1984) 4451–4459.
- [26] G.J. Van Berkel, S.A. McLuckey, G.L. Glish, Electrochemical origin of radical cations observed in electrospray ionization mass spectra, *Anal. Chem.* 64 (1992) 1586–1593.
- [27] F. Charbonnier, C. Rolando, F. Saru, P. Hapiot, J. Pinson, Short time-scale observation of an electrospray current, *Rapid Commun. Mass Spectrom.* 7 (1993) 707–710.
- [28] A.T. Blades, M.G. Ikononou, P. Kebarle, Mechanism of electrospray mass spectrometry. Electrospray as an electrolysis cell, *Anal. Chem.* 63 (1991) 2109–2114.
- [29] G.J. Van Berkel, F. Zhou, Characterization of an Electrospray Ion Source as a Controlled-Current Electrolytic Cell, *Anal. Chem.* 67 (1995) 2916–2923.
- [30] G.J. Van Berkel, F. Zhou, Electrospray as a Controlled-Current Electrolytic Cell: Electrochemical Ionization of Neutral Analytes for Detection by Electrospray Mass Spectrometry, *Anal. Chem.* 67 (1995) 3958–3964.
- [31] A. Dupont, J.-P. Gisselbrecht, E. Leize, L. Wagner, A. Van Dorsselaer, Electrospray mass spectrometry of electrochemically ionized molecules: Application to the study of fullerenes, *Tetrahedron Lett.* 35 (1994) 6083–6086.
- [32] F. Zhou, G.J. Van Berkel, Electrochemistry Combined Online with Electrospray Mass Spectrometry, *Anal. Chem.* 67 (1995) 3643–3649.
- [33] G. Diehl, A. Liesener, U. Karst, Liquid chromatography with post-column electrochemical treatment and mass spectrometric detection of non-polar compounds, *Analyst.* 126 (2001) 288–290.
- [34] Y. Esaka, N. Okumura, B. Uno, M. Goto, Electrophoretic analysis of quinone anion radicals in acetonitrile solutions using an on-line radical generator, *Electrophoresis* 24 (2003) 1635–1640.
- [35] F. Matysik, Electrochemically assisted injection – a new approach for hyphenation of electrochemistry with capillary-based separation systems, *Electrochem. Commun.* 5 (2003) 1021–1024.
- [36] R. Scholz, F.-M. Matysik, A novel approach for the separation of neutral analytes by means of electrochemically assisted injection coupled to capillary electrophoresis-mass spectrometry, *Analyst* 136 (2011) 1562–1565.
- [37] U. Karst, Electrochemistry/Mass Spectrometry (EC/MS)—A New Tool To Study Drug Metabolism and Reaction Mechanisms, *Angew. Chemie Int. Ed.* 43 (2004) 2476–2478.
- [38] J. Gun, S. Bharathi, V. Gutkin, D. Rizkov, A. Voloshenko, R. Shelkov, S. Sladkevich, N. Kyi, M. Rona, Y. Wolanov, D. Rizkov, M. Koch, S. Mizrahi, P. V. Pridkochenko, A. Modestov, O. Lev, Highlights in Coupled Electrochemical Flow Cell-Mass Spectrometry, *EC/MS, Isr. J. Chem.* 50 (2010) 360–373.
- [39] W. Lohmann, A. Baumann, U. Karst, Electrochemistry and LC-MS for Metabolite Generation and Identification: Tools, Technologies, and Trends, *LCGC North Am.* 28 (2010) 470–478.
- [40] I. Stassen, G. Hambitzer, Anodic oxidation of aniline and N-alkylanilines in aqueous sulphuric acid studied by electrochemical thermospray mass spectrometry, *J. Electroanal. Chem.* 440 (1997) 219–228.

- [41] W. Lu, X. Xu, R.B. Cole, On-Line Linear Sweep Voltammetry–Electrospray Mass Spectrometry, *Anal. Chem.* 69 (1997) 2478–2484.
- [42] U. Jurva, H. V. Wikström, A.P. Bruins, In vitro mimicry of metabolic oxidation reactions by electrochemistry/mass spectrometry, *Rapid Commun. Mass Spectrom.* 14 (2000) 529–533.
- [43] M. Krausa, W. Vielstich, Study of the electrocatalytic influence of Pt/Ru and Ru on the oxidation of residues of small organic molecules, *J. Electroanal. Chem.* 379 (1994) 307–314.
- [44] A. Baumann, W. Lohmann, S. Jahn, U. Karst, On-line electrochemistry/electrospray ionization mass spectrometry (EC/ESI-MS) for the generation and identification of nucleotide oxidation products, *Electroanalysis* 22 (2010) 286–292.
- [45] H. Faber, D. Melles, C. Brauckmann, C.A. Wehe, K. Wentker, U. Karst, Simulation of the oxidative metabolism of diclofenac by electrochemistry/(liquid chromatography)/mass spectrometry, *Anal. Bioanal. Chem.* 403 (2012) 345–354.
- [46] L. Telgmann, H. Faber, S. Jahn, D. Melles, H. Simon, M. Sperling, U. Karst, Identification and quantification of potential metabolites of Gd-based contrast agents by electrochemistry/separations/mass spectrometry, *J. Chromatogr. A* 1240 (2012) 147–155.
- [47] S. Jahn, H. Faber, R. Zazzeroni, U. Karst, Electrochemistry/mass spectrometry as a tool in the investigation of the potent skin sensitizer p-phenylenediamine and its reactivity toward nucleophiles, *Rapid Commun. Mass Spectrom.* 26 (2012) 1453–1464.
- [48] W. Lohmann, U. Karst, Electrochemistry meets enzymes: instrumental on-line simulation of oxidative and conjugative metabolism reactions of toremifene, *Anal. Bioanal. Chem.* 394 (2009) 1341–1348.
- [49] H.A. Laitinen, I.M. Kolthoff, Voltammetry with Stationary Microelectrodes of Platinum Wire., *J. Phys. Chem.* 45 (1941) 1061–1079.
- [50] T. Herl, F.-M. Matysik, Characterization of electrochemical flow cell configurations with implemented disposable electrodes for the direct coupling to mass spectrometry, *Tech. Mess.* 84 (2017) 672–682.
- [51] J. Roscher, H. Faber, M. Stoffels, O. Hachmöller, J. Happe, U. Karst, Nonaqueous capillary electrophoresis as separation technique to support metabolism studies by means of electrochemistry and mass spectrometry, *Electrophoresis* 35 (2014) 2386–2391.
- [52] A.A. Abd-El-Latif, C.J. Bondue, S. Ernst, M. Hegemann, J.K. Kaul, M. Khodayari, E. Mostafa, A. Stefanova, H. Baltruschat, Insights into electrochemical reactions by differential electrochemical mass spectrometry, *TrAC Trends Anal. Chem.* 70 (2015) 4–13.
- [53] U. Jurva, H. V. Wikström, L. Weidolf, A.P. Bruins, Comparison between electrochemistry/mass spectrometry and cytochrome P450 catalyzed oxidation reactions, *Rapid Commun. Mass Spectrom.* 17 (2003) 800–810.
- [54] T. Johansson, L. Weidolf, U. Jurva, Mimicry of phase I drug metabolism – novel methods for metabolite characterization and synthesis, *Rapid Commun. Mass Spectrom.* 21 (2007) 2323–2331.
- [55] H.P. Permentier, A.P. Bruins, Electrochemical oxidation and cleavage of proteins with on-line mass spectrometric detection: Development of an instrumental alternative to enzymatic protein digestion, *J. Am. Soc. Mass Spectrom.* 15 (2004) 1707–1716.
- [56] W. Lohmann, U. Karst, Generation and Identification of Reactive Metabolites by Electrochemistry and Immobilized Enzymes Coupled On-Line to Liquid Chromatography/Mass Spectrometry, *Anal. Chem.* 79 (2007) 6831–6839.
- [57] R. Erb, S. Plattner, F. Pitterl, H.-J. Brouwer, H. Oberacher, An optimized electrochemistry-liquid chromatography-mass spectrometry method for studying guanosine oxidation, *Electrophoresis* 33 (2012) 614–621.
- [58] P. Palatzky, F.-M. Matysik, Development and characterization of a novel semiautomated arrangement for electrochemically assisted injection in combination with capillary electrophoresis time-of-flight mass spectrometry, *Electrophoresis* 33 (2012) 2689–2694.

- [59] P. Palatzky, A. Zöpfl, T. Hirsch, F.-M. Matysik, Electrochemically Assisted Injection in Combination with Capillary Electrophoresis-Mass Spectrometry (EAI-CE-MS) - Mechanistic and Quantitative Studies of the Reduction of 4-Nitrotoluene at Various Carbon-Based Screen-Printed Electrodes, *Electroanalysis* 25 (2013) 117–122.
- [60] E.L. Clark, M.R. Singh, Y. Kwon, A.T. Bell, Differential Electrochemical Mass Spectrometer Cell Design for Online Quantification of Products Produced during Electrochemical Reduction of CO₂, *Anal. Chem.* 87 (2015) 8013–8020.
- [61] E.L. Clark, A.T. Bell, Direct Observation of the Local Reaction Environment during the Electrochemical Reduction of CO₂, *J. Am. Chem. Soc.* 140 (2018) 7012–7020.
- [62] S. Shen, Y. Hong, F. Zhu, Z. Cao, Y. Li, F. Ke, J. Fan, L. Zhou, L. Wu, P. Dai, M. Cai, L. Huang, Z. Zhou, J. Li, Q. Wu, S. Sun, Tuning Electrochemical Properties of Li-Rich Layered Oxide Cathodes by Adjusting Co/Ni Ratios and Mechanism Investigation Using in situ X-ray Diffraction and Online Continuous Flow Differential Electrochemical Mass Spectrometry, *ACS Appl. Mater. Interfaces* 10 (2018) 12666–12677.
- [63] J. Mateos-Santiago, M.L. Hernández-Pichardo, L. Lartundo-Rojas, A. Manzo-Robledo, Methanol Electro-Oxidation on Pt–Carbon Vulcan Catalyst Modified with WO_x Nanostructures: An Approach to the Reaction Sequence Using DEMS, *Ind. Eng. Chem. Res.* 56 (2017) 161–167.
- [64] S. Möller, S. Barwe, J. Masa, D. Wintrich, S. Seisel, H. Baltruschat, W. Schuhmann, Online Monitoring of Electrochemical Carbon Corrosion in Alkaline Electrolytes by Differential Electrochemical Mass Spectrometry, *Angew. Chemie Int. Ed.* 59 (2020) 1585–1589.
- [65] B. Pozniak, I. Treufeld, D. Scherson, Hydroxylamine Oxidation on Polycrystalline Gold Electrodes in Aqueous Electrolytes: Quantitative On-Line Mass Spectrometry under Forced Convection, *ChemPhysChem.* 20 (2019) 3128–3133.
- [66] S. Cheng, Q. Wu, H.D. Dewald, H. Chen, Online Monitoring of Methanol Electro-Oxidation Reactions by Ambient Mass Spectrometry, *J. Am. Soc. Mass Spectrom.* 28 (2017) 1005–1012.
- [67] S.-J. Liu, Z.-W. Yu, L. Qiao, B.-H. Liu, Electrochemistry-mass spectrometry for mechanism study of oxygen reduction at water/oil interface, *Sci. Rep.* 7 (2017) 46669.
- [68] C. Gu, X. Nie, J. Jiang, Z. Chen, Y. Dong, X. Zhang, J. Liu, Z. Yu, Z. Zhu, J. Liu, X. Liu, Y. Shao, Mechanistic Study of Oxygen Reduction at Liquid/Liquid Interfaces by Hybrid Ultramicroelectrodes and Mass Spectrometry, *J. Am. Chem. Soc.* 141 (2019) 13212–13221.
- [69] H. Svengren, M. Chamoun, J. Grins, M. Johnsson, Water Splitting Catalysis Studied by using Real-Time Faradaic Efficiency Obtained through Coupled Electrolysis and Mass Spectrometry, *ChemElectroChem* 5 (2018) 44–50.
- [70] P. Khanipour, M. Löffler, A.M. Reichert, F.T. Haase, K.J.J. Mayrhofer, I. Katsounaros, Electrochemical Real-Time Mass Spectrometry (EC-RTMS): Monitoring Electrochemical Reaction Products in Real Time, *Angew. Chemie Int. Ed.* 58 (2019) 7273–7277.
- [71] J. Xu, T. Zhu, K. Chingin, Y. Liu, H. Zhang, H. Chen, Sequential Formation of Analyte Ions Originated from Bulk Alloys for Ambient Mass Spectrometry Analysis, *Anal. Chem.* 90 (2018) 13832–13836.
- [72] L. Song, J. Xu, D. Zhong, K. Chingin, Y. Qu, H. Chen, Rapid detection of metal impurities on the surfaces of intact objects with irregular shapes using electrochemical mass spectrometry, *Analyst* 144 (2019) 3505–3510.
- [73] P. Jovanovič, M. Može, E. Gričar, M. Šala, F. Ruiz-Zepeda, M. Bele, G. Marolt, N. Hodnik, Effect of Particle Size on the Corrosion Behaviour of Gold in the Presence of Chloride Impurities: An EFC-ICP-MS Potentiodynamic Study, *Coatings* 9 (2019) 10.
- [74] P. Jovanovič, A. Pavlišič, V.S. Šelih, M. Šala, N. Hodnik, M. Bele, S. Hočevar, M. Gabersček, New Insight into Platinum Dissolution from Nanoparticulate Platinum-Based Electrocatalysts Using Highly Sensitive In Situ Concentration Measurements, *ChemCatChem* 6 (2014) 449–453.
- [75] P. Jovanovič, V.S. Šelih, M. Šala, N. Hodnik, In situ electrochemical dissolution of platinum and gold in organic-based solvent, *Npj Mater. Degrad.* 2 (2018) 9.

- [76] M. Ledendecker, S. Geiger, K. Hengge, J. Lim, S. Cherevko, A.M. Mingers, D. Göhl, G. V. Fortunato, D. Jalalpoor, F. Schüth, C. Scheu, K.J.J. Mayrhofer, Towards maximized utilization of iridium for the acidic oxygen evolution reaction, *Nano Res.* 12 (2019) 2275–2280.
- [77] O. Kasian, J.-P. Grote, S. Geiger, S. Cherevko, K.J.J. Mayrhofer, The Common Intermediates of Oxygen Evolution and Dissolution Reactions during Water Electrolysis on Iridium, *Angew. Chemie Int. Ed.* 57 (2018) 2488–2491.
- [78] W.D. Looi, L. Chamand, B. Brown, A. Brajter-Toth, Role of Electrochemistry in Desorption Ionization Mass Spectrometry (LS DESI MS) of Aqueous Samples Containing Electrolyte Salts, *Anal. Chem.* 89 (2017) 603–610.
- [79] Z. Wang, Y. Zhang, B. Liu, K. Wu, S. Thevuthasan, D.R. Baer, Z. Zhu, X.-Y. Yu, F. Wang, In Situ Mass Spectrometric Monitoring of the Dynamic Electrochemical Process at the Electrode–Electrolyte Interface: a SIMS Approach, *Anal. Chem.* 89 (2017) 960–965.
- [80] R. Narayanan, P. Basuri, S.K. Jana, A. Mahendranath, S. Bose, T. Pradeep, In situ monitoring of electrochemical reactions through CNT-assisted paper cell mass spectrometry, *Analyst* 144 (2019) 5404–5412.
- [81] A.A. Folgueiras-Amador, K. Philipps, S. Guilbaud, J. Poelakker, T. Wirth, An Easy-to-Machine Electrochemical Flow Microreactor: Efficient Synthesis of Isoindolinone and Flow Functionalization, *Angew. Chemie Int. Ed.* 56 (2017) 15446–15450.
- [82] K. Watts, W. Gattrell, T. Wirth, A practical microreactor for electrochemistry in flow, *Beilstein J. Org. Chem.* 7 (2011) 1108–1114.
- [83] K. Arai, K. Watts, T. Wirth, Difluoro- and Trifluoromethylation of Electron-Deficient Alkenes in an Electrochemical Microreactor, *ChemistryOpen*. 3 (2014) 23–28.
- [84] K. Arai, T. Wirth, Rapid Electrochemical Deprotection of the Isonicotinylxycarbonyl Group from Carbonates and Thiocarbonates in a Microfluidic Reactor, *Org. Process Res. Dev.* 18 (2014) 1377–1381.
- [85] Q. Wan, S. Chen, A.K. Badu-Tawiah, An integrated mass spectrometry platform enables picomole-scale real-time electrosynthetic reaction screening and discovery, *Chem. Sci.* 9 (2018) 5724–5729.
- [86] J. Keller, H. Haase, M. Koch, Electrochemical simulation of biotransformation reactions of citrinin and dihydroergocristine compared to UV irradiation and Fenton-like reaction, *Anal. Bioanal. Chem.* 409 (2017) 4037–4045.
- [87] L. Kotthoff, J. Lisek, T. Schwerdtle, M. Koch, Prediction of Transformation Products of Monensin by Electrochemistry Compared to Microsomal Assay and Hydrolysis, *Molecules* 24 (2019) 2732.
- [88] S. Colombo, G. Coliva, A. Kraj, J.-P. Chervet, M. Fedorova, P. Domingues, M.R. Domingues, Electrochemical oxidation of phosphatidylethanolamines studied by mass spectrometry, *J. Mass Spectrom.* 53 (2018) 223–233.
- [89] C. Kallinich, S. Schefer, S. Rohn, Analysis of Protein-Phenolic Compound Modifications Using Electrochemistry Coupled to Mass Spectrometry, *Molecules* 23 (2018) 264.
- [90] L. Navarro Suarez, S. Thein, C. Kallinich, S. Rohn, Electrochemical Oxidation as a Tool for Generating Vitamin D Metabolites, *Molecules* 24 (2019) 2369.
- [91] L. Zhu, Y. Shao, H. Xiao, B. Santiago-Schübel, H. Meyer-Alert, S. Schiwly, D. Yin, H. Hollert, S. Küppers, Electrochemical simulation of triclosan metabolism and toxicological evaluation, *Sci. Total Environ.* 622–623 (2018) 1193–1201.
- [92] K. Pietruk, M. Piątkowska, M. Olejnik, Electrochemical reduction of azo dyes mimicking their biotransformation to more toxic products, *J. Vet. Res.* 63 (2019) 433–438.
- [93] I. Iftikhar, K.M.A. El-Nour, A. Brajter-Toth, Detection of transient dopamine antioxidant radicals using electrochemistry in electrospray ionization mass spectrometry, *Electrochim. Acta* 249 (2017) 145–154.

- [94] I. Iftikhar, K.M.A. El-Nour, A. Brajter-Toth, DOPA and Adrenaline Oxidation Kinetics and Intermediates Identified by Electrospray Ionization Mass Spectrometry in Real Time, *ChemElectroChem* 5 (2018) 1056–1063.
- [95] F.T.G. van den Brink, T. Zhang, L. Ma, J. Bomer, M. Odijk, W. Olthuis, H.P. Permentier, R. Bischoff, A. van den Berg, Electrochemical Protein Cleavage in a Microfluidic Cell with Integrated Boron Doped Diamond Electrodes, *Anal. Chem.* 88 (2016) 9190–9198.
- [96] J. Pei, C.-C. Hsu, Y. Wang, K. Yu, Corona discharge-induced reduction of quinones in negative electrospray ionization mass spectrometry, *RSC Adv.* 7 (2017) 43540–43545.
- [97] C.N. Cramer, C.D. Kelstrup, J. V. Olsen, K.F. Haselmann, P.K. Nielsen, Generic Workflow for Mapping of Complex Disulfide Bonds Using In-Source Reduction and Extracted Ion Chromatograms from Data-Dependent Mass Spectrometry, *Anal. Chem.* 90 (2018) 8202–8210.
- [98] S. Tang, H. Cheng, X. Yan, On-Demand Electrochemical Epoxidation in Nano-Electrospray Ionization Mass Spectrometry to Locate Carbon-Carbon Double Bonds, *Angew. Chemie Int. Ed.* 59 (2020) 209–214.
- [99] J. He, N. Li, D. Zhang, G. Zheng, H. Zhang, K. Yu, J. Jiang, Real-time monitoring of ciprofloxacin degradation in an electro-Fenton-like system using electrochemical-mass spectrometry, *Environ. Sci. Water Res. Technol.* 6 (2020) 181–188.
- [100] L.M. Frensemeier, L. Büter, M. Vogel, U. Karst, Investigation of the oxidative transformation of roxarsone by electrochemistry coupled to hydrophilic interaction liquid chromatography/mass spectrometry, *J. Anal. At. Spectrom.* 32 (2017) 153–161.
- [101] L.M. Frensemeier, J. Mayr, G. Koellensperger, B.K. Keppler, C.R. Kowol, U. Karst, Structure elucidation and quantification of the reduction products of anticancer Pt(IV) prodrugs by electrochemistry/mass spectrometry (EC-MS), *Analyst* 143 (2018) 1997–2001.
- [102] T.F. Mekonnen, U. Panne, M. Koch, Electrochemistry coupled online to liquid chromatography-mass spectrometry for fast simulation of biotransformation reactions of the insecticide chlorpyrifos, *Anal. Bioanal. Chem.* 409 (2017) 3359–3368.
- [103] T.F. Mekonnen, U. Panne, M. Koch, Prediction of biotransformation products of the fungicide fluopyram by electrochemistry coupled online to liquid chromatography-mass spectrometry and comparison with in vitro microsomal assays, *Anal. Bioanal. Chem.* 410 (2018) 2607–2617.
- [104] C. Xu, Q. Zheng, P. Zhao, J. Paterson, H. Chen, A New Quantification Method Using Electrochemical Mass Spectrometry, *J. Am. Soc. Mass Spectrom.* 30 (2019) 685–693.
- [105] P. Zhao, R.N. Zare, H. Chen, Absolute Quantitation of Oxidizable Peptides by Coulometric Mass Spectrometry, *J. Am. Soc. Mass Spectrom.* 30 (2019) 2398–2407.
- [106] P. Zhao, Y. Guo, H.D. Dewald, H. Chen, Improvements for absolute quantitation using electrochemical mass spectrometry, *Int. J. Mass Spectrom.* 443 (2019) 41–45.
- [107] L. Büter, L.M. Frensemeier, M. Vogel, U. Karst, Dual reductive/oxidative electrochemistry/liquid chromatography/mass spectrometry: Towards peptide and protein modification, separation and identification, *J. Chromatogr. A* 1479 (2017) 153–160.
- [108] T. Zhang, M.P. de Vries, H.P. Permentier, R. Bischoff, Specific Affinity Enrichment of Electrochemically Cleaved Peptides Based on Cu(II)-Mediated Spirolactone Tagging, *Anal. Chem.* 89 (2017) 7123–7129.
- [109] T. Herl, N. Heigl, F.-M. Matysik, Development of a miniaturized injection cell for online electrochemistry–capillary electrophoresis–mass spectrometry, *Monatshfte Für Chemie - Chem. Mon.* 149 (2018) 1685–1691.
- [110] T. Herl, L. Taraba, D. Böhm, F.-M. Matysik, Electrooxidation of cytosine on bare screen-printed carbon electrodes studied by online electrochemistry-capillary electrophoresis-mass spectrometry, *Electrochem. Commun.* 99 (2019) 41–45.

- [111] T. Herl, F.-M. Matysik, Investigation of the Electrooxidation of Thymine on Screen-Printed Carbon Electrodes by Hyphenation of Electrochemistry and Mass Spectrometry, *Anal. Chem.* 92 (2020) 6374–6381.
- [112] B. Liu, X.-Y. Yu, Z. Zhu, X. Hua, L. Yang, Z. Wang, In situ chemical probing of the electrode–electrolyte interface by ToF-SIMS, *Lab Chip.* 14 (2014) 855–859.
- [113] J. Yu, Y. Zhou, X. Hua, S. Liu, Z. Zhu, X.-Y. Yu, Capturing the transient species at the electrode–electrolyte interface by in situ dynamic molecular imaging, *Chem. Commun.* 52 (2016) 10952–10955.
- [114] C. Lübbert, W. Peukert, How to avoid interfering electrochemical reactions in ESI-MS analysis, *J. Mass Spectrom.* 54 (2019) 301–310.
- [115] R. Scholz, P. Palatzky, F.-M. Matysik, Simulation of oxidative stress of guanosine and 8-oxo-7,8-dihydroguanosine by electrochemically assisted injection–capillary electrophoresis–mass spectrometry, *Anal. Bioanal. Chem.* 406 (2014) 687–694.
- [116] M. Cindric, M. Vojs, F.-M. Matysik, Characterization of the Oxidative Behavior of Cyclic Nucleotides Using Electrochemistry-Mass Spectrometry, *Electroanalysis* 27 (2015) 234–241.
- [117] A. Potęga, D. Garwolińska, A.M. Nowicka, M. Fau, A. Kot-Wasik, Z. Mazerska, Phase I and phase II metabolism simulation of antitumor-active 2-hydroxyacridinone with electrochemistry coupled on-line with mass spectrometry, *Xenobiotica* 49 (2019) 922–934.
- [118] A. Potęga, D. Żelaszczyk, Z. Mazerska, Electrochemical simulation of metabolism for antitumor-active imidazoacridinone C-1311 and in silico prediction of drug metabolic reactions, *J. Pharm. Biomed. Anal.* 169 (2019) 269–278.
- [119] S. Studzińska, L. Sיעińska, B. Buszewski, On-line electrochemistry/electrospray ionization mass spectrometry (EC-ESI-MS) system for the study of nucleosides and nucleotides oxidation products, *J. Pharm. Biomed. Anal.* 158 (2018) 416–424.
- [120] M. Szultka-Młyńska, S. Bajkacz, M. Kaca, I. Baranowska, B. Buszewski, Electrochemical simulation of three novel cardiovascular drugs phase I metabolism and development of a new method for determination of them by liquid chromatography coupled with tandem mass spectrometry, *J. Chromatogr. B* 1093–1094 (2018) 100–112.
- [121] M. Szultka-Młyńska, S. Bajkacz, I. Baranowska, B. Buszewski, Structural characterization of electrochemically and in vivo generated potential metabolites of selected cardiovascular drugs by EC-UHPLC/ESI-MS using an experimental design approach, *Talanta* 176 (2018) 262–276.
- [122] F. Mao, K. Yu, J. He, Q. Zhou, G. Zhang, W. Wang, N. Li, H. Zhang, J. Jiang, Real-time monitoring of electroreduction and labelling of disulfide-bonded peptides and proteins by mass spectrometry, *Analyst* 144 (2019) 6898–6904.
- [123] L. Cui, Y. Ma, M. Li, Z. Wei, Q. Fei, Y. Huan, H. Li, L. Zheng, Disulfide linkage assignment based on reducing electrochemistry and mass spectrometry using a lead electrode, *Talanta* 199 (2019) 643–651.
- [124] T. Wigger, A. Seidel, U. Karst, Electrochemistry coupled to (LC-)MS for the simulation of oxidative biotransformation reactions of PAHs, *Chemosphere* 176 (2017) 202–211.
- [125] S. Colombo, G. Coliva, A. Kraj, J.-P. Chervet, M. Fedorova, P. Domingues, M.R. Domingues, Oxidative metabolism of phosphatidylethanolamines predicted by electrochemistry-mass spectrometry, *Free Radic. Biol. Med.* 108 (2017) S62.
- [126] Y. Lai, R.J.R. Jones, Y. Wang, L. Zhou, J.M. Gregoire, Scanning Electrochemical Flow Cell with Online Mass Spectroscopy for Accelerated Screening of Carbon Dioxide Reduction Electrocatalysts, *ACS Comb. Sci.* 21 (2019) 692–704.
- [127] T. Gul, R. Bischoff, H.P. Permentier, Mechanism of aromatic hydroxylation of lidocaine at a Pt electrode under acidic conditions, *Electrochim. Acta* 224 (2017) 636–641.
- [128] D. Falck, W.M.A. Niessen, Solution-phase electrochemistry-nuclear magnetic resonance of small organic molecules, *TrAC Trends Anal. Chem.* 70 (2015) 31–39.

4. Experimental

In this chapter, an overview of the most important chemicals, materials, and instruments is given. Instrumental setups and general procedures are shortly described. Exact details of the conducted experiments are given in the respective chapters in the results section.

4.1 Materials and instruments

4.1.1 Chemicals

In Table 4.1, the most important chemicals used in the experiments are listed in alphabetical order. Purity was analytical grade or higher, if not stated otherwise. Aqueous solutions were prepared using Milli-Q water ($18 \text{ M}\Omega \text{ cm}^{-1}$) provided by a Milli-Q Advantage A10 system (Merck Millipore, Darmstadt, Germany). Non-aqueous solutions were degassed at 50 mbar for 30 min prior to use. The exact solution specifications used in the single experiments are described in the respective chapters in the results section.

Table 4.1 List of most important chemicals

Substance	Abbreviation	Supplier
Acetic acid, glacial	HOAc	Sigma-Aldrich, St. Louis, MO, USA
Acetonitrile	ACN	Merck, Darmstadt, Germany
Ammonia, 25%	NH ₃	Merck, Darmstadt, Germany
Ammonium acetate	NH ₄ OAc	Merck, Darmstadt, Germany
Ammonium hydrogencarbonate	NH ₄ HCO ₃	Roth, Karlsruhe, Germany
Caffeine, 99%	Caff	ABCR, Karlsruhe, Germany
Cytosine, $\geq 99\%$	Cyt	Sigma-Aldrich, St. Louis, MO, USA
Decamethylferrocene, 99%	dMFC	ABCR, Karlsruhe, Germany
di-Sodium hydrogenphosphate	Na ₂ HPO ₄	Merck, Darmstadt, Germany
Ferrocene, 98%	Fc	Riedel-de-Haën, Seelze, Germany
Ferrocenemethanol, 99%	FcMeOH	ABCR, Karlsruhe, Germany
Formic acid, 98-100%	FA	Merck, Darmstadt, Germany
Hydrochloric acid, 1 M	HCl	Merck, Darmstadt, Germany
Hydrochloric acid, conc.	HCl	Merck, Darmstadt, Germany
Isopropanol	iPrOH	Roth, Karlsruhe, Germany
Sodium carbonate	Na ₂ CO ₃	Roth, Karlsruhe, Germany
Sodium dihydrogenphosphate	NaH ₂ PO ₄	Merck, Darmstadt, Germany
Sodium hydrogencarbonate	NaHCO ₃	Merck, Darmstadt, Germany
Sodium hydroxide, 0.1 M	NaOH	Merck, Darmstadt, Germany
Thymine, $\geq 99\%$	Thy	Sigma-Aldrich, St. Louis, MO, USA

4.1.2 Consumables

In Table 4.2 the most important consumables are listed:

Table 4.2 List of consumables

Consumable	Supplier
Fused silica capillary, ID 25 μm , OD 360 μm	Polymicro Technologies, Phoenix, AZ, USA
Fused silica capillary, ID 50 μm , OD 360 μm	Polymicro Technologies, Phoenix, AZ, USA
Screen-printed carbon electrode, DRP-110	DropSens, Llanera, Spain
Gold thin-film electrode, ED-SE1-Au	Micrux Technologies, Oviedo, Spain
Platinum thin-film electrode, ED-SE1-Pt	Micrux Technologies, Oviedo, Spain

4.1.3 Instruments

In Table 4.3, the most important commercially available instruments used in this thesis are summarized.

Table 4.3 List of instruments

Instrument	Supplier
μ Autolab III potentiostat	Metrohm Autolab B. V., Utrecht, The Netherlands
μ Stat 200 potentiostat	DropSens, Llanera, Spain
PalmSens 3 potentiostat	PalmSens BV, Houten, The Netherlands
Coulochem II potentiostat	ESA Biosciences Inc., Chelmsford, USA
Lambda 1010 UV/VIS detector	Bischoff Analysentechnik und -geräte GmbH, Leonberg, Germany
MicrOTOF mass spectrometer	Bruker Daltonics, Bremen, Germany
Type A-99 syringe pump	Razel Scientific Instruments, Saint Albans, VT, USA
Microinjection syringe pump	World Precision Instruments, Sarasota, FL, USA
Type 601553 syringe pump	KD Scientific, Holliston, MA, USA
Flow cell, model FLWCL	DropSens, Llanera, Spain
Flow cell, model ED-FLOW-CELL	Micrux Technologies, Oviedo, Spain

4.1.4 Software

All software used for data evaluation and presentation is listed in Table 4.4:

Table 4.4 List of software

Software	Supplier
NOVA 2.0	Metrohm Autolab B. V., Utrecht, The Netherlands
DropView	DropSens, Llanera, Spain
PSTrace 4.6	PalmSens BV, Houten, The Netherlands
MicrOTOF Control 2.3	Bruker Daltonics, Bremen, Germany
Compass DataAnalysis 4.0	Bruker Daltonics, Bremen, Germany
Microsoft Office 365	Microsoft Corporation, Redmond, WA, USA
Origin 2018	OriginLab Corporation, Northampton, MA, USA
Blender 3D Creation Suite	Blender Foundation, Amsterdam, The Netherlands

4.1.5 Handling of capillaries

Fused silica capillaries were cut to the desired length by carving the polyimide coating with a ceramic cutter and carefully breaking the capillary. During preparation, the capillaries were flushed with water by applying pressure with a syringe via a septum. The polyimide coating was removed at the capillary tips with a micro torch and remaining particles were removed with a razorblade and a soft cloth soaked with isopropanol. The capillary tips were polished using a laboratory-constructed polishing machine and micro abrasive sheets (Precision Surfaces International, Houston, TX, USA) with a grain size of 30 μm for rough polishing and 9 μm for fine polishing. The detection end of the capillaries was polished to a planar edge. The injection end was polished to a planar edge for EC-MS measurements and to an angle of 15° for EC-CE-MS measurements, as illustrated in Figure 4.1.

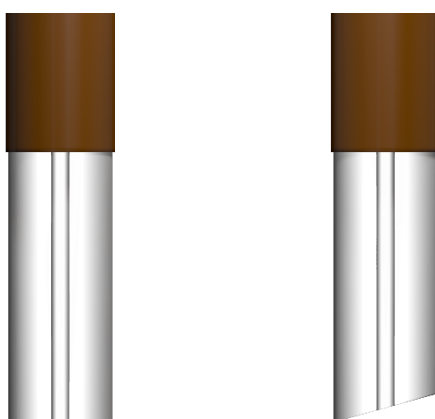


Figure 4.1 Illustration of polished capillary tips at the injection end for EC-MS (left) and EC-CE-MS (right).

Prior to measurements, the capillaries were conditioned by flushing with 0.1 M NaOH for 10 min, followed by Milli-Q water for 5 min, and separation buffer for at least 30 min. When not in use, capillaries were flushed with water.

4.1.6 Handling of electrodes

Screen-printed carbon electrodes (SPCEs, DRP-110, DropSens, Llanera, Spain), thin-film gold electrodes (ED-SE1-Au, Micrux Technologies, Oviedo, Spain), and thin-film platinum electrodes (ED-SE1-Pt, Micrux Technologies, Oviedo, Spain) were used during the experiments. The SPCEs exhibited a carbon WE, a carbon AE, and a silver quasi-RE. The thin-film electrodes had all electrode structures fabricated from gold or platinum, respectively. All electrodes were used as received without particular cleaning or pretreatment protocols. Screen-printed electrodes were flushed with water and dried with nitrogen between measurements. Thin-film electrodes were washed with water or isopropanol and dried with nitrogen. Due to the electrode materials, screen-printed electrodes were limited to the application in aqueous solvents, as the carbon inks were not solvent-resistant. Thin-film electrodes were solvent-resistant and could therefore be used in acetonitrile-based media. Figure 4.2 shows a comparison of the different electrodes.

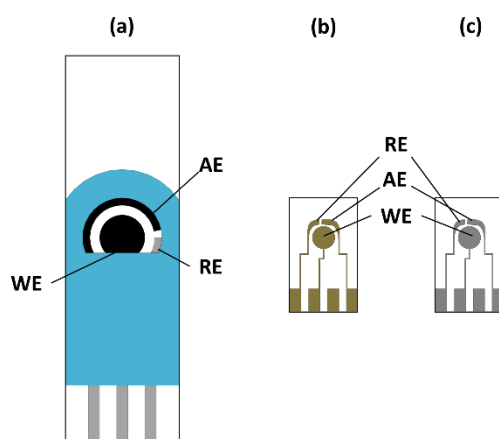


Figure 4.2 Drawings of a screen-printed carbon electrode (a), a thin-film gold electrode (b), and a thin-film platinum electrode (c). The relative sizes are shown to scale. Working electrode (WE), auxiliary electrode (AE), and quasireference electrode (RE) are marked.

4.1.7 Mass spectrometer configuration

A micrOTOF time-of-flight mass spectrometer (Bruker Daltonics, Bremen, Germany) was used as mass selective detector in most measurements. It was equipped with a coaxial sheath liquid electrospray ionization (ESI) interface (Agilent Technologies, Waldbronn, Germany). A fused silica capillary with an outer diameter of 360 μm was installed in the center of the sprayer. A sheath liquid flow was added with a syringe pump (KD Scientific, Holliston, MA, USA) in order to enhance the flow rate for the formation of a stable spray and to close the electrical circuit between the CE effluent and the grounded stainless-steel sprayer. A nebulizer gas supported spray formation and solvent evaporation. To monitor the quality of the electrospray, the ESI source was equipped with a microscope camera (DigiMicro 1.3, dnt, Dietzenbach, Germany) and a laboratory-constructed laser illumination. Thus, spray conditions could be optimized during operation based on the MS signals and optical feedback.

4.2 Instrumentation and methods

4.2.1 Instrumental setup for EC-MS

EC-MS measurements were carried out by direct coupling of electrochemical flow cells with integrated disposable electrodes to MS. The solutions to be investigated were filled into a 1 mL glass syringe and transported to the respective flow cell with a syringe pump. A PEEK capillary was used to connect syringe and flow cell. The effluent of the flow cell was guided to the ESI interface of the MS system via a fused silica capillary. The exact details of the flow cell configuration are described in [1]. The capillary was installed via PEEK fittings and capillary sleeves for 360 μm OD capillaries (Upchurch Scientific, Oak Harbor, WA, USA). A general scheme of the setup is depicted in Figure 4.3. Three different flow cells were available. Commercially available polymethylmethacrylate (PMMA) flow cells by DropSens (model FLWCL, DropSens, Llanera, Spain) and Micrux (model ED-FLOW-CELL, Micrux Technologies, Oviedo, Spain) were suitable for measurements of aqueous samples. To facilitate measurement of non-aqueous solutions, a flow cell with a polyetheretherketone (PEEK) cover, based on the Micrux-type flow cell, was manufactured by the fine-mechanical and electronic workshops of the University of Regensburg. During EC-MS measurements, the sample was continuously infused to the flow cell at a constant flow rate. A constant potential pulse or a potential sweep were applied after a certain period of time and the oxidation products were detected by mass spectrometry. Further details can be found in the respective chapters of the results section.

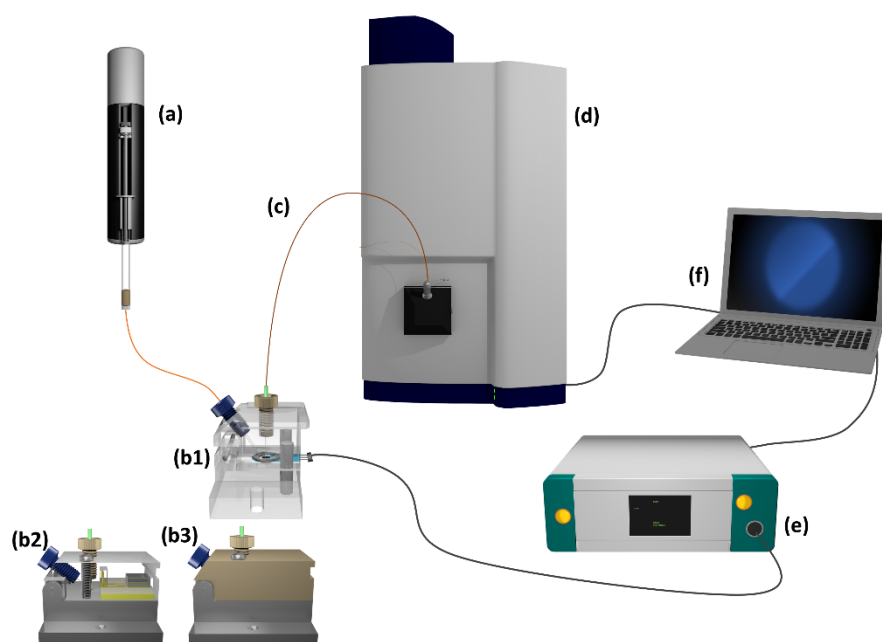


Figure 4.3 General setup for EC-MS measurements. Syringe pump (a), PMMA flow cell for DropSens electrodes (b1), PMMA flow cell for Micrux electrodes (b2), PEEK flow cell for Micrux electrodes (b3), fused silica capillary (c), time-of-flight mass spectrometer (d), potentiostat (e), computer (f).

4.2.2 Instrumental setup for EC-CE-MS

EC-CE-MS measurements were carried out with a fully automated injection device developed by Matysik and coworkers [2]. It consisted of a bottom part with a slot for electrode and buffer reservoirs, which was moveable horizontally, and a top part with a PEEK fitting (Upchurch Scientific) for installation of the capillary, which was moveable vertically. Both were controlled by servo motors and the injection sequence was programmed by a software developed by the electronic workshop of the University of Regensburg. The beveled injection end of the capillary was positioned directly onto the working electrode surface of screen-printed or thin-film electrodes for hydrodynamic sample injection. The injection device and an enlarged view of the injection position are schematically shown in Figure 4.4. A scheme of the general setup for EC-CE-MS is depicted in Figure 4.5. The electrode potential was controlled by a potentiostat. High-voltage was applied by an external high-voltage source. A time-of-flight mass spectrometer equipped with a coaxial sheath liquid electrospray ionization interface was used as detector. All parts of the setup that were in contact with high voltage were placed in a PMMA box for safety reasons. EC-CE-MS measurements were carried out as follows: The sample solution was placed onto the electrode. A constant oxidation potential was applied for a certain period of time. At the end of the oxidation, the capillary tip was placed directly on the center of the working electrode surface while the oxidation potential was still applied. Sample injection took place hydrodynamically by a difference in height between the injection end and the detection end of the capillary and the suction pressure of the ESI interface. After injection, the capillary was automatically moved back into the buffer reservoir, the potentiostat was plugged off, and the separation voltage was applied. Further experimental details are described in the respective parts of the results section.

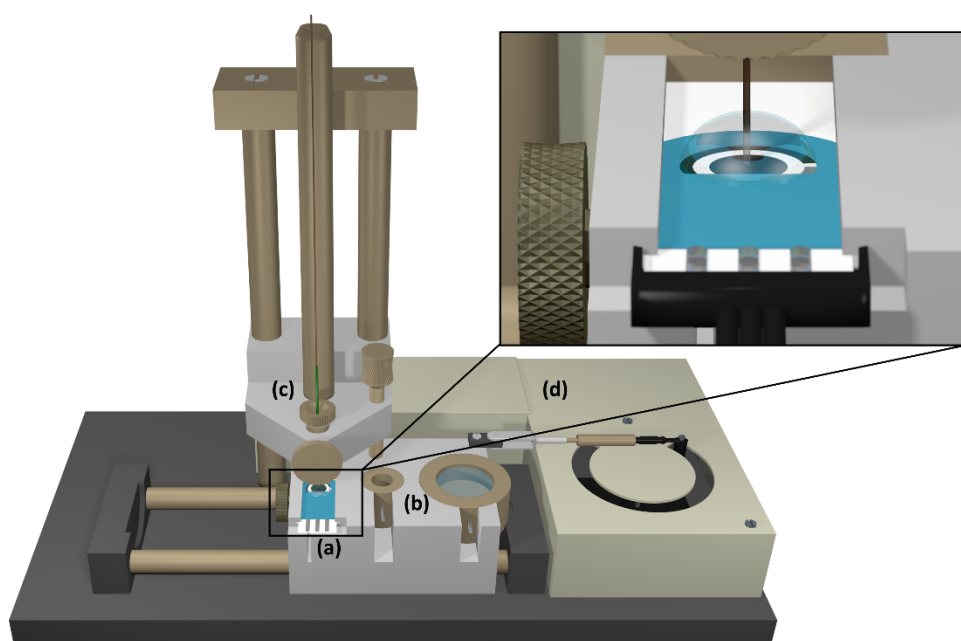


Figure 4.4 Illustration of the fully automated injection device for EC-CE-MS measurements. The inset shows a closer look at the injection position of the capillary tip on the working electrode surface. Screen-printed electrode (a), buffer reservoirs (b), capillary installed in PEEK fitting (c), housing for servo motors (d).

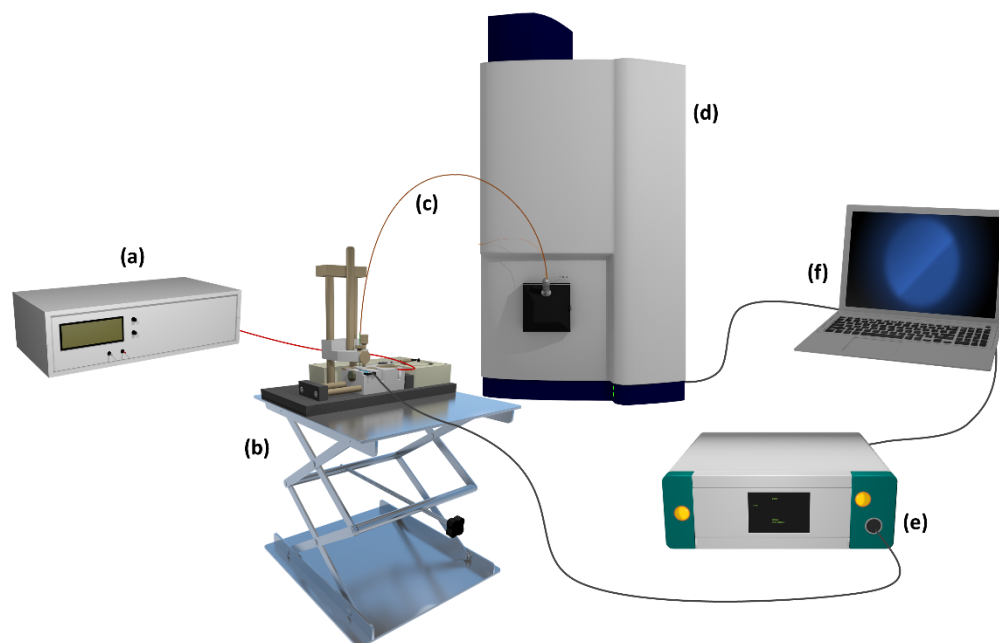


Figure 4.5 Setup for EC-CE-MS measurements. High-voltage source (a), injection device with integrated disposable electrode and buffer reservoirs (b), fused silica capillary (c), time-of-flight mass spectrometer (d), potentiostat (e), computer (f).

References

- [1] T. Herl, F.-M. Matysik, Characterization of electrochemical flow cell configurations with implemented disposable electrodes for the direct coupling to mass spectrometry, *Tech. Mess.* 84 (2017) 672-682.
- [2] P. Palatzky, A. Zöpfl, T. Hirsch, F.-M. Matysik, Electrochemically Assisted Injection in Combination with Capillary Electrophoresis-Mass Spectrometry (EAI-CE-MS) - Mechanistic and Quantitative Studies of the Reduction of 4-Nitrotoluene at Various Carbon-Based Screen-Printed Electrodes, *Electroanalysis* 25 (2013) 117-122.

5. Results and discussion

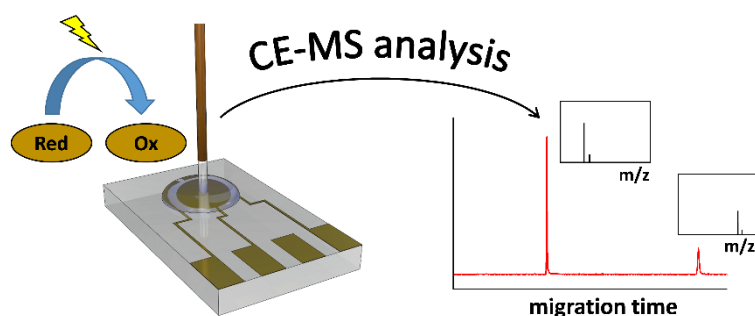
5.1 Development of a miniaturized injection cell for online electrochemistry-capillary electrophoresis-mass spectrometry

This chapter was published in the journal *Monatshefte für Chemie - Chemical Monthly*. The layout specifications of the journal were changed for uniformity. Copyright 2018 Springer Nature.

T. Herl, N. Heigl, F.-M. Matysik, *Monatsh. Chem.* **2018**, *149*, 1685-1691.

Abstract

The elucidation of oxidation or reduction pathways is important for the electrochemical characterization of compounds of interest. In this context, hyphenation of electrochemistry and mass spectrometry is frequently applied to identify products of electrochemical reactions. In this contribution, the development of a novel miniaturized injection cell for online electrochemistry-capillary electrophoresis-mass spectrometry (EC-CE-MS) is presented. It is based on disposable thin-film electrodes, which allow for high flexibility and fast replacement of electrode materials. Thus, high costs and time-consuming maintenance procedures can be avoided, which makes this approach interesting for routine applications. The cell was designed to be suitable for investigations in aqueous and particularly non-aqueous solutions making it a universal tool for a broad range of analytical problems. EC-CE-MS measurements of different ferrocene derivatives in non-aqueous solutions were carried out to characterize the cell. Oxidation products of ferrocene and ferrocenemethanol were electrochemically generated and could be separated from the decamethylferricenium cation. The importance of fast CE-MS analysis of instable oxidation products was demonstrated by evaluating the signal of the ferriceniummethanol cation depending on the time gap between electrochemical generation and detection.



5.1.1 Introduction

Electrochemical methods are of high relevance in many fields of research. They are essential tools for studies in the context of material sciences such as corrosion studies [1], the development of energy carriers [2], microbial fuel cells [3], or electrosynthetic processes [4]. Electrochemistry is also widely applied in bioanalytical studies such as the electrochemical simulation of oxidative stress [5–8] or metabolic processes [9–17].

Pure electrochemical investigations such as cyclic voltammetry are well suited for the characterization of redox activities and reversibility of redox processes [18], but lack of qualitative information regarding mechanistic details. Thus, hyphenation to powerful detection techniques is in demand to obtain additional information on processes taking place on the electrode surface. In this context, hyphenation of electrochemistry (EC) to electrospray ionization-mass spectrometry (ESI-MS) is a frequently applied method, as recent reviews point out [16, 19]. ESI-MS offers high sensitivity and the possibility of identifying products of electrochemical reactions by their molecular masses and isotopic patterns with low fragmentation in the ionization process [20]. Thus, this technique can help in the elucidation of possible reaction mechanisms. However, EC and ESI have to be decoupled as electrochemical cells are operated at low voltages, while in ESI high-voltage conditions are applied [21]. This can be achieved by using setups with grounded ESI interfaces [22].

Typical approaches to EC-MS comprise the direct coupling of electrochemical flow cells such as coulometric flow-through cells with porous electrodes or thin-layer flow cells with planar electrodes to mass spectrometry [4, 19, 23, 24]. Furthermore, efforts towards miniaturized setups using microfluidic electrochemical cells and nanoscale electrochemical reactors were made [25]. The advantage of such an approach is the simplicity of the experimental setup and the possibility of very fast detection within seconds [26], as the analytes are directly transported to MS via pumps. However, based on the cell type, the dependence of the conversion efficiency on the flow rate and the electrode surface area has to be kept in mind [23, 24]. An innovative approach to EC as online sample preparation technique for ESI-MS was developed by Dyrťová et al [27], who coupled an electrochemical cell with switchable working electrodes to ESI-MS in order to ionize even non-polar organic compounds by adduct formation with electrochemically generated reactive metallic ions.

However, there are also some limitations of direct EC-MS. In complex samples, additional separation steps are necessary, as ion suppression effects in the ion source of MS can influence the detection, especially if mixtures of products are formed or if product and educt species show significant differences in their ionization properties. Thus, a quantification of oxidation or reduction products is difficult. Overlapping mass spectra can prevent the clear identification of individual species. Moreover, the separation behavior can give important additional information on the analytes, such as the presence of functional groups or polarity.

Hyphenation to separation techniques is often achieved by coupling EC to HPLC via electrochemical flow cells installed prior to or after the separation column [7, 13, 24]. However, the instrumental setups for this purpose are quite complex as different pumps and valves are needed, if EC is carried out before HPLC [19]. Another disadvantage that can arise is the compatibility between the conditions needed for electrochemical reactions and the separation conditions [13]. Contrary to direct EC-MS, the time gap between formation and detection of products is longer if a separation step is carried out after oxidation or reduction. Typical analysis times are in the range of several minutes [7, 14, 23]. Working with reversed phase HPLC-MS it has to be considered that non-polar analytes are usually favored for HPLC, but polar analytes are better compatible to ESI-MS conditions [28].

Due to the aspects mentioned above, capillary electrophoresis (CE) is the method to be preferred in some cases. It offers fast separation and low solvent consumption [29, 30] and is suitable for separation of charged species. Thus, it is an ideal separation method for many biomolecules that contain functional groups which can be protonated or deprotonated depending on pH. In contrast to HPLC, separations are possible under nearly physiological conditions [5] and can be carried out in the same electrolyte as the oxidation or reduction, so that the migration behavior in CE is representative for the state of charge of the analytes in the electrolyte. Due to the charge-dependent migration behavior, CE allows for differentiation between ions, which are generated by electrochemical processes and ions generated in the ionization prior to MS detection. This information can not be obtained in direct EC-MS or EC-HPLC-MS.

First online EC-CE approaches were established in 2003 [31, 32] using batch electrolysis cells and classical three-electrode setups. Thus, they had the disadvantage of time-consuming electrode maintenance procedures, which are necessary to avoid electrode fouling and require experienced users. Additionally, a comparably high sample volume is needed. In contrast to that, Palatzky et al. [33] developed a fully automated device for online EC-CE-MS based on disposable screen-printed electrodes (SPEs). Hence, compared to classical cells, significantly lower sample consumption (about 50 μL is sufficient), easy replacement of electrodes avoiding time-consuming cleaning and polishing procedures, and high flexibility concerning electrode materials could be achieved. The electrochemical cell consisted of a droplet of solution placed onto the three-electrode structure of the electrode and sample injection into the CE-system was achieved by placing the separation capillary into this droplet directly above the working electrode. However, this system was not compatible to non-aqueous solutions due to the screen-printed electrode materials, which is a major drawback when it comes to the investigation of analytes that are not readily soluble or stable [31] in water.

This contribution presents an instrumental approach to online EC-CE-MS with disposable electrodes, which is applicable under non-aqueous conditions. It is based on the existing fully automated EAI-CE-MS device described in [33]. To allow for investigations in non-aqueous solutions, different problems had to be addressed. As already mentioned above, screen-printed electrodes are attacked by organic

solvents, so that alternative electrode types had to be used. Commercially available solvent-resistant thin-film electrodes are fabricated of metal electrode materials on glass substrates instead of carbon inks and thus are ideal for this purpose [26]. However, simply applying droplets of solution onto the electrode surface as it could be done with aqueous solutions [5, 33] was not possible, as organic solvents easily spread due to low surface tension. This can lead to electrical shortcuts and corrosion problems, when the liquid flows into electrical contacts. Therefore, the cell volume had to be delimited physically in order to prevent spreading of the liquid. To overcome these problems, a novel miniaturized injection cell for online EC-CE-MS with integrated thin-film electrodes was developed, capable of measurements in aqueous and especially non-aqueous media. A model mixture consisting of ferrocene (Fc), ferrocenemethanol (FcMeOH), and dcamethylferrocene (dMFC) was used to characterize this injection cell. The importance of short separation times was demonstrated by evaluation of the dependency of FcMeOH⁺ signal on the separation time.

5.1.2 Experimental

Reagents and chemicals

The following chemicals were used, all of analytical grade or higher if not stated otherwise: acetic acid (Sigma Aldrich, MO, USA), acetonitrile, ammonium acetate (both Merck, Darmstadt, Germany), dcamethylferrocene (purity 99%, ABCR, Karlsruhe, Germany), formic acid (Merck, Darmstadt, Germany), ferrocene (purity 98%, Riedel-de-Haën, Seelze, Germany), ferrocenemethanol (purity 99%, ABCR, Karlsruhe, Germany), isopropanol (Roth, Karlsruhe, Germany).

Instrumentation

For EC-CE-MS measurements, the fully automated CE system developed by Palatzky et al. [33] was used. The setup was installed in a plexiglass box and connected to a high voltage supply (HCN 7E 35000, FuG Elektronik, Schechen, Germany). A micrOTOF time-of-flight mass spectrometer (Bruker Daltonics, Bremen, Germany), equipped with a coaxial sheath liquid ESI interface (Agilent Technologies, Waldbronn, Germany), was used for detection. It was operated in positive ion mode. A mixture of isopropanol:water:formic acid (49.9:49.9:0.2, v:v:v) was added as sheath liquid at a flow rate of 8 $\mu\text{L min}^{-1}$ with a syringe pump (KS Scientific, Holliston, MA, USA). Separations were carried out in fused silica capillaries (Polymicro Technologies, AZ, USA) with an outer diameter of 360 μm , an inner diameter of 25 μm , and a length of 35 cm. The detection end of the capillary was polished to a plane edge while the injection end of the capillary was polished to an angle of 15°. The capillaries were preconditioned by flushing with 0.1 mol dm⁻³ NaOH for 10 min, followed by water for 5 min and background electrolyte (BGE) for CE separation (ACN/10 mmol dm⁻³ NH₄OAc/1 mol dm⁻³ HOAc) for at least 30 min. A thin-film electrode with gold working, counter, and quasireference electrode (ED-SE1-Au, Micrux Technologies, Oviedo, Spain) was used for the oxidation. All potentials given are referred to the Au quasireference electrode and all electrochemical measurements were carried out in

ACN/10 mmol dm⁻³ NH₄OAc/1 mol dm⁻³ HOAc as BGE. The electrode was installed in the novel injection cell described in detail in the results and discussion section. A μ STAT 200 potentiostat (DropSens, Llanera, Spain) controlled by Dropview 200 software was used for applying potentials. A schematic illustration of the experimental setup is depicted in Figure 5.1.1.

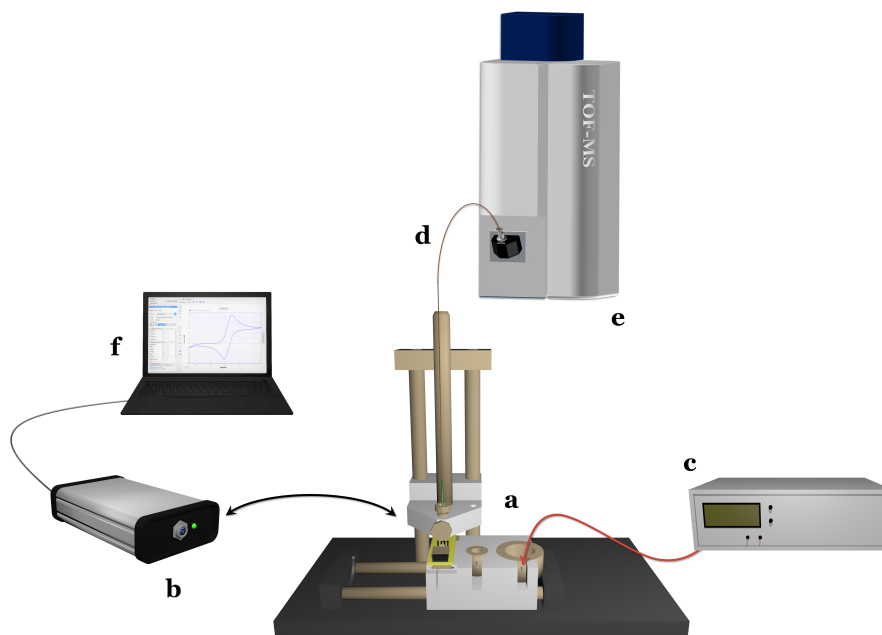


Figure 5.1.1 Illustration of the instrumental setup used for EC-CE-MS measurements: (a) injection unit with novel injection cell and electrolyte reservoirs, (b) potentiostat, (c) high voltage source, (d) fused silica capillary, (e) mass spectrometer, (f) computer.

Experimental procedures

For evaluation of the cell performance, a solution of 1.5 mmol dm⁻³ Fc, 1 mmol dm⁻³ FcMeOH, and 40 μ mol dm⁻³ dMFC in BGE was used. Fast detection studies were carried out with a solution of 1 mmol dm⁻³ FcMeOH in BGE. For the CE protocol, 8 mm³ of sample solution were filled into the cell. The sample was hydrodynamically injected into the CE system by placing the tapered end of the separation capillary onto the working electrode surface for 2 s at a difference in height of 18 cm between the injection end of the capillary and the detection end of the capillary (hydrostatic pressure). After the injection, the capillary was automatically placed into the 2 mL BGE reservoir and the separation voltage denoted in detail in the respective measurements in the results section was applied. Measurements were carried out without previous oxidation and after oxidation at 0.5 V for 10 s (injection during the last 2 s of oxidation). For data evaluation the extracted ion signals of Fc (m/z 186.01), FcMeOH (m/z 199.02; m/z 216.02), and dMFC (m/z 326.20) were used.

The parameters for the MS detection were as follows: Acquisition: ion polarity: positive; mass range: 100-350 m/z ; spectra rate 5 Hz; Source: end plate offset: -500 v; capillary: -4000 V; nebulizer: 1.0 bar; dry gas: 4.0 L/min; dry temperature: 190 °C; Transfer: capillary exit: 75.0 V; skimmer 1: 25.3 V;

hexapole 1: 23.0 V; hexapole RF: 65.0 Vpp; skimmer 2: 23.0 V; lens 1 transfer: 38.0 μ s; lens 1 pre pulse storage: 6.0 μ s.

5.1.3 Results and discussion

Design and fabrication of the injection cell

The developed injection cell was based on commercial Micrux thin-film electrodes (size 10 mm x 6 mm, working electrode diameter 1 mm). The cell geometry was adapted to the existing EC-CE-MS setup [33] to allow for the usage of thin-film electrodes without changing the injection unit. Instead of a SPE, the injection cell with integrated thin-film electrode was installed in the injection unit. Due to electrode and cell dimensions, small sample volumes of only 10 μ L or lower were sufficient for EC-CE-MS measurements, which is especially advantageous if only limited amount of sample is available. A schematic illustration of the final injection cell prototype is shown in Figure 5.1.2.

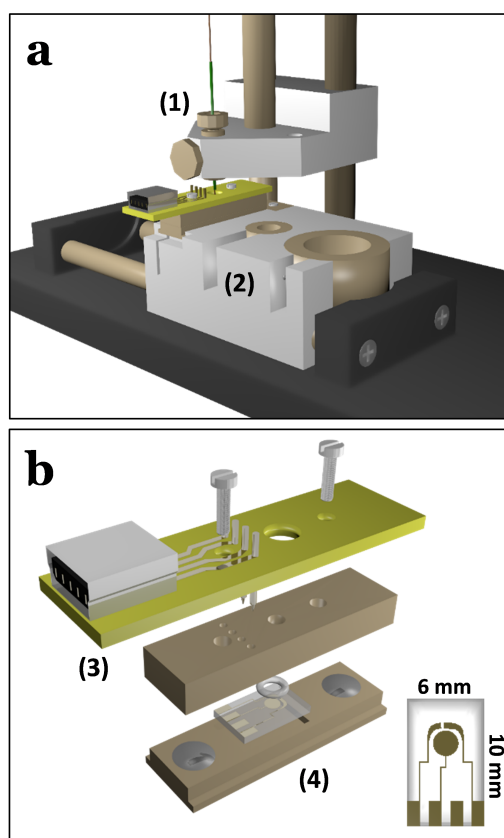


Figure 5.1.2 Illustrations of (a) the injection cell in the setup at injection position and (b) exploded view of injection cell. The cell is installed in the bottom part (2) of the EC-CE-MS device next to buffer reservoirs for CE separation. The separation capillary (1) is installed in the top part. The injection cell consists of a bottom piece (4) with electrode slot and a cover piece (3) with electrical contacts. A silicone sealing ring prevents leakage of the sample.

Polyether ether ketone (PEEK), a highly chemical resistant and mechanically stable material, was used for fabrication of the cell body. To prevent leakage, a sealing ring was integrated at the bottom of the open cell chamber. Thus, spreading of droplets could be avoided. As commercially available O-ring materials were attacked by organic solvents, a custom silicone sealing ring with appropriate dimensions

(inner diameter 2 mm, outer diameter 4 mm, thickness 1 mm) was prepared. The electrical contact to the implemented thin-film electrode was achieved via spring contact probes. To facilitate a fast assembling and disassembling of the cell, magnets were integrated to keep the cell closed. Due to materials and modularity of the cell it could be cleaned easily and was suitable for measurements in aqueous as well as non-aqueous solutions. Electrodes could easily be exchanged, which allowed for high flexibility regarding electrode materials. When installed in the EC-CE-MS device, a fully automated hydrodynamic injection of sample directly from the working electrode surface was possible by placing the tapered tip of the fused silica separation capillary onto the electrode surface. The overall experimental setup is illustrated in Figure 5.1.1 in the experimental section.

EC-CE-MS experiments

By CE-MS, a fast separation and detection of neutral and particularly cationic species was possible applying a positive high voltage at the injection end of the capillary (detection end of capillary installed in grounded ESI sprayer). Figure 5.1.3a shows a CE-MS measurement that was carried out at a separation voltage of 18 kV (2.4 μ A) without previous oxidation using a model mixture of Fc, FcMeOH, and dMFC. The three model substances showed different behavior regarding state of charge and detectability. In the case of dMFC, the migration behavior in CE and the respective mass detected in MS indicated that only the cationic dMFC⁺ (m/z 326.20) was present in solution even without electrochemical oxidation. This is because in dMFC Fe(II) is easily oxidized to Fe(III) by dissolved oxygen forming a stable cationic complex [32, 34]. This behavior is well known as already reported in 1990 by Bashkin and Kinlen [35]. FcMeOH was migrating with the EOF, showing that it was neutral in solution. The detected mass (m/z 199.02) indicated a loss of the hydroxyl group during the ionization process, whereas no protonation or oxidation in the ESI source could be observed under the applied conditions. Non-oxidized Fc could not be detected due to its hydrophobicity and thus poor ionization efficiency in ESI. Unlike Dyrtrtová et al [36], who used a NaClO₄/HClO₄ electrolyte, we could not observe a protonation or oxidation of Fc in solution or in the ESI source. In contrast to dMFC, Fc and FcMeOH exhibited no peaks corresponding to cationic species in CE separation without previous electrochemical oxidation. By electrochemical oxidation at 0.5 V for 10 s, the cationic ferricenium (m/z 186.01) and ferriceniummethanol species (m/z 216.02) were formed, as could be confirmed by the m/z values and the migration behavior in CE. A representative electropherogram is shown in Figure 5.1.3b. Fc⁺ and FcMeOH⁺ were migrating to the cathode faster than dMFC⁺. The results demonstrated the importance of CE separation: The migration behavior in CE and the comparison of the electropherograms before and after oxidation facilitated the distinction between cationic species that are present in solution and species formed in the ionization process, which is not possible without separation step.

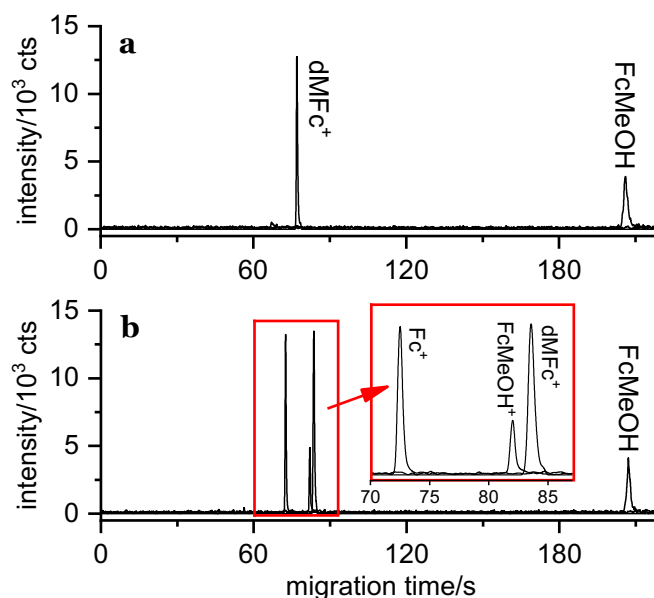


Figure 5.1.3 Electropherograms of the model mixture Fc, FcMeOH and dMFC without oxidation (a) and after oxidation at 0.5 V for 10 s (b). The inset in (b) shows an enlarged view of the separated cationic species $dMFC^+$ (m/z 326.20), $FcMeOH^+$ (m/z 216.02) and Fc^+ (m/z 186.01). The migration time of FcMeOH marks the EOF. Before oxidation, only $dMFC^+$ and FcMeOH (m/z 199.02) were visible. After oxidation, additional peaks of $FcMeOH^+$ and Fc^+ were present. Separation voltage 18 kV (2.4 μ A); capillary: ID = 25 μ m, L = 35 cm; separation in ACN/10 mmol dm^{-3} NH_4OAc /1 mmol dm^{-3} HOAc; 2 s hydrodynamic injection.

The results showed that electrochemical sample pretreatment and online analysis of oxidation products could be achieved within a short time scale. Very short oxidation times of only 10 s (injection during last 2 s of oxidation) were enough to generate a sufficient amount of product species for detection. The electrochemical generation and detection of Fc^+ and $FcMeOH^+$ were feasible within 90 s and both were separated from $dMFC^+$.

Fast online analysis of oxidation products

Besides high-throughput aspects, short analysis times are crucial for the investigation of reactive or instable species in order to allow for a reliable identification and sensitive detection. To demonstrate that, the detection of $FcMeOH^+$ was investigated depending on the separation conditions. As in the case of FcMeOH both, the cationic and the neutral species were detectable, the peak of neutral FcMeOH could be used as internal standard for characterization of the analytical performance. The time gap between generation and detection of $FcMeOH^+$ was varied by changing the separation voltage and thus the migration time. Representative electropherograms measured after oxidation are illustrated in Figure 5.1.4. As visible in the measurements, the ratio of the $FcMeOH^+$ peak to the FcMeOH peak continuously increased with higher separation voltage meaning faster migration. This indicated the decomposition of the cation over time, as after longer migration less amount of cation could be detected. As depicted in Figure 5.1.4a, the detection of both species took quite long and the signal corresponding to the cationic species was comparably small when applying a separation voltage of 2 kV, while at a separation voltage of 18 kV, a fast detection, narrow peaks and a high intensity of the $FcMeOH^+$ peak were observed as shown in Figure 5.1.4e.

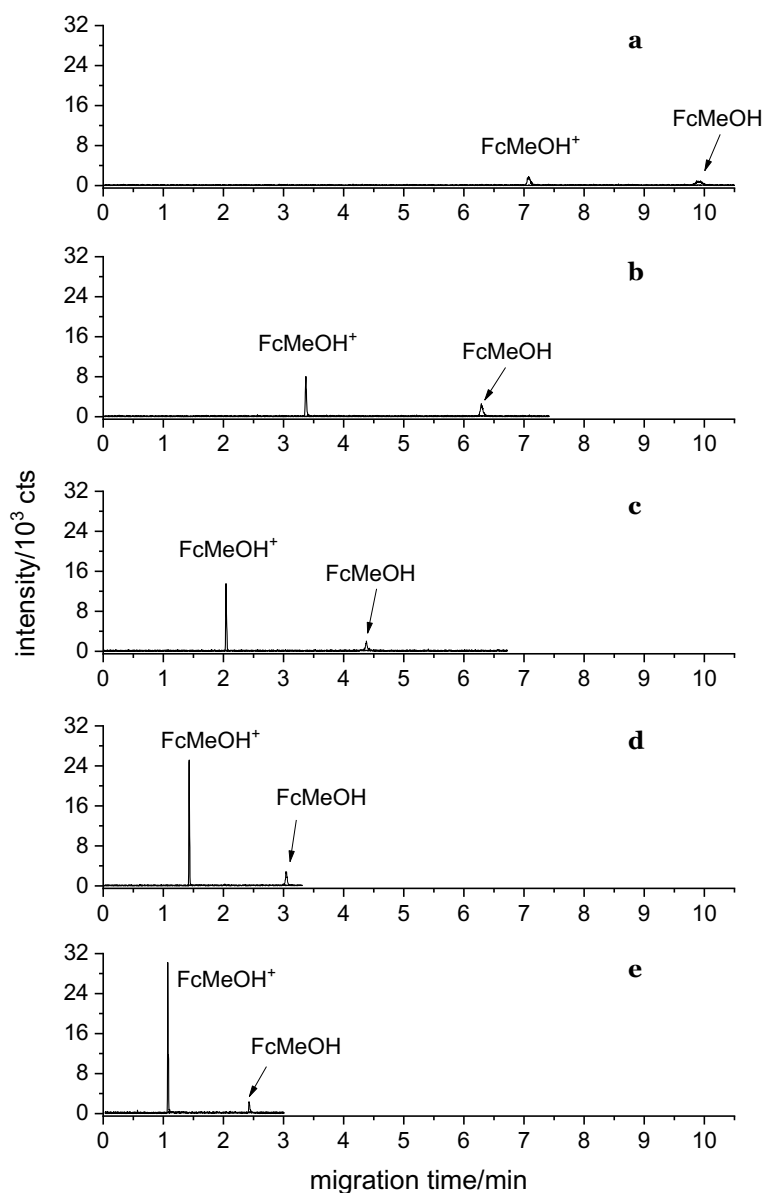


Figure 5.1.4 EC-CE-MS measurements of FcMeOH (m/z 199.02, 216.02) after oxidation at 0.5 V for 10 s. Separations were carried out at different separation voltages: (a) 2 kV (0.7 μ A), (b) 6 kV (1.3 μ A), (c) 10 kV (1.8 μ A), (d) 14 kV (2.1 μ A), (e) 18 kV (2.4 μ A). Capillary: ID = 25 μ m, L = 35 cm; separation in ACN/10 mmol dm⁻³ NH₄OAc/1 mmol dm⁻³ HOAc; 2 s hydrodynamic injection.

Further evaluation of the experimental data led to the results illustrated in Figure 5.1.5. The peak area obtained for FcMeOH⁺ normalized to the peak area corresponding to FcMeOH was plotted versus the migration time of the respective FcMeOH⁺ peak. Due to the fully automated oxidation and injection procedures, the measurements showed a good reproducibility regarding migration times and amount of cation formed. The time between generation and detection of FcMeOH⁺ could precisely be controlled by the high voltage. At short migration times, a significantly larger signal for the cationic species was obtained, so that the sensitivity of the system could be enhanced by applying higher separation voltages. These results indicate that this method is promising for sensitive detection of instable oxidation or reduction products due to the possibility of fast online analysis.

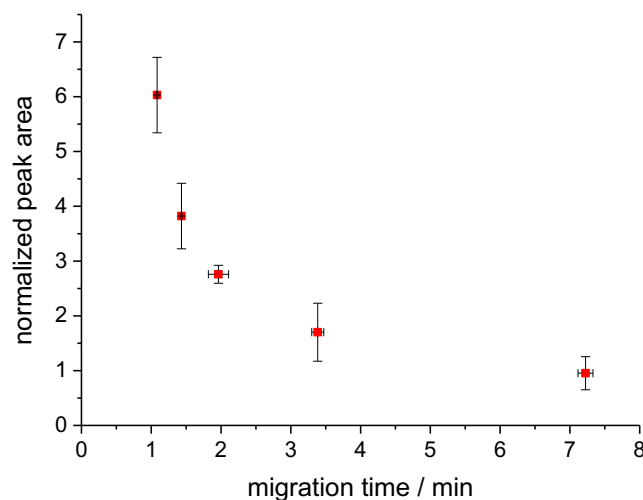


Figure 5.1.5 Peak area of FcMeOH^+ (normalized to the peak area of the FcMeOH signal) vs. migration time of FcMeOH^+ . The migration times were controlled by the separation voltages of 18, 14, 10, 6, and 2 kV (from left to right). The standard deviations of migration times and peak ratios ($n = 3$) are indicated by error bars.

5.1.4 Conclusion

A miniaturized injection cell for online EC-CE-MS was developed and characterized. It was capable of handling very small sample volumes of 10 μL or lower. Electrodes and injection cell were solvent-resistant, so that online investigations of electrochemical reactions in aqueous and particularly non-aqueous media were possible. The integration of disposable thin-film electrodes leads to a high flexibility in electrode materials and to an easy exchange of electrodes, which is minimizing artifacts due to adsorption or electrode fouling. Time-consuming electrode maintenance procedures that usually need experienced users can be avoided. In online EC-CE-MS using ferrocene derivatives, short analysis times within few minutes from generation to detection of oxidized species were possible. Fc^+ and FcMeOH^+ could be generated and separated from dMFC^+ within less than 90 s. Due to that, the method is suitable for the investigation of instable products, which was demonstrated by evaluating the signal of electrochemically generated FcMeOH^+ depending on separation speed. Fully automated oxidation and injection procedures allowed for reproducible measurements and a reliable control of the time gap between formation and detection of oxidized species.

In conclusion, this novel setup extends the applicability of online EC-CE-MS based on disposable electrodes to analytes that are only soluble in organic solvents, which was not possible using screen-printed electrodes. The high flexibility and possibility of fast online analysis make this setup attractive for further applications, such as kinetic studies or electrochemical simulation of metabolic processes with particular focus on reactive species.

References

- [1] F. Arjmand, A. Adriaens, Microcapillary electrochemical droplet cells: Applications in solid-state surface analysis, *J. Solid State Electrochem.* 18 (2014) 1779–1788.
- [2] S. Chandrasekaran, J.S. Chung, E.J. Kim, S.H. Hur, Advanced Nano-Structured Materials for Photocatalytic Water Splitting, *J. Electrochem. Sci. Technol.* 7 (2016) 1–12.
- [3] A.D. Tharali, N. Sain, W.J. Osborne, Microbial fuel cells in bioelectricity production, *Front. Life Sci.* 9 (2016) 252–266.
- [4] T. Gul, R. Bischoff, H.P. Permentier, Electrosynthesis methods and approaches for the preparative production of metabolites from parent drugs, *TrAC Trends Anal. Chem.* 70 (2015) 58–66.
- [5] R. Scholz, P. Palatzky, F.-M. Matysik, Simulation of oxidative stress of guanosine and 8-oxo-7,8-dihydroguanosine by electrochemically assisted injection–capillary electrophoresis–mass spectrometry, *Anal. Bioanal. Chem.* 406 (2014) 687–694.
- [6] M. Cindric, M. Vojs, F.-M. Matysik, Characterization of the Oxidative Behavior of Cyclic Nucleotides Using Electrochemistry-Mass Spectrometry, *Electroanalysis* 27 (2015) 234–241.
- [7] R. Erb, S. Plattner, F. Pitterl, H.-J. Brouwer, H. Oberacher, An optimized electrochemistry-liquid chromatography-mass spectrometry method for studying guanosine oxidation, *Electrophoresis* 33 (2012) 614–621.
- [8] A. Baumann, W. Lohmann, S. Jahn, U. Karst, On-line electrochemistry/electrospray ionization mass spectrometry (EC/ESI-MS) for the generation and identification of nucleotide oxidation products, *Electroanalysis* 22 (2010) 286–292.
- [9] U. Karst, Electrochemistry/Mass Spectrometry (EC/MS)—A New Tool To Study Drug Metabolism and Reaction Mechanisms, *Angew. Chem. Int. Ed.* 43 (2004) 2476–2478.
- [10] U. Jurva, H. V. Wikström, A.P. Bruins, In vitro mimicry of metabolic oxidation reactions by electrochemistry/mass spectrometry, *Rapid Commun. Mass Spectrom.* 14 (2000) 529–533.
- [11] U. Jurva, H. V. Wikström, L. Weidolf, A.P. Bruins, Comparison between electrochemistry/mass spectrometry and cytochrome P450 catalyzed oxidation reactions, *Rapid Commun. Mass Spectrom.* 17 (2003) 800–810.
- [12] T. Johansson, L. Weidolf, U. Jurva, Mimicry of phase I drug metabolism – novel methods for metabolite characterization and synthesis, *Rapid Commun. Mass Spectrom.* 21 (2007) 2323–2331.
- [13] H. Faber, M. Vogel, U. Karst, Electrochemistry/mass spectrometry as a tool in metabolism studies—A review, *Anal. Chim. Acta* 834 (2014) 9–21.
- [14] E. Nouri-Nigjeh, H.P. Permentier, R. Bischoff, A.P. Bruins, Lidocaine Oxidation by Electrogenerated Reactive Oxygen Species in the Light of Oxidative Drug Metabolism, *Anal. Chem.* 82 (2010) 7625–7633.
- [15] T. Yuan, H. Permentier, R. Bischoff, Surface-modified electrodes in the mimicry of oxidative drug metabolism, *TrAC Trends Anal. Chem.* 70 (2015) 50–57.
- [16] U. Bussy, R. Boisseau, C. Thobie-Gautier, M. Boujtita, Electrochemistry-mass spectrometry to study reactive drug metabolites and CYP450 simulations, *TrAC Trends Anal. Chem.* 70 (2015) 67–73.
- [17] U. Jurva, L. Weidolf, Electrochemical generation of drug metabolites with applications in drug discovery and development, *TrAC Trends Anal. Chem.* 70 (2015) 92–99.
- [18] A.J. Bard, L.R. Faulkner, *Electrochemical Methods: Fundamentals and Applications*, 2nd ed., Wiley & Sons, Hoboken, NJ, 2001.
- [19] L. Portychová, K.A. Schug, Instrumentation and applications of electrochemistry coupled to mass spectrometry for studying xenobiotic metabolism: A review, *Anal. Chim. Acta* 993 (2017) 1–21.

- [20] J.B. Fenn, M. Mann, C.K. Meng, S.F. Wong, C.M. Whitehouse, Electrospray ionization for mass spectrometry of large biomolecules, *Science* 246 (1989) 64–71.
- [21] F. Zhou, G.J. Van Berkel, Electrochemistry Combined Online with Electrospray Mass Spectrometry, *Anal. Chem.* 67 (1995) 3643–3649.
- [22] P. Liu, Q. Zheng, H.D. Dewald, R. Zhou, H. Chen, The study of electrochemistry with ambient mass spectrometry, *TrAC Trends Anal. Chem.* 70 (2015) 20–30.
- [23] W. Lohmann, A. Baumann, U. Karst, Electrochemistry and LC–MS for Metabolite Generation and Identification: Tools, Technologies, and Trends, *LCGC N. Am.* 28 (2010) 470–478.
- [24] A.P. Bruins, An overview of electrochemistry combined with mass spectrometry, *TrAC Trends Anal. Chem.* 70 (2015) 14–19.
- [25] F.T.G. van den Brink, W. Olthuis, A. van den Berg, M. Odijk, Miniaturization of electrochemical cells for mass spectrometry, *TrAC Trends Anal. Chem.* 70 (2015) 40–49.
- [26] T. Herl, F.-M. Matysik, Characterization of electrochemical flow cell configurations with implemented disposable electrodes for the direct coupling to mass spectrometry, *Tech. Mess.* 84 (2017) 672–682.
- [27] J. Jaklová Dyrtrtová, M. Jakl, T. Navrátil, J. Cvačka, O. Pačes, An electrochemical device generating metal ion adducts of organic compounds for electrospray mass spectrometry, *Electrochim. Acta* 211 (2016) 787–793.
- [28] G. Diehl, A. Liesener, U. Karst, Liquid chromatography with post-column electrochemical treatment and mass spectrometric detection of non-polar compounds, *Analyst* 126 (2001) 288–290.
- [29] X. Wang, K. Li, E. Adams, A. Van Schepdael, Capillary electrophoresis-mass spectrometry in metabolomics: the potential for driving drug discovery and development., *Curr. Drug Metab.* 14 (2013) 807–813.
- [30] J.J.P. Mark, P. Piccinelli, F.-M. Matysik, Very fast capillary electrophoresis with electrochemical detection for high-throughput analysis using short, vertically aligned capillaries, *Anal. Bioanal. Chem.* 406 (2014) 6069–6073.
- [31] Y. Esaka, N. Okumura, B. Uno, M. Goto, Electrophoretic analysis of quinone anion radicals in acetonitrile solutions using an on-line radical generator, *Electrophoresis* 24 (2003) 1635–1640.
- [32] F. Matysik, Electrochemically assisted injection – a new approach for hyphenation of electrochemistry with capillary-based separation systems, *Electrochem. Commun.* 5 (2003) 1021–1024.
- [33] P. Palatzky, A. Zöpfl, T. Hirsch, F.-M. Matysik, Electrochemically Assisted Injection in Combination with Capillary Electrophoresis-Mass Spectrometry (EAI-CE-MS) - Mechanistic and Quantitative Studies of the Reduction of 4-Nitrotoluene at Various Carbon-Based Screen-Printed Electrodes, *Electroanalysis* 25 (2013) 117–122.
- [34] A. Singh, D.R. Chowdhury, A. Paul, A kinetic study of ferrocenium cation decomposition utilizing an integrated electrochemical methodology composed of cyclic voltammetry and amperometry, *Analyst* 139 (2014) 5747–5754.
- [35] J.K. Bashkin, P.J. Kinlen, Oxygen-Stable Ferrocene Reference Electrodes, *Inorg. Chem.* 29 (1990) 4507–4509.
- [36] J.J. Dyrtrtová, M. Jakl, T. Navrátil, D. Schröder, A hyphenation of stripping voltammetry with electrospray ionization mass spectrometry; An effect of sodium perchlorate on ferrocene oxidation, *Int. J. Electrochem. Sci.* 8 (2013) 1623–1634.

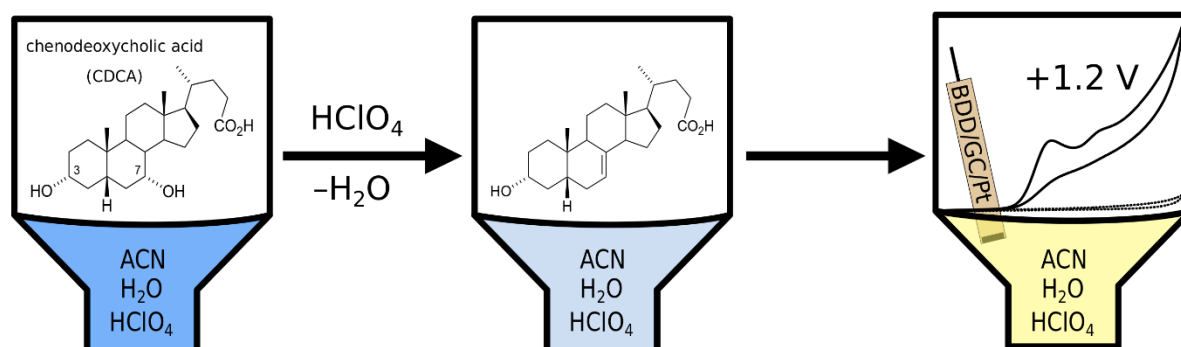
5.2 Bile acids: Electrochemical oxidation on bare electrodes after acid-induced dehydration

This chapter was published in the journal *Electrochemistry Communications*. The layout specifications of the journal were changed for uniformity. Copyright 2017 Elsevier B. V.

J. Klouda, J. Berek, P. Kočovský, T. Herl, F.-M. Matysik, K. Nesměrák, K. Schwarzová-Pecková, *Electrochem. Commun.* **2018**, *86*, 99-103.

Abstract

Bile acids and sterols in general have long been considered practically inactive for direct redox processes. Herein, a novel way of electrochemical oxidation of primary bile acids is reported, involving an initial acid-induced dehydration step, as confirmed by capillary electrophoresis – mass spectrometry, thereby extending the electrochemical activity of the steroid core. Oxidation potentials were found to be ca +1.2 V vs. Ag/AgNO₃ in acetonitrile on boron doped diamond, glassy carbon, and platinum electrodes in a mixed acetonitrile-aqueous medium employing perchloric acid as a chemical reagent, and as a supporting electrolyte for the voltammetric measurements. The chemical step proved to be effective only for primary bile acids, possessing an axial 7 α -hydroxyl group, which is a prerequisite for providing a well-developed voltammetric signal. Preliminary results show that other steroids, *e.g.*, cholesterol, can also be oxidized by employing a similar approach.



5.2.1 Introduction

Biosynthesis of the bile acids (BAs) is an important pathway for the metabolism and excretion of cholesterol in mammals [1]. Depending on the place of formation, literature discerns primary BAs, which originate in the liver, and secondary BAs that are formed by bacterial transformation of the primary BAs in the gut [2]. The most common primary BAs in humans are cholic (**1**; CA) and chenodeoxycholic (**2**; CDCA) acids.

The lack of double bonds or any fluorescent or electrochemically active groups in the molecules of BAs significantly limits the range of methods useful for their determination [3]. Gas chromatography after derivatization and HPLC in combination with mass spectrometry are commonly utilized for quantitation of individual BAs [4–6]. Other methods are based on detection of the products of enzymatic reactions, frequently using 3 α -hydroxysteroid dehydrogenase as the key enzyme [7]. Electrochemical biosensors detecting the enzymatically generated NADH [8,9] or hydrogen peroxide [10] represent another strategy. Other reports on utilization of electrochemical methods for quantitation of BAs are scarce, as shown in our recent review [11]. BAs give electrochemical signal on mercury electrodes at far negative potentials [12,13], presumably as a result of catalytic hydrogen evolution from the carboxyl group in the side chain. Alternatively, electrooxidation has been reported in studies employing chromatographic separation with pulsed amperometric detection on gold [14,15] or porous graphite electrodes [16]. These studies, however, are mainly focused on the chromatographic aspects of the methods, rather than on the electrochemical processes themselves. Indirect oxidation using NaCl as a mediator succeeded in conversion of the hydroxyl groups of cholic acid into keto groups [17,18]. No study sufficiently characterizing the direct electrochemical oxidation of BAs has been published to date. Reports on steroids lacking any or possessing only isolated double bonds, including cholesterol, are scarce [11].

Herein, we present anodic oxidation of primary BAs on bare platinum, glassy carbon (GC), and boron doped diamond (BDD) electrodes in a mixed medium of acetonitrile - water - perchloric acid, where perchloric acid serves as a dehydrating reagent. Such an introduction of a double bond into the steroid skeleton can potentially increase the electrochemical activity. In the case of cholesterol, the double bond, together with the respective allylic positions, was identified as one of the sites of the electrochemical attack [19]. This approach, based on acid-induced dehydration, has also enabled a spectrometric determination of cholesterol (Liebermann-Burchard reaction) [20–22]. The proposed electrochemical approach could find application in the diagnosis of disorders of BA synthesis. A block in the biosynthesis of BAs in most cases results in a deficiency of the primary BAs [23].

5.2.2 Experimental

Cholic (**1**), chenodeoxycholic (**2**), ursodeoxycholic (**3**), deoxycholic (**4**), lithocholic (**5**) acids, and cholesterol (all of > 99% purity, structures in Figure 5.2.1C) were purchased from Sigma-Aldrich. All other commercially available chemicals were of analytical grade (if not stated otherwise).

Voltammetry was performed using a potentiostat PalmSens 2.0 with PSTrace 4.8 software. BDD ($A = 7.07 \text{ mm}^2$, Windsor Scientific, UK), GC ($A = 3.14 \text{ mm}^2$), or platinum ($A = 7.07 \text{ mm}^2$; both Metrohm, Switzerland) working electrodes were used, routinely polished using alumina prior to each scan. Electrochemical cells with integrated reference electrode (Ag wire in $0.1 \text{ mol L}^{-1} \text{ AgNO}_3$, $1 \text{ mol L}^{-1} \text{ NaClO}_4$ in acetonitrile, separated from the measured solution by a salt bridge containing $0.5 \text{ mol L}^{-1} \text{ NaClO}_4$ in acetonitrile) and a platinum foil counter electrode were employed. All experiments were carried out under the temperature of 21°C . The contact time of the BA and HClO_4 and their concentrations are given in the caption of each voltammogram.

A modification of the previously described setup was used for capillary electrophoresis-mass spectrometry (CE-MS) [24]. The sample was hydrodynamically injected from an implemented PEEK cell: Sample volume $10 \mu\text{L}$; injection time 2 s ; separation voltage 18 kV . Parameters of fused silica capillary: Inner diameter $25 \mu\text{m}$, outer diameter $360 \mu\text{m}$, length 50 cm . Separation buffer: acetonitrile/ 1 mol L^{-1} acetic acid/ 10 mmol L^{-1} ammonium acetate. A Bruker micrOTOF (Bruker Daltonics, Germany) time-of-flight mass spectrometer equipped with a coaxial sheath liquid electrospray ionization (ESI) interface (Agilent, Waldbronn, Germany) was operated in positive ion mode; the mass range set $100\text{--}480 \text{ m/z}$; spectra rate 5 Hz . Source: ESI voltage: -4000 V (grounded sprayer tip), plate offset: -500 V ; nebulizer: 1.0 bar ; dry gas: 4.0 L min^{-1} ; dry temperature: 190°C . Transfer: capillary exit: 75.0 V ; skimmer 1: 25.3 V ; hexapole 1: 23.0 V ; hexapole RF: 65.0 Vpp ; skimmer 2: 23.0 V ; lens 1 transfer: $38.0 \mu\text{s}$; lens 1 pre pulse storage: $6.0 \mu\text{s}$. Sheath liquid (2-propanol:water:formic acid, $49.9:49.9:0.2$, $v/v/v$) was introduced by a syringe pump (KD Scientific, Holliston, MA, USA) with a flow rate of 0.48 mL h^{-1} .

5.2.3 Results and discussion

5.2.3.1 Voltammetric response of bile acids in the acetonitrile-water-perchloric acid medium

Electrochemical oxidation of two primary CA (**1**) and CDCA (**2**), and three secondary BAs, deoxycholic acid (**3**, DCA), lithocholic acid (**4**, LCA), and ursodeoxycholic acid (**5**, UDCA) in a mixed medium of acetonitrile-water containing perchloric acid was investigated.

Respective cyclic voltammograms on BDD electrode are presented in Figure 5.2.1A (curves *a-c*). The overall process proved to be highly dependent on the structure. Only primary BAs with the axial 7α -hydroxyl group (CA, CDCA) afforded well-developed irreversible anodic signals at around $+1.2 \text{ V}$ (curves *a, b*), ca $2.25\times$ higher for CDCA than CA, increasing in time (Figure 5.2.1B). The difference in current densities for the different BAs can be rationalized by different, temperature-dependent rates at which each of the BAs undergoes the dehydration reaction. Such low oxidation potential has not been reported to date. That applies not only to BAs, but to any other steroid-based compounds, lacking any or possessing only isolated double bonds, including cholesterol. A proof of its oxidizability at $+1.5 \text{ V}$ under the same conditions as those for BAs is presented by the voltammogram in Figure 5.2.1A, curve *d*. The voltammograms of the secondary BAs, namely DCA and LCA lacking the 7α -hydroxyl group

and UDCA possessing 7 β -hydroxyl group, are featureless around this potential (shown for UDCA in Figure 5.2.1A, curve *c*).

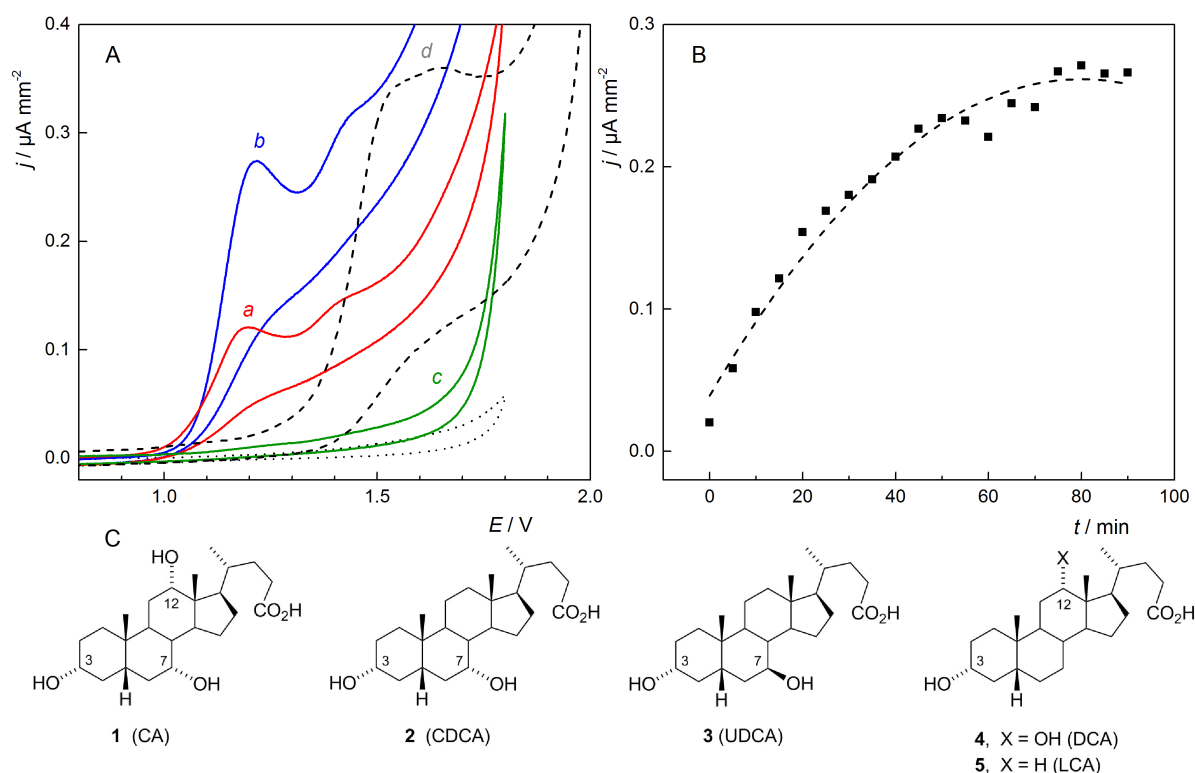


Figure 5.2.1 (A) Cyclic voltammograms of (a) CA, (b) CDCA, (c) UDCA ($c = 9 \times 10^{-5} \text{ mol L}^{-1}$), and (d) cholesterol ($c = 5 \times 10^{-5} \text{ mol L}^{-1}$) in acetonitrile containing $0.1 \text{ mol L}^{-1} \text{ HClO}_4$ and 0.43% H_2O on BDD electrode. Voltammograms recorded 90 minutes after the solutions were prepared from the stock solution and the supporting electrolyte. Supporting electrolyte in dotted line, scan rate 50 mV s^{-1} . (B) In-time development of the first CV peak height of CDCA ($c = 9 \times 10^{-5} \text{ mol L}^{-1}$). (C) Structural formulas of the BAs.

Obviously, the presence of the 7 α -hydroxyl group is the crucial factor enabling the development of the anodic signal. Note that its anti-periplanar position to the hydrogen atom at C(8) is likely to allow ready dehydration on protonation with HClO_4 . The latter reaction was identified as the rate determining step leading to time dependency of the voltammetric signal, reaching a stabilized current value after approximately 75 min (Figure 5.2.1B). Figure 5.2.2 shows that the oxidation process can be achieved on various bare electrode materials including BDD, GC, and platinum with comparable positive potentials. The highest signal/background ratio is provided by BDD, which predestines this material for analytical applications. Preliminary voltammetric experiments on this electrode material suggest linear concentration dependences with detection limits in the micromolar concentration range for both BAs.

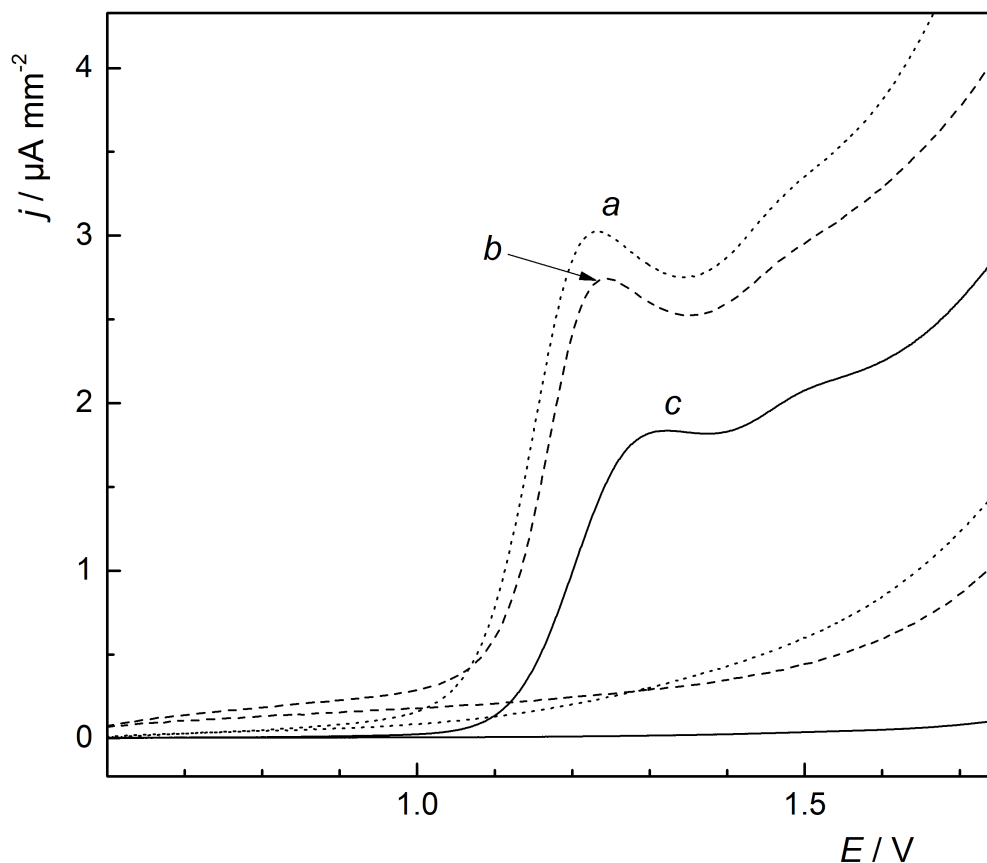


Figure 5.2.2 Linear sweep voltammograms for CDCA ($c = 9 \times 10^{-4} \text{ mol L}^{-1}$) and supporting electrolyte on (a) Pt, (b) GC, and (c) BDD electrodes. Supporting electrolyte: acetonitrile containing $0.1 \text{ mol L}^{-1} \text{ HClO}_4$ and 0.43% H_2O . Voltammograms were recorded 70 minutes after the preparation of the solutions, scan rate 50 mV s^{-1} .

5.2.3.2 CE-MS elucidation of reaction steps

CE-MS measurements were used to confirm the dehydration reaction steps and to investigate its other products and products of electrochemical oxidation. The proposed mechanism for the CDCA (**2**) ($m/z = 410.33$; $\text{CDCA} \cdot \text{NH}_4^+$ adduct) chemical reaction step is shown in Figure 5.2.3B based on CE-MS measurements of the reaction mixture containing CDCA in acetonitrile/ HClO_4 solution (water content 0.43%) (Figure 5.2.3A). In principle, the dehydration can produce the corresponding Δ^6 or Δ^7 alkene ($m/z = 392.32$; $(\text{CDCA} - \text{H}_2\text{O}) \text{NH}_4^+$ adduct); the latter structure (**6**) is more likely, as it should be thermodynamically preferred (Zaitsev's rule) but the structure has not been confirmed at this stage. Nevertheless, dehydration of 7α -hydroxy derivatives on treatment with POCl_3 in pyridine at room temperature is known to afford the thermodynamically favored Δ^7 -alkenes (Zaitsev rule) [25]. Therefore, formation of the Δ^7 -alkene (**6**) in our case seems very likely. After a longer period (inset in Figure 5.2.3A), a new signal was found at $m/z = 416.32$ (H^+ adduct), corresponding to the loss of another hydroxyl and addition of the acetamide group (**7**). This is also supported by the migration behavior in CE that indicated a positive charge of the latter species (**7**), presumably due to protonation of the amide group (Figure 5.2.3A). Formation of such a product can be rationalized by Ritter reaction [26], starting with an attack of the Lewis basic nitrogen of the acetonitrile at a cationic species (presumably generated

by protonation of the double bond), followed by hydrolysis of the iminium intermediate with the water that is present. Elucidation of the exact structure of this product will be the subject of future investigation.

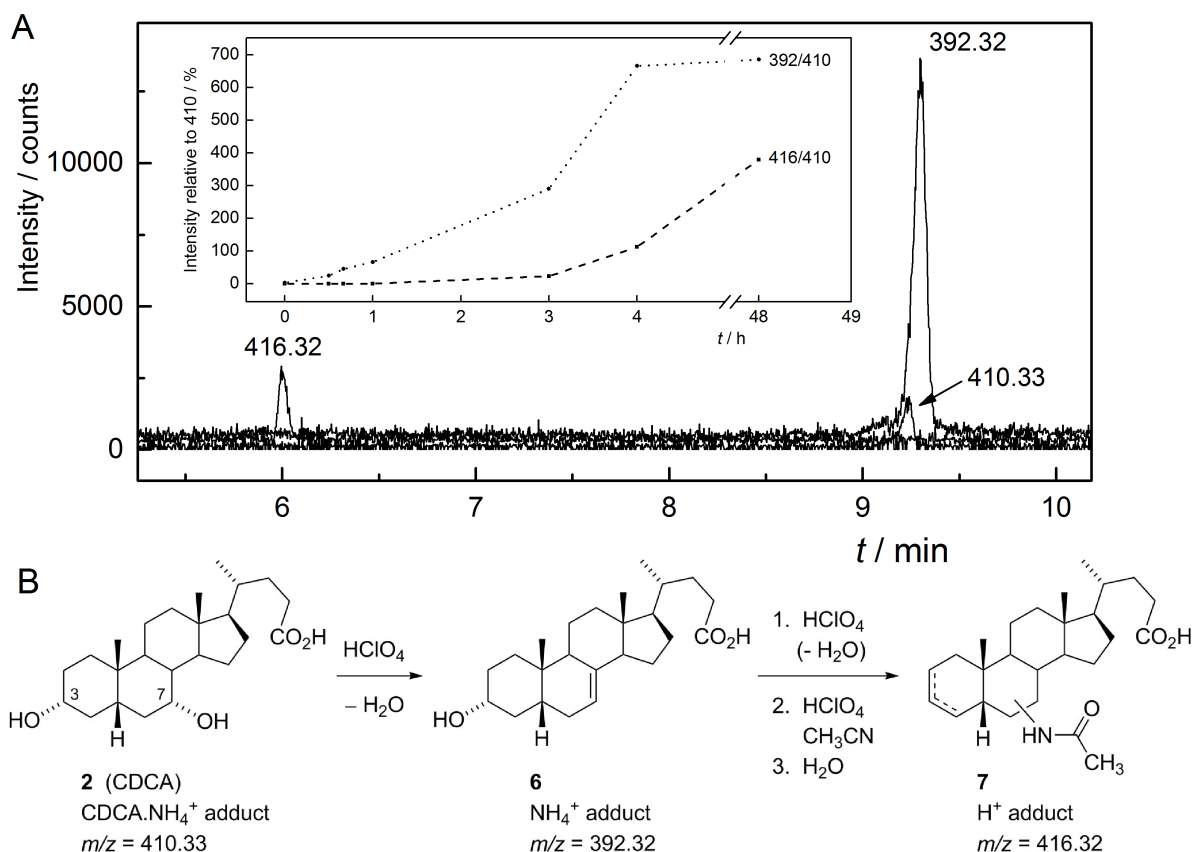


Figure 5.2.3 (A) CE-MS of solution containing CDCA ($c = 9 \times 10^{-4} \text{ mol L}^{-1}$) in acetonitrile containing $0.1 \text{ mol L}^{-1} \text{ HClO}_4$ and $0.43\% \text{ H}_2\text{O}$ obtained after 4 hours. Three selected ion traces are shown (m/z 392.32, 410.33, 416.32). Inset: In-time development of ratio between respective peaks. (B) The proposed reaction mechanism for CDCA dehydration.

The rise in voltammetric signal intensity correlates with the gradual rise of the peak attributed to dehydrated steroid (**6**) in the CE-MS measurements. The introduction of double bond(s) into the steroid skeleton enables the oxidation process, as unsaturated compounds are more prone to the removal of an electron from a bonding π -orbital (HOMO) and formation of a reactive radical cation. The exact mechanism and structure of the products of both chemical and electrochemical reaction steps are under investigation. In general, formation of a number of reaction products is expected, as dehydration of steroids, promoted by aqueous acidic systems, often leads to backbone rearrangements and other transformations [20, 27, 28]. Further, oxidative properties of perchloric acid itself have to be considered together with the fact, that beside the final products of dehydration reaction the intermediates can undergo electrochemical oxidation.

5.2.3.3 Solvent, supporting electrolyte and water effects on voltammetric signals

The effects of the media used and the water content on the overall process were further investigated. The choice of the solvent must respect its safe miscibility with strong acids in view of the associated hazards. Furthermore, the solvent must provide sufficient potential limit that enables electrochemical oxidation within the potential window of the respective electrode material. Acetonitrile, a weak electron donor, fulfils both requirements. With other tested miscible solvents, no signal for BAs was observed, presumably as a consequence of incomplete dehydration reaction (nitromethane) or decomposition of the solvent preceding the electrochemical reaction of the primary BAs (tetrahydrofuran). The second key factor is the choice of the supporting electrolyte, which should also function as a dehydration agent. Experiments were carried out with HClO_4 , H_2SO_4 , H_3PO_4 , and HCl (all 0.1 mol L^{-1}), containing respective concentrations of water in the solutions (%): 0.43, 0.02, 0.10, and 0.57. Only the presence of HClO_4 as the strongest among the inorganic acids used, enabled the dehydration step and consequently the electrochemical oxidation of the reaction products. Nevertheless, for other steroids with the core already activated by the presence of double bond(s), the use of other inorganic acids for further dehydration can be foreseen [20], as indicated by our preliminary experiments with cholesterol. Importantly, the voltammetric signal is not developed when using water-free medium, such as acetonitrile with NaClO_4 as supporting electrolyte, or the same medium with water present, confirming the necessity of the presence of a strong acid for inducing the dehydration reaction.

The initial water content proved to be an important factor influencing the chemical reaction step. The minimum amount in the solution (0.43 %) is given by its presence in the concentrated solution of perchloric acid (70 %). On the other hand, with water concentration higher than 2 % v/v, only negligible voltammetric signal was obtained as the dehydration step was apparently inhibited. However, once the dehydration starts and the electrochemically active species are formed, increasing the water:acetonitrile ratio does not lead to any substantial decrease of the voltammetric signal. This finding is important for prospective applications in HPLC with electrochemical detection of steroids requiring variability in water content for their successful separation.

5.2.4 Conclusion

For the first time an approach offering anodic electrochemical oxidation of bile acids in mixed organic-aqueous medium at reasonably low potential is presented. The signal can be obtained on various electrodes (BDD, GC, Pt). The saturated steroid core, known to be electrochemically inert, is activated by introduction of double bond(s) (via dehydration). This takes place directly in the medium of acetonitrile-water containing HClO_4 , the latter also serving as the supporting electrolyte. Only primary BAs, possessing the axial 7α -hydroxyl group, can undergo the acid-induced dehydration step, which nevertheless proceeds rather slowly. Therefore, the voltammetric signal is time dependent. Identification of the products of both chemical and electrochemical reaction steps is under investigation. Applicability to cholesterol was also confirmed. Based on the current work development of voltammetric methods

and methods based on amperometric detection in liquid flow techniques can be envisaged. The novel approach presented here, inspired by enzyme-based or acid-induced dehydration reactions, can be viewed as a promising step on the way to a long-sought after tool aiming at implementation of electrochemical methods for characterization and detection of steroids that are currently deemed to be electrochemically inert.

Acknowledgement

This research was carried out within the framework of Specific University Research (SVV 260440). Financial support from the Czech Science Foundation (project P206/12/G151) and Grant Agency of the Charles University (project GAUK 1440217) is gratefully acknowledged.

References

- [1] I. Björkhem, Mechanism of bile acid biosynthesis in mammalian liver, in: H. Danielsson, J. Sjövall (Eds.), *Sterols and Bile Acids*, 12th ed., Elsevier, Amsterdam, 1985, pp. 231–272.
- [2] D.W. Russell, K.D. Setchell, Bile acid biosynthesis, *Biochemistry* 31 (1992) 4737–4749.
- [3] W.J. Griffiths, J. Sjövall, Bile acids: Analysis in biological fluids and tissues, *J. Lipid Res.* 51 (2010) 23–41.
- [4] G. Kakiyama, A. Muto, H. Takei, H. Nittono, T. Murai, T. Kurosawa, A.F. Hofmann, W.M. Pandak, J.S. Bajaj, A simple and accurate HPLC method for fecal bile acid profile in healthy and cirrhotic subjects: Validation by GC-MS and LC-MS, *J. Lipid Res.* 55 (2014) 978–990.
- [5] H.L.J. Makin, C.H.L. Shackleton, J.W. Honour, Extraction, purification and measurement of steroids by high-performance liquid chromatography, gas-liquid chromatography and mass spectrometry. In H.L.J. Makin, D.B. Gower (Eds.), *Steroid Analysis*, Springer, New York, 2010, pp. 137–141.
- [6] S.I. Sayin, A. Wahlström, J. Felin, S. Jäntti, H.-U. Marschall, K. Bamberg, B. Angelin, T. Hyötyläinen, M. Orešič, F. Bäckhed, Gut microbiota regulates bile acid metabolism by reducing the levels of tauro-beta-muricholic acid, a naturally occurring FXR antagonist, *Cell Metab.* 17 (2013) 225–235.
- [7] G. Zhang, A. Cong, G. Xu, C. Li, R. Yang, T. Xia, An enzymatic cycling method for the determination of serum total bile acids with recombinant 3α -hydroxysteroid dehydrogenase, *Biochem. Biophys. Res. Commun.* 326 (2005) 87–92.
- [8] D. Lawrance, C. Williamson, M.G. Boutelle, A.E.G. Cass, Development of a disposable bile acid biosensor for use in the management of cholestasis, *Anal. Methods* 7 (2015) 3714–3719.
- [9] X. Zhang, M. Zhu, B. Xu, Y. Cui, G. Tian, Z. Shi, M. Ding, Indirect electrochemical detection for total bile acids in human serum, *Biosens. Bioelectron.* 85 (2016) 563–567.
- [10] S. Koide, N. Ito, I. Karube, Development of a micro-planar amperometric bile acid biosensor for urinalysis, *Biosens. Bioelectron.* 22 (2007) 2079–2085.
- [11] J. Klouda, J. Barek, K. Nesměrāk, K. Schwarzová-Pecková, Non-Enzymatic electrochemistry in characterization and analysis of steroid compounds, *Crit. Rev. Anal. Chem.* 47 (2017) 384–404.
- [12] T. Ferri, L. Campanella, G. De Angelis, Differential-pulse polarographic determination of cholic acids, *Analyst* 109 (1984) 923–925.
- [13] U.T. Yilmaz, D. Uzun, H. Yilmaz, A new method for rapid and sensitive determination of cholic acid in gallbladder bile using voltammetric techniques, *Microchem. J.* 122 (2015) 159–163.
- [14] R. Dekker, R. van der Meer, C. Olieman, Sensitive pulsed amperometric detection of free and conjugated bile acids in combination with gradient reversed-phase HPLC, *Chromatographia* 31 (1991) 549–553.
- [15] M.F. Chaplin, Analysis of bile acids and their conjugates using high-pH anion-exchange chromatography with pulsed amperometric detection, *J. Chromatogr. B Biomed. Sci. Appl.* 664 (1995) 431–434.
- [16] S. Scalia, S. Tirendi, P. Pazzi, E. Bousquet, Assay of free bile acids in pharmaceutical preparations by HPLC with electrochemical detection, *Int. J. Pharm.* 115 (1995) 249–253.
- [17] F. Bonfatti, A. De Battisti, S. Ferro, A. Medici, P. Pedrini, Electrosynthesis of dehydrocholic acid from cholic acid, *J. Appl. Electrochem.* 30 (2000) 995–998.
- [18] A. Medici, P. Pedrini, A. De Battisti, G. Fantin, M. Fogagnolo, A. Guerrini, Anodic electrochemical oxidation of cholic acid, *Steroids* 66 (2001) 63–69.
- [19] J.W. Morzycki, A. Sobkowiak, Electrochemical oxidation of cholesterol, *Beilstein J. Org. Chem.* 11 (2015) 392–402.
- [20] Q. Xiong, W.K. Wilson, J. Pang, The Liebermann-Burchard reaction: Sulfonation, desaturation, and rearrangement of cholesterol in acid, *Lipids* 42 (2007) 87–96.

- [21] W.D. Brown, Determination of serum cholesterol with perchloric acid, *Aust. J. Exp. Biol. Med. Sci.* 37 (1959) 523–531.
- [22] T.C. Huang, C.P. Chen, V. Wefler, A. Raftery, A stable reagent for the Liebermann-Burchard reaction. Application to rapid serum cholesterol determination, *Anal. Chem.* 33 (1961) 1405–1407.
- [23] F.M. Vaz, S. Ferdinandusse, Bile acid analysis in human disorders of bile acid biosynthesis, *Mol. Asp. Med.* 56 (2017) 10–24.
- [24] P. Palatzky, A. Zöpfel, T. Hirsch, F.-M. Matysik, Electrochemically assisted injection in combination with capillary electrophoresis-mass spectrometry (EAI-CE-MS) – mechanistic and quantitative studies of the reduction of 4-nitrotoluene at various carbon-based screen-printed electrodes, *Electroanalysis* 25 (2013) 117–122.
- [25] E. Berner, A. Lardon, T. Reichstein, Über Gallensäuren und Verwandte Stoffe: 3 α ,12 α -Dioxy-cholen-(7)-säure, *Helv. Chim. Acta* 30 (1947) 1542–1553.
- [26] R. Bishop, Ritter-type reactions, in: B.M. Trost, I. Fleming (Eds.), *Comprehensive organic synthesis*, Elsevier, Amsterdam, 1991, pp. 261–300.
- [27] R. De Marco, A. Leggio, A. Liguori, F. Perri, C. Siciliano, Transformations of 3-hydroxy steroids with Lewis and anhydrous protic acids: The case of pregn-4-en-3 β ,17 α ,20 β -triol, *Chem. Biol. Drug Des.* 78 (2011) 269–276.
- [28] P. Kočovský, Back-bone rearrangements of steroids and related systems, *Chem. Listy* 73 (1979) 583–613.

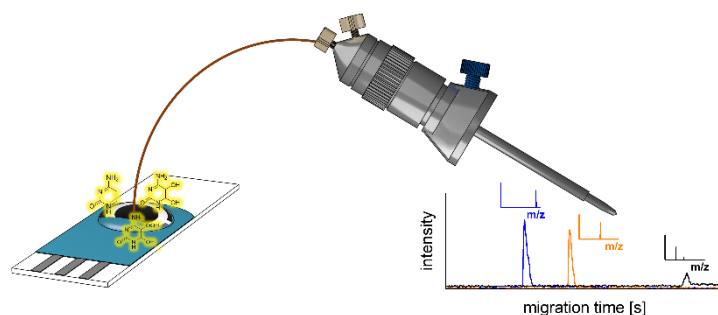
5.3 Electrooxidation of cytosine on bare screen-printed carbon electrodes studied by online electrochemistry-capillary electrophoresis-mass spectrometry

This chapter was published in the journal *Electrochemistry Communications*. The layout specifications of the journal were changed for uniformity. Copyright 2019 The Authors. Published by Elsevier B. V.

T. Herl, L. Taraba, D. Böhm, F.-M. Matysik, *Electrochem. Commun.* **2019**, 99, 41-45.

Abstract

The electrooxidation of cytosine on common commercially available screen-printed carbon electrodes was investigated. To characterize the processes on the electrode surface, the oxidation products were analyzed by online electrochemistry-capillary electrophoresis-mass spectrometry. Capillary electrophoresis was the ideal separation technique as all occurring species were positively charged at acidic separation conditions. Comparing the results to literature data on cytosine oxidation by one electron oxidants, the compound 6-hydroxy-5-hydroperoxy-5,6-dihydrocytosine was identified as the main oxidation product that could be detected on the screen-printed carbon electrode material. This product species was found to be rather stable over an investigated period of 60 minutes under the conditions present in our experiments. A small amount of cytosine glycol was detected, probably formed as decomposition product. During oxidation in acetate electrolyte, a side reaction with the electrolyte took place forming an artificial product, which was not the case in hydrogencarbonate electrolyte. This showed that products have to be investigated carefully in the context of the background electrolyte to avoid misinterpretations.



5.3.1 Introduction

The nucleobase cytosine is an important analytical target in research studies regarding DNA damage or mutations [1,2]. Various investigations are concerned with the identification of base, nucleoside and nucleotide oxidation products. However, in this context mainly chemical or irradiation processes based on hydroxyl radicals, one-electron oxidants and UV- or γ -irradiation are widely applied as described by Wagner and Cadet [3,4]. Typical mechanisms proposed in literature are one-electron oxidation to a cytosine radical cation or addition of a hydroxyl radical followed by subsequent reactions like hydration or deprotonation. Amongst others, 5-hydroxycytosine, 5-hydroxyuracil, 5,6-dihydroxy-5,6-dihydrouracil, 5-hydroxyhydantoin and 1-carbamoyl-4,5-dihydroxy-2-oxoimidazolidine were described as stable oxidation products [5]. Compared to the methods described above, sophisticated mechanistic studies in the context of electrochemical oxidation of cytosine are scarce in comparison for instance to guanine, which is more readily oxidizable and thus well investigated [6–8]. However, different analytical applications for electrochemical determination of cytosine or related species exist [9–13] and are referred to as cheap alternatives to expensive instrumental techniques [14]. Thus, it is important to investigate the mechanism of electrochemical cytosine oxidation.

Early studies on the electrochemical behavior of cytosine were solely dealing with polarographic reduction [15,16] until it was shown that it can be oxidized at glassy carbon electrode materials where it was considered inactive for a long time [17]. Brotons et al. [18] reported in-house fabricated tailored screen-printed graphite electrodes that were used for oxidation of all nucleobases including cytosine and methylcytosine. The general application of carbon materials for electrooxidation was recently reviewed by Brotons et al. [14]. Some examples for the characterization of electrochemically generated oxidation products of cytosine species can be found in literature dealing for example with the investigation of 2'-deoxycytidine-5'-monophosphate [19], cytidine-3',5'-cyclic monophosphate [20], or 5-halocytosine oxidation [21]. However, investigations on cytosine itself are predominantly concerned with voltammetric characterization but not with product identification, even if some mechanistic steps are proposed [14]. Nevertheless, the identification of oxidation products is of fundamental importance to understand the processes happening on the electrode surface depending on electrode materials and oxidation conditions, especially if electrochemistry is used to mimic physiological conditions. Next to the commonly applied hyphenation of electrochemical flow cells to MS or HPLC-MS [22], electrochemistry-capillary electrophoresis-mass spectrometry (EC-CE-MS) is the method of choice if charged product species are formed [23].

In this study, the electrooxidation of cytosine on widely used commercial screen-printed carbon electrodes was investigated by online EC-CE-MS. The application of disposable electrodes [24] offered the advantages of simple electrochemical setup, user-friendliness, low costs, low sample consumption, and easy replacement of electrodes avoiding electrode fouling. Because of these features, this approach is potentially interesting for future routine applications. Electrooxidation of cytosine combined with CE

separation allowed for the characterization and interference-free detection of individual product species based on the pH-dependent migration behavior. Oxidation as well as separation were carried out under different conditions and products were characterized by MS and MS/MS detection.

5.3.2 Experimental

All chemicals were of analytical grade, if not stated otherwise. Solutions were prepared with Milli-Q water ($18.2 \text{ M}\Omega \text{ cm}^{-1}$, Milli-Q Advantage A10 system, Merck Millipore, Darmstadt, Germany). Solutions of 1 mM cytosine (purity $\geq 99\%$, Sigma-Aldrich, St. Louis, MO, USA) in 100 mM NH_4OAc (Merck) at pH 7 or NH_4HCO_3 (Roth, Karlsruhe, Germany) at pH 8 were prepared. Caffeine at a concentration of 100 μM served as EOF marker. As electrolyte for CE separations, 50 mM NH_4OAc (pH 7) or 50 mM HOAc (pH 3) (Sigma-Aldrich) were used.

Electrode potentials were controlled by a $\mu\text{Autolab III}$ potentiostat and NOVA 2.0 software (Metrohm Autolab B.V., Utrecht, The Netherlands). Voltammetric studies were carried out by applying droplets of 50 μL cytosine solution on screen-printed carbon electrodes (SPCEs, DRP-110, DropSens, Llanera, Spain) and cycling the potential at a scan rate of 50 mV s^{-1} .

The setup developed by Palatzky et al [24] was used for EC-CE-MS. Volumes of 50 μL of cytosine solution were applied onto the SPCE and CE measurements were done prior to and after oxidation at 1.4 V for 15 s (injection during last 10 s). Sample was hydrodynamically injected by placing the beveled tip (15°) of the capillary onto the center of the working electrode (height difference of 17 cm between injection and detection end of capillary). A separation voltage of 20 kV was applied and a fused silica capillary with an ID of 25 μm , an OD of 360 μm and a length of 35 cm was used. The MS detector was a micrOTOF mass spectrometer (Bruker Daltonics, Bremen, Germany) equipped with a grounded coaxial sheath liquid electrospray ionization interface (Agilent, Waldbronn, Germany). A solution of 2-propanol:water:formic acid 49.9:49.9:0.2 v/v/v was added as sheath liquid with a syringe pump (KD Scientific, Holliston, MA, USA) at a flow rate of 8 $\mu\text{L min}^{-1}$. The MS was operated in positive ion mode (mass range m/z 50-450, spectra rate 3 Hz, nebulizer 1.0 bar, dry gas 4.0 L min^{-1} , dry temperature 250°C). MS/MS measurements were carried out with an Agilent QTOF MS system (positive ion mode, mass range m/z 50-400, MS spectra rate 4 Hz, MS/MS spectra rate 6 Hz, collision energy 10 eV, nebulizer 1 bar, dry gas 10 L min^{-1} , dry temperature 180°C).

5.3.3 Results and discussion

5.3.3.1 Cyclic voltammetry of cytosine on bare SPCE

The electrolytes for electrochemical oxidation of cytosine were selected to be compatible to ESI-MS measurements. Additionally, the pH was chosen close to neutral to simulate physiological conditions. For the electrochemical characterization of cytosine, NH_4OAc was more suitable than NH_4HCO_3 due to the larger anodic potential window (Figure 5.3.1A) leading to a more pronounced oxidation peak compared to NH_4HCO_3 (Figure 5.3.1B). Cytosine exhibited an oxidation wave at 1.3 V. Based on the

cyclic voltammograms, an oxidation potential of 1.4 V was chosen for oxidation in EC-CE measurements to ensure diffusion-controlled processes.

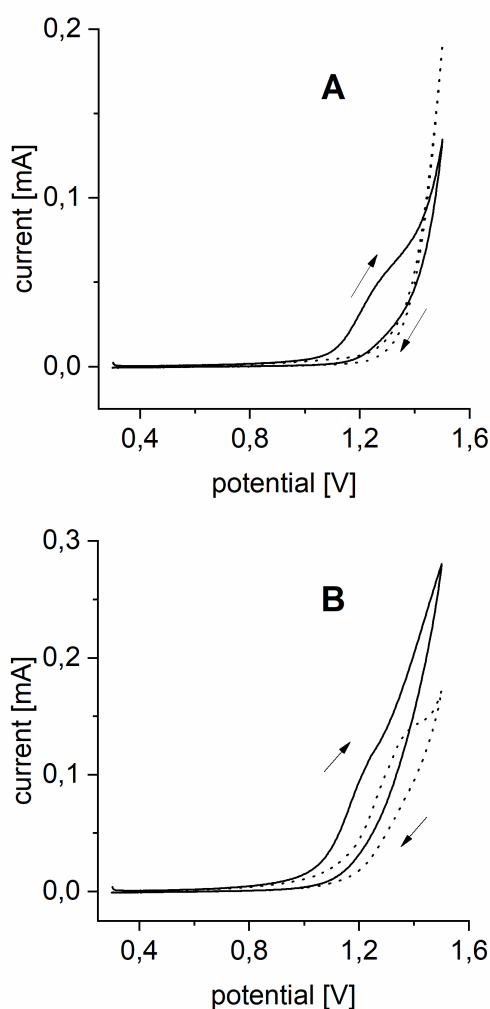


Figure 5.3.1 Cyclic voltammograms of 1 mM cytosine in 100 mM NH_4OAc (A) and 100 mM NH_4HCO_3 (B) on a SPCE. The dotted lines represent voltammograms in background electrolytes. Scan rate was 50 mV s^{-1} .

5.3.3.2 Migration behavior of cytosine and oxidation products

During separation in NH_4OAc at neutral pH (Figures 5.3.2A+B), cytosine and its oxidation products were migrating close to the electroosmotic flow (EOF), marking the migration of neutral species (EOF marker caffeine). At these conditions, only one oxidation product (m/z 162.051), identified as $\text{C}_4\text{H}_8\text{N}_3\text{O}_4$ (**1**, $[\text{M}+\text{H}]^+$) was detected. When separation was done in HOAc (pH 3), cytosine and its oxidation products could be fully separated and were migrating faster than the EOF meaning that they carried a positive charge due to protonation in solution (Figure 5.3.2C). After oxidation in NH_4OAc , three product species were detected (Figure 5.3.2C+5.3.3A): product **1** and, additionally, products with m/z 204.061 (**2**, $\text{C}_6\text{H}_{10}\text{N}_3\text{O}_5$, $[\text{M}+\text{H}]^+$) and m/z 146.058 (**3**, $\text{C}_4\text{H}_8\text{N}_3\text{O}_3$, $[\text{M}+\text{H}]^+$). **2** and **3** were probably suppressed under neutral pH due to overlap with the other peaks. After oxidation in NH_4HCO_3 in place of NH_4OAc , only products **1** and **3** were detected (Figure 5.3.3B) under the same separation conditions. This means that in the case of NH_4OAc a reaction with the electrolyte took place. This step was competing with

formation of the other products, as only minor amounts of **1** and **3** were detected relative to the cytosine peak compared to NH_4HCO_3 . Product **3** was only generated in very small amounts. Investigations on product stability (electrolysis in acetate electrolyte for 20 minutes followed by consecutive CE-MS measurements) are shown in the inset in Figure 5.3.3A and revealed that product **1** was the main product and was quite stable with only a small decrease in signal intensity within an hour under the present conditions. Product **2** showed a fast decomposition within 5 minutes after oxidation and exhibited a much smaller peak area after 20 minutes oxidation compared to injection directly from the electrode after oxidation. The small peak for **3** remained at a constant level.

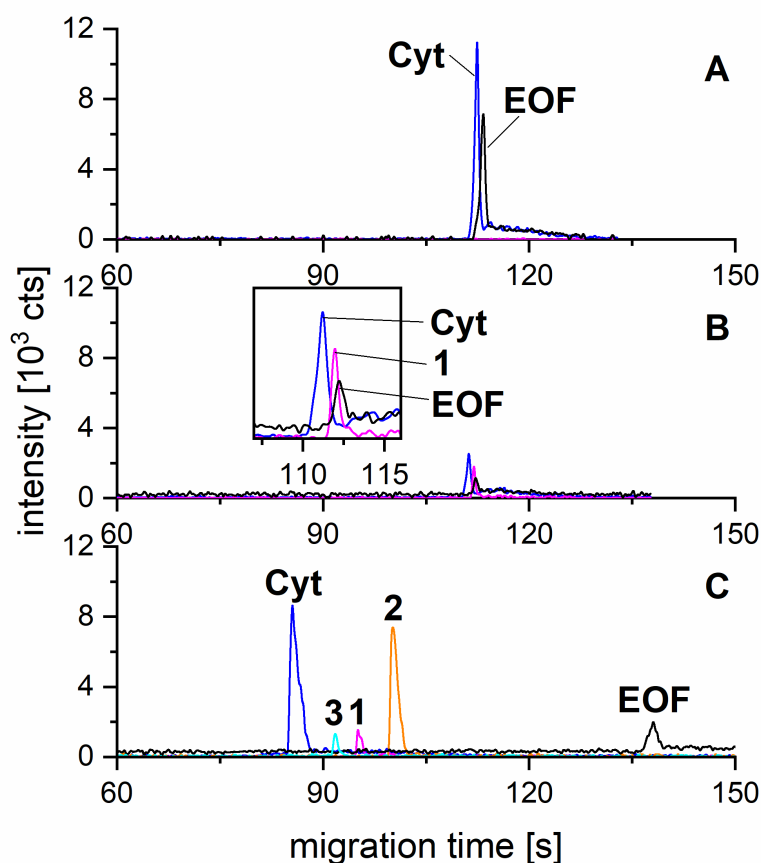


Figure 5.3.2 CE-MS measurements of 1 mM cytosine in 100 mM NH_4OAc (pH 7) without prior oxidation (A) and after oxidation on SPCE at 1.4 V for 15 s (B+C). Separation in 50 mM NH_4OAc at pH 7 (A+B) and 50 mM HOAc at pH 3 (C). Extracted ion electropherograms ($[\text{M}+\text{H}]^+$ traces) of cytosine (Cyt, blue, m/z 112.051), product **1** (magenta, m/z 162.051), product **2** (orange, m/z 204.061), product **3** (cyan, m/z 146.058), and EOF marker caffeine (black, m/z 195.074) are shown. Separation at 20 kV, capillary ID 25 μm , L 35 cm, 10 s hydrodynamic injection.

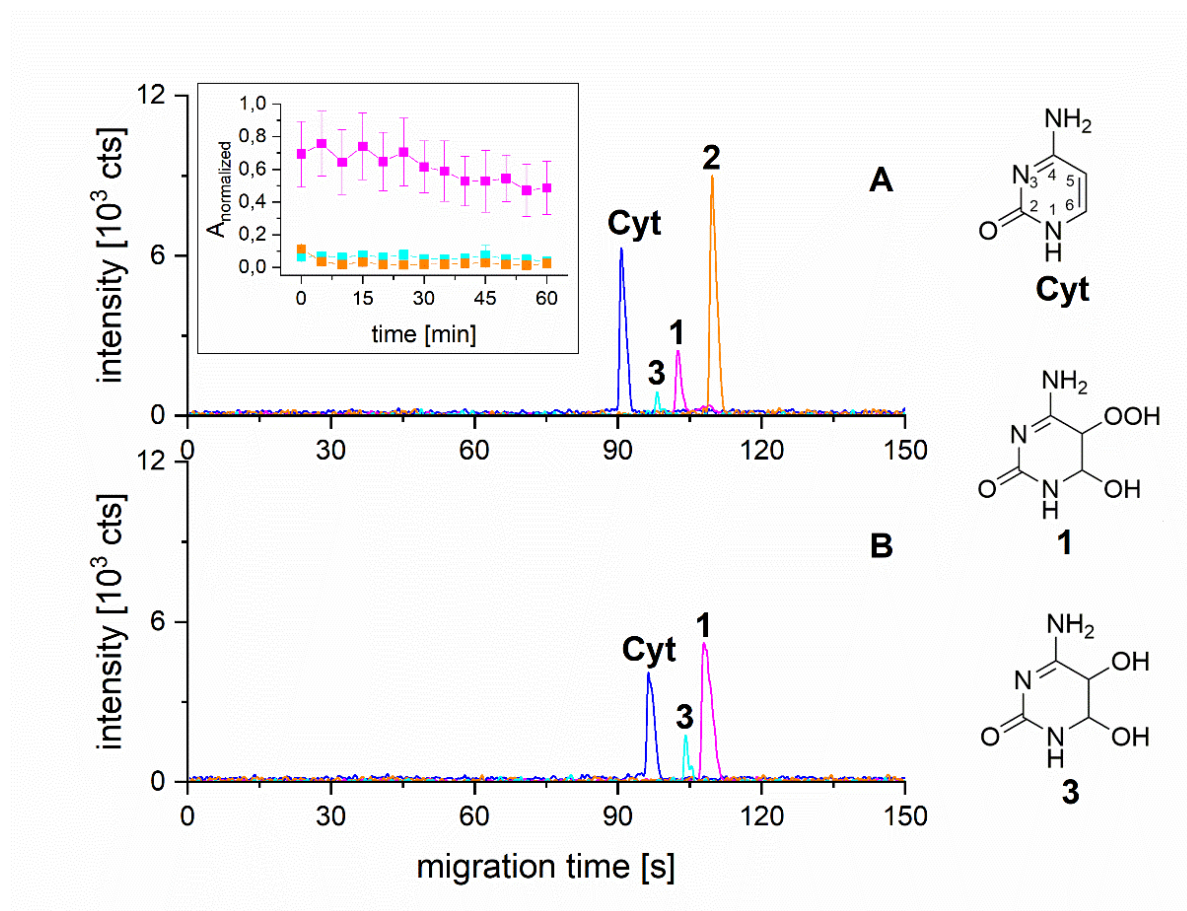


Figure 5.3.3 EC-CE-MS measurements of 1 mM cytosine in 100 mM NH₄OAc at pH 7 (A) and 100 mM NH₄HCO₃ at pH 8 (B) after oxidation on SPCE at 1.4 V for 15 s. Separation in 50 mM HOAc (pH 3) at 20 kV. Extracted ion electropherograms of cytosine (Cyt, blue, m/z 112.051), product 1 (magenta, m/z 162.051), product 2 (orange, m/z 204.061), and product 3 (cyan, m/z 146.058). Capillary ID 25 μ m, L 35 cm, 10 s hydrodynamic injection. The proposed structures are shown on the right side. Product 2 was assigned to a reaction with acetate electrolyte. The inset in 5.3.3A shows the development of peak areas normalized to cytosine over time after oxidation in NH₄OAc for 20 minutes.

5.3.3.3 MS/MS measurements

EC-CE-MS/MS measurements with collision-induced dissociation were carried out to obtain additional structural information. In the cytosine spectrum, a deamination (-17 m/z) and loss of HNCO (-43 m/z) were observed (Figure 5.3.4A). The spectra of 1 and 2 were similar to each other (Figures 5.3.4B+C). A characteristic fragment occurring in both cases was m/z 144.039, exhibiting a molecular formula of C₄H₆N₃O₃ ([M+H]⁺). This species can be assigned to dehydration (-18 m/z) of 1. Product 2 showed a loss of acetic acid (-60 m/z) instead. This was the final proof that product 2 was not a primary oxidation product of cytosine but rather an artifact caused by reaction with the electrolyte. The signal intensity obtained for 3 was too low for MS/MS measurements.

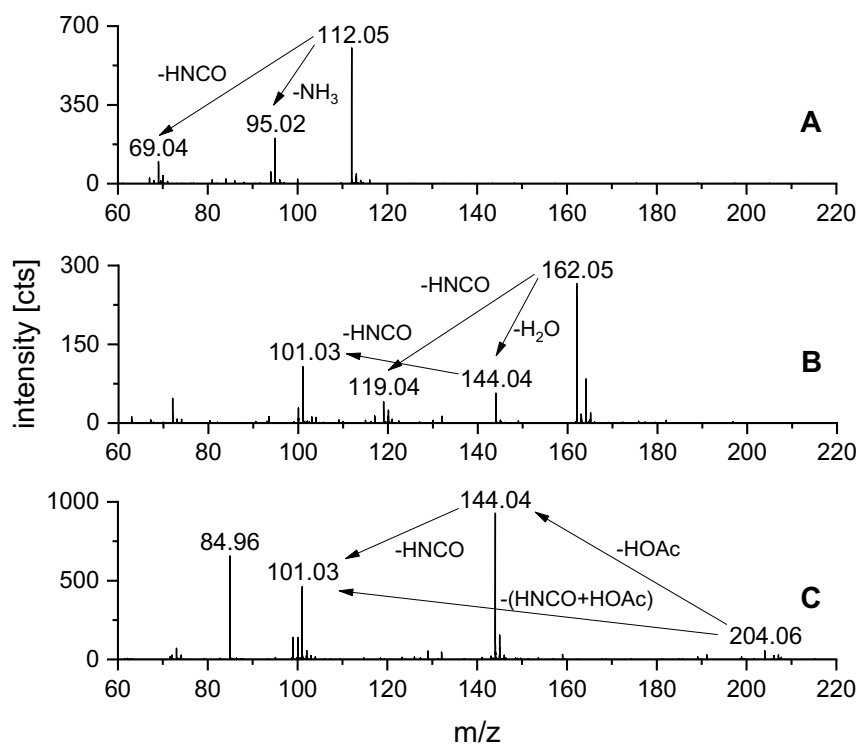


Figure 5.3.4 Mass spectra of cytosine (A), **1** (B) and **2** (C) after collision-induced dissociation (collision energy 10 eV). Assignment of fragments adapted from [25].

5.3.3.4 Oxidation mechanism

Based on the results obtained, we propose an electrochemical oxidation mechanism starting with the formation of a cytosine radical cation by oxidation of the double bond between C5 and C6, similar as described for one-electron oxidants [3] and already reported in the recent review by Brotons et al [14]. By hydration of the radical cation [26], hydroxyl adduct radicals are formed [3] predominantly resulting in 6-hydroxy-5,6-dihydrocytos-5-yl radicals [27]. These react fast and quantitatively with oxygen to 6-hydroxy-5-hydroperoxyradicals [26, 28] followed by reduction for example by superoxide radical anions [28] and protonation to 6-hydroxy-5-hydroperoxy-5,6-dihydrocytosine **1** ($C_4H_7N_3O_4$, structure shown in Figure 5.3.3) as main product of the electrochemical oxidation. The formation of 5-hydroxy-6-hydroperoxy-5,6-dihydrocytosine that can not be distinguished from **1** with our methods can be ruled out as it would result from a reaction of cytosine with hydroxyl radicals forming 5-hydroxy-5,6-dihydrocyto-6-yl radicals [28]. Considering the electrode material, a hydroxyl radical based mechanism is negligible, as SPCEs are known for oxidations involving direct electron transfer in contrast to for example boron doped diamond generating hydroxyl radicals [20]. Imidazolidine decomposition products commonly described particularly for 5-hydroxy-6-hydroperoxy-5,6-dihydrocytosine [27] were not observed. As MS/MS measurements showed comparable fragmentation patterns, product **1** and product **2** may have been formed via a similar mechanism starting from the cytosine radical cation. However, as already stated, product **2** was an artifact formed by reaction with the electrolyte. A possible mechanism for the formation of **2** can be explained by nucleophilic addition of acetate to the cytosine radical cation instead of initial hydration finally leading to 6-acetoxy-5-hydroperoxy-5,6-

dihydrocytosine ($C_6H_9N_3O_5$). Nucleophilic additions of radical cations were previously reported in the context of crosslink reactions between guanine radical cations and thymine [29]. Product **2** decomposed quite fast (see inset in Figure 5.3.3). As can be found in literature [27], 6-hydroxy-5-hydroperoxides of cytosine decompose to 5,6-glycols. Thus, cytosine glycol **3** ($C_4H_7N_3O_3$, structure shown in Figure 5.3.3), which was also detected, can be interpreted as decomposition product formed by reduction of the hydroperoxide of product **1** [28]. It has to be stated that we could not distinguish possible cis and trans isomers of products **1** and **3**. Product **1** is often referred to as instable intermediate in literature, undergoing subsequent reactions [3,5, 30]. However, in our experiments we measured only a slow decay of signal intensity within one hour and no decomposition products besides cytosine glycol were detected. This might be due to the rather low amount of products generated via electrochemistry compared to other methods, so that the concentration of decomposition products was too low to detect. Additionally, fast sample preparation and analysis by online EC-CE-MS without isolation and preconcentration steps allows for a short time interval between generation and detection of products, limiting decomposition.

5.3.4 Conclusion

EC-CE-MS was applied to investigate the electrochemical oxidation of cytosine and to identify oxidation products. Cytosine was oxidizable on widely used commercial screen-printed carbon electrodes using MS compatible electrolytes. Online CE-MS allowed for a fast detection of electrogenerated species. CE was well suited for separation as all analytes were positively charged at acidic separation conditions. The results indicated the formation of 5,6-hydroperoxy-hydroxy species as main products that were quite stable within an investigated period of one hour showing only minor decrease in signal intensity under the present conditions. Cytosine glycol was detected in small amount, probably as decomposition product formed by reduction of hydroperoxides. When oxidation was carried out in acetate-containing electrolyte, an additional product was found in contrast to oxidation in hydrogencarbonate. In further investigations, this species could be attributed to reaction with the electrolyte so that it could finally be identified as artifact instead of a primary oxidation product of cytosine. This illustrates that results have to be interpreted carefully. The results showed that online EC-CE-MS can contribute to the investigation of electrochemical reactions enabling the identification of final oxidation products. In the future, this method may be of rising interest for routine applications due to the advantages of screen-printed electrodes like easy replaceability, simple setup, and low sample volumes. Furthermore, it might be an attractive complementary method for simulation of oxidative stress under physiological conditions, avoiding the addition of chemical oxidants or irradiation sources.

Acknowledgement

Josef Kiermaier of the MS department of the central analytical services at the University of Regensburg is gratefully acknowledged for his help with MS/MS measurements. This research did not receive any specific grant from funding agencies in the public, commercial, or not-for-profit sectors.

References

- [1] C.S. Nabel, S.A. Manning, R.M. Kohli, The curious chemical biology of cytosine: Deamination, methylation, and oxidation as modulators of genomic potential, *ACS Chem. Biol.* 7 (2012) 20–30.
- [2] G.S. Madugundu, J. Cadet, J.R. Wagner, Hydroxyl-radical-induced oxidation of 5-methylcytosine in isolated and cellular DNA, *Nucleic Acids Res.* 42 (2014) 7450–7460.
- [3] J.R. Wagner, J. Cadet, Oxidation reactions of cytosine DNA components by hydroxyl radical and one-electron oxidants in aerated aqueous solutions, *Acc. Chem. Res.* 43 (2010) 564–571.
- [4] J. Cadet, J. Richard Wagner, DNA base damage by reactive oxygen species, oxidizing agents, and UV radiation, *Cold Spring Harb. Perspect. Biol.* 5 (2013).
- [5] F. Samson-Thibault, G.S. Madugundu, S. Gao, J. Cadet, J.R. Wagner, Profiling Cytosine Oxidation in DNA by LC-MS/MS, *Chem. Res. Toxicol.* 25 (2012) 1902–1911.
- [6] F. Pitterl, J.P. Chervet, H. Oberacher, Electrochemical simulation of oxidation processes involving nucleic acids monitored with electrospray ionization - Mass spectrometry, *Anal. Bioanal. Chem.* 397 (2010) 1203–1215.
- [7] R. Erb, S. Plattner, F. Pitterl, H.-J. Brouwer, H. Oberacher, An optimized electrochemistry-liquid chromatography-mass spectrometry method for studying guanosine oxidation, *Electrophoresis* 33 (2012) 614–621.
- [8] R. Scholz, P. Palatzky, F.-M. Matysik, Simulation of oxidative stress of guanosine and 8-oxo-7,8-dihydroguanosine by electrochemically assisted injection–capillary electrophoresis–mass spectrometry, *Anal. Bioanal. Chem.* 406 (2014) 687–694.
- [9] A.M. Oliveira-Brett, J.A.P. Piedade, L.A. Silva, V.C. Diculescu, Voltammetric determination of all DNA nucleotides, *Anal. Biochem.* 332 (2004) 321–329.
- [10] J. Jankowska-Śliwińska, M. Dawgul, J. Kruk, D.G. Pijanowska, Comparison of electrochemical determination of purines and pyrimidines by means of carbon, graphite and gold paste electrodes, *Int. J. Electrochem. Sci.* 12 (2017) 2329–2343.
- [11] D. Kato, N. Sekioka, A. Ueda, R. Kurita, S. Hirono, K. Suzuki, O. Niwa, Nanohybrid carbon film for electrochemical detection of SNPs without hybridization or labeling, *Angew. Chem. Int. Ed.* 47 (2008) 6681–6684.
- [12] D. Kato, K. Goto, S.I. Fujii, A. Takatsu, S. Hirono, O. Niwa, Electrochemical DNA methylation detection for enzymatically digested CpG oligonucleotides, *Anal. Chem.* 83 (2011) 7595–7599.
- [13] H. Li, X. Wang, Z. Wang, W. Zhao, Simultaneous determination of guanine, adenine, thymine and cytosine with a simple electrochemical method, *J. Solid State Electrochem.* 20 (2016) 2223–2230.
- [14] A. Brotons, F.J. Vidal-Iglesias, J. Solla-Gullón, J. Iniesta, Carbon materials for the electrooxidation of nucleobases, nucleosides and nucleotides toward cytosine methylation detection: A review, *Anal. Methods* 8 (2016) 702–715.
- [15] D.L. Smith, P.J. Elving, Electrochemical Reduction of Pyrimidine, Cytosine and Related Compounds: Polarography and Macroscale Electrolysis, *J. Am. Chem. Soc.* 84 (1962) 2741–2747.
- [16] J.W. Webb, B. Janik, P.J. Elving, Cytosine Nucleoside-nucleotide Series. Electrochemical Study of Reduction Mechanism, Association, and Adsorption, *J. Am. Chem. Soc.* 95 (1973) 991–1003.
- [17] A.M. Oliveira Brett, F.-M. Matysik, Voltammetric and sonovoltammetric studies on the oxidation of thymine and cytosine at a glassy carbon electrode, *J. Electroanal. Chem.* 429 (1997) 95–99.
- [18] A. Brotons, L.A. Mas, J.P. Metters, C.E. Banks, J. Iniesta, Voltammetric behaviour of free DNA bases, methylcytosine and oligonucleotides at disposable screen printed graphite electrode platforms., *Analyst* 138 (2013) 5239–49.

- [19] A. Baumann, W. Lohmann, S. Jahn, U. Karst, On-line electrochemistry/electrospray ionization mass spectrometry (EC/ESI-MS) for the generation and identification of nucleotide oxidation products, *Electroanalysis* 22 (2010) 286–292.
- [20] M. Cindric, M. Vojs, F.-M. Matysik, Characterization of the Oxidative Behavior of Cyclic Nucleotides Using Electrochemistry-Mass Spectrometry, *Electroanalysis* 27 (2015) 234–241.
- [21] I. Sanjuán, A.N. Martín-Gómez, J. Graham, N. Hernández-Ibáñez, C. Banks, T. Thiemann, J. Iniesta, The electrochemistry of 5-halocytosines at carbon based electrodes towards epigenetic sensing, *Electrochim. Acta* 282 (2018) 459–468.
- [22] H. Faber, M. Vogel, U. Karst, Electrochemistry/mass spectrometry as a tool in metabolism studies—A review, *Anal. Chim. Acta* 834 (2014) 9–21.
- [23] M. Cindric, F.-M. Matysik, Coupling electrochemistry to capillary electrophoresis-mass spectrometry, *TrAC Trends Anal. Chem.* 70 (2015) 122–127.
- [24] P. Palatzky, A. Zöpfl, T. Hirsch, F.-M. Matysik, Electrochemically Assisted Injection in Combination with Capillary Electrophoresis-Mass Spectrometry (EAI-CE-MS) - Mechanistic and Quantitative Studies of the Reduction of 4-Nitrotoluene at Various Carbon-Based Screen-Printed Electrodes, *Electroanalysis* 25 (2013) 117–122.
- [25] S.S. Jensen, X. Ariza, P. Nielsen, J. Vilarrasa, F. Kirpekar, Collision-induced dissociation of cytidine and its derivatives, *J. Mass Spectrom.* 42 (2007) 49–57.
- [26] J.R. Wagner, J.E. Van Lier, C. Decarroz, M. Berger, J. Cadet, Photodynamic methods for oxy radical-induced DNA damage, *Methods Enzymol.* 186 (1990) 502–511.
- [27] S. Tremblay, T. Gantchev, L. Tremblay, P. Lavigne, J. Cadet, J.R. Wagner, Oxidation of 2'-Deoxycytidine to Four Interconverting Diastereomers of N¹-Carbamoyl-4,5-dihydroxy-2-oxoimidazolidine Nucleosides, *J. Org. Chem.* 72 (2007) 3672–3678.
- [28] J.R. Wagner, C. Decarroz, M. Berger, J. Cadet, Hydroxyl-Radical-Induced Decomposition of 2'-Deoxycytidine in Aerated Aqueous Solutions, *J. Am. Chem. Soc.* 121 (1999) 4101–4110.
- [29] J. Cadet, K.J.A. Davies, M.H. Medeiros, P. Di Mascio, J.R. Wagner, Formation and repair of oxidatively generated damage in cellular DNA, *Free Radic. Biol. Med.* 107 (2017) 13–34.
- [30] J. Cadet, J.R. Wagner, V. Shafirovich, N.E. Geacintov, One-electron oxidation reactions of purine and pyrimidine bases in cellular DNA, *Int. J. Radiat. Biol.* 90 (2014) 423–432.

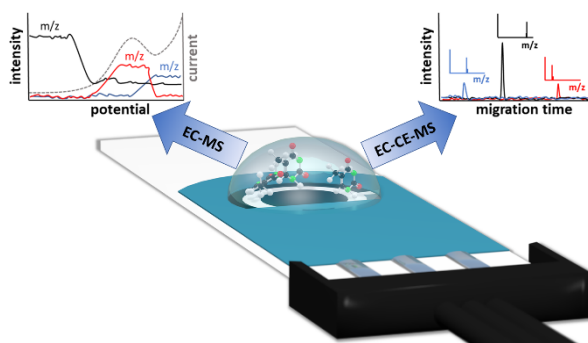
5.4 Investigation of the electrooxidation of thymine on screen-printed carbon electrodes by hyphenation of electrochemistry and mass spectrometry

This chapter was published in the journal *Analytical Chemistry*. The layout specifications of the journal were changed for uniformity. Copyright 2020 American Chemical Society.

T. Herl, F.-M. Matysik, *Anal. Chem.* **2020**, *92*, 6374-6381.

Abstract

The electrooxidation of thymine on screen-printed carbon electrodes was investigated utilizing different complementary instrumental approaches. The potential-dependent product profile was obtained by recording real-time mass voltammograms. Electrochemical flow cells with integrated disposable electrodes were directly coupled with mass spectrometry to facilitate a very fast detection of electrogenerated species. Thymine dimers were found at a potential of about 1.1 V in ammonium acetate (pH 7.0) and 1.25 V in ammonium hydrogen carbonate electrolyte (pH 8.0). Electrochemistry-capillary electrophoresis-mass spectrometry measurements revealed that two isobaric isomers of a dimeric oxidation product were formed. Separations at different time intervals between end of oxidation and start of separation showed that these were hydrated over time. An investigation of the pK_a values by changing the separation conditions in electrochemistry-capillary electrophoresis-ultraviolet-visible spectroscopy measurements allowed for further characterization of the primary oxidation products. The results showed that both isomers exhibited two deprotonation steps. The oxidation products were further characterized by high-performance liquid chromatography-tandem mass spectrometry. Based on the obtained data, the main oxidation products of thymine in aqueous solution could most likely be identified as N(1)-C(5') and N(1)-C(6') linked dimer species evolving into the corresponding dimer hydrates over time. The presented methods for online characterization of electrochemically pretreated samples showed that not only mass spectrometric data can be obtained by electrochemistry-mass spectrometry but also further characterizations such as the investigation of product stability and the pH-dependent protonation or deprotonation behavior are possible. This is valid not only for stable oxidation products but also for intermediates, as analysis can be carried out within a short time scale. Thus, a vast amount of valuable experimental data can be acquired, which can help in understanding electrooxidation processes.



5.4.1 Introduction

Developing methods for the investigation of nucleobase oxidation is important to improve the understanding of DNA damage caused by oxidative processes. In simulative studies, different methods can be applied for oxidation for example based on hydroxyl-radical [1] or radiation-mediated reactions [2–4]. Oxidative processes of purine and pyrimidine bases as well as DNA have been reviewed extensively by Cadet et al [5,6]. Being considered electrochemically inactive on carbon-based electrode materials for long time [7], cytosine and thymine can as well be oxidized electrochemically on glassy carbon electrodes [8], analogous to the well-investigated guanine [9]. Electrochemical oxidation is an attractive alternative to chemical and irradiative processes for simulation of oxidative stress due to the simple setup and well-controllable parameters such as the selection of electrode materials, oxidation potentials, and reaction time. Next to electrochemical simulation of oxidative processes, the electrochemical detection of nucleobases and modified nucleobases is applied in DNA sensing as reviewed by Hocek and Fojta [10]. Different carbon-based electrode materials for nucleobase oxidation were reviewed by Brotons et al [11]. Next to bare and modified glassy carbon, graphite, and gold paste electrodes [11–13], screen-printed platforms are also suitable for oxidation of DNA bases [14,15]. Regardless of the oxidation method, sophisticated analytical methods for the identification of oxidation products are needed to understand mechanistic details. Different instrumental approaches are available such as coupling of electrochemical flow cells to MS (EC-MS) or hyphenation of electrochemistry with separation methods like high-performance liquid chromatography or capillary electrophoresis combined with mass spectrometric detection (EC-HPLC-MS, EC-CE-MS) as recently reviewed by Portychová and Schug [16] in the context of xenobiotic metabolism. EC-MS and, in particular, electrochemical real-time mass spectrometry (EC-RTMS) measurements are characterized by a fast detection of electrogenerated species and allow for the investigation of reactive intermediates and dynamic processes such as the determination of oxidation products under potential sweep conditions [17]. By establishing flow cell configurations with very low dead volumes very fast transfer times to MS can be achieved [18]. However, if a separation step is added, additional information such as polarity of occurring structures can be obtained and fragmentation of respective peaks in MS can be investigated [19]. Using screen-printed platforms for oxidation offers different advantages. Screen-printed electrodes (SPEs) are easy to use and can easily be replaced avoiding time-consuming electrode maintenance procedures. Thus, they are suitable for routine and high-throughput investigations as a constant performance can be ensured. Additionally, only low amounts of sample solution are needed so that a sufficient number of measurements can be carried out even if the sample volume is limited [20]. Using capillary electrophoresis as a separation method, the oxidized sample can be injected into the capillary directly from the electrode surface allowing for a fast analysis and an efficient transfer into the separation system even at short electrolysis times [21]. Capillary electrophoresis facilitates not only separation but also further investigation of molecular properties of analytes based on the pH-dependent migration behavior. Thus, acidic and basic groups can be characterized and pK_a values can be determined [22]. Concerning

thymine oxidation, different oxidation products are described in literature including hydroxy and hydroperoxy species [23]. Besides that, thymine is also known for dimerization caused by UV-irradiation resulting in cyclobutene-pyrimidine dimers and (6-4) lesions [24–29]. Dimeric species caused by oxidation instead of photodimerization are much less described [3,30].

In this study, the investigation of electrochemical oxidation of thymine on bare screen-printed carbon electrodes (SPCEs) is presented. In contrast to cytosine, which we previously investigated with similar methods [31], thymine showed barely monomeric oxidation products. Instead, mainly dimeric oxidation products were detected under the applied conditions. The electrogenerated dimeric oxidation products of thymine were characterized by EC-MS, EC-CE-MS, EC-CE-UV/VIS, and EC-HPLC-MS/MS.

5.4.2 Experimental

Chemicals and solutions

Solutions of 1 and 0.1 mM thymine (T, purity \geq 99%, Sigma-Aldrich, St. Louis, MO, USA) were prepared by dissolution in aqueous solutions of 50 mM ammonium acetate (NH_4OAc , Merck KGaA, Darmstadt, Germany) at pH 7.0 or 50 mM ammonium hydrogen carbonate (NH_4HCO_3 , Roth, Karlsruhe, Germany) at pH 8.0 as electrolytes. 50 mM acetic acid (HOAc, Sigma-Aldrich) at pH 3.0, 50 mM NH_4OAc at pH 7.0, and 50 mM NH_4HCO_3 (Roth) at pH 10.0 were used as separation buffers for EC-CE-MS measurements (pH adjusted with NH_3 or HOAc). For EC-CE-UV/VIS measurements, 20 mM phosphate buffer ($\text{NaH}_2\text{PO}_4/\text{Na}_2\text{HPO}_4$) or 20 mM carbonate buffer ($\text{NaHCO}_3/\text{Na}_2\text{CO}_3$) were used as buffers in pH ranges of 6–8 and 9–11, respectively (pH adjusted with concentrated HCl or 1 M NaOH). 100 μM caffeine (C) was used as an EOF marker in EC-CE-MS measurements, and 0.1 mg mL^{-1} C was used as an EOF marker in EC-CE-UV/VIS measurements. Isopropanol (iPrOH, LC-MS grade) was obtained from Roth. All solutions were prepared with Milli-Q water ($18.2 \text{ M}\Omega \text{ cm}^{-1}$) provided by a Milli-Q Advantage A 10 system (Merck), and all chemicals were of analytical grade or higher if not stated otherwise.

Instruments

Oxidation of thymine was carried out on screen-printed carbon electrodes (DRP-110, DropSens, Llanera, Spain) that were used as received. Potentials were applied using a $\mu\text{Autolab III}$ potentiostat controlled by NOVA 2.0 software (Metrohm Autolab B. V., Utrecht, The Netherlands) in EC-MS and EC-CE-MS measurements or an ESA Coulochem II potentiostat (ESA Biosciences Inc., MA, USA) in EC-CE-UV/VIS measurements. A Bruker micrOTOF mass spectrometer (Bruker Daltonics, Bremen, Germany), equipped with a coaxial sheath liquid electrospray ionization interface (Agilent Technologies, Waldbronn, Germany) was used for MS detection. Sheath liquid (iPrOH/ H_2O /FA 49.9:49.9:0.2 v/v/v for EC-CE-MS and iPrOH/FA 99.8:0.2 v/v for EC-MS) was provided by a syringe pump (Type 161553, KD Scientific, Holliston, MA, USA) and a 1 mL glass syringe (ILS, Stützerbach, Germany) at a flow rate of 0.48 mL h^{-1} . The MS was operated in positive mode using the following

settings: mass range m/z 50-450, spectra rate 3 Hz, nebulizer 1.0 bar, dry gas 4.0 L min^{-1} , dry temperature $250 \text{ }^\circ\text{C}$. A Lambda 1010 UV/VIS detector (Bischoff Analysentechnik und -geräte GmbH, Leonberg, Germany) was used for UV/VIS detection at a wavelength of 250 nm. HPLC-MS measurements were carried out with an HPLC-Q-TOF-MS system (model 6540, Agilent Technologies) using the following parameters: Column: YMC-Triart C18, 1.9 μm , $75 \times 2 \text{ mm}$, 12 nm; Solvent A: $\text{H}_2\text{O} + 0.1\%$ formic acid, Solvent B: ACN + 0.1% formic acid, Gradient: 0 min 100% A/0% B, 4 min 100% A/0% B, 8 min 2% A/98% B, 9 min 2% A/98% B, 9.1 min 100% A/0% B, 10.1 min 100% A/0% B; flow rate 0.4 mL min^{-1} ; injected volume: $2.5 \text{ }\mu\text{L}$. Ion source: AJS ESI; dry gas temperature $300 \text{ }^\circ\text{C}$; dry gas flow 8 L min^{-1} ; nebulizer gas pressure 2.8 bar; sheath gas temperature $300 \text{ }^\circ\text{C}$; sheath gas flow 10 L min^{-1} . Collision induced dissociation of target species at 10 and 20 eV.

Instrumental setups and parameters

A schematic overview of the instrumental setups is depicted in Figure 5.4.1. For voltammetric studies, $50 \text{ }\mu\text{L}$ of 1 mM thymine solutions were applied onto screen-printed electrodes and potential scans were carried out at a scan rate of 50 mV s^{-1} . As illustrated in Figure 5.4.1A, EC-MS measurements were carried out by coupling an electrochemical flow cell with integrated SPCE (DRP-FLWCL, DropSens) to MS via a fused silica capillary ($50 \text{ }\mu\text{m} \times 21 \text{ cm}$, Polymicro Technologies, AZ, USA), which was installed in the cell using a modified PEEK fitting and sleeve as described previously [18]. The solutions were transported to the detector by a microinjection syringe pump (World Precision Instruments, Sarasota, FL, USA) equipped with a 1 mL glass syringe (Hamilton Company, Reno, NV, USA) at a flow rate of $16 \text{ }\mu\text{L min}^{-1}$, corresponding to a fast transfer time of 1-2 s between generation at the electrode and detection in MS (experimentally determined by using ferrocene methanol as model system at an oxidation potential of 0.5 V). Due to this fast detection of products, the real-time response of the product composition while scanning a potential ramp from 0 to 2 V at 10 mV s^{-1} could be recorded. Solutions of 1 mM and 0.1 mM thymine in 50 mM NH_4OAc (pH 7.0) or 50 mM NH_4HCO_3 (pH 8.0) were used.

EC-CE-MS (Figure 5.4.1B) and EC-CE-UV/VIS measurements (Figure 5.4.1C) were carried out using laboratory-constructed CE systems, as described elsewhere [21,32]. Samples were hydrodynamically injected into the separation capillary by placing the injection end of the capillary directly onto the working electrode surface during oxidation. The capillary tip was polished to an angle of 15° at the injection end with a laboratory-constructed polishing machine using lapping foils with a grain size of 30 and $9 \text{ }\mu\text{m}$ to ensure a reproducible injection position. For EC-CE-MS measurements, an oxidation potential of 1.2 V was applied for 15 s and injection was carried out in the last 10 s of oxidation. For EC-CE-UV/VIS measurements, oxidation was carried out at 1.2 V for 60 s and injection took place in the last 15 s. After injection, a separation voltage of 18 kV was applied. Capillary dimensions were $25 \text{ }\mu\text{m} \times 35 \text{ cm}$ for EC-CE-MS measurements and $50 \text{ }\mu\text{m} \times 50 \text{ cm}$ (effective length to detector 35 cm) for EC-CE-UV/VIS measurements. The choice of separation buffers is described in the respective parts

of the results section. Solutions of 1 mM thymine in 50 mM NH_4OAc (pH 7.0) were used for the investigations. HPLC-MS measurements were carried out after offline oxidation on an SPCE at 1.2 V for 180 s and transferring the 50 μL droplet into a sample vial.

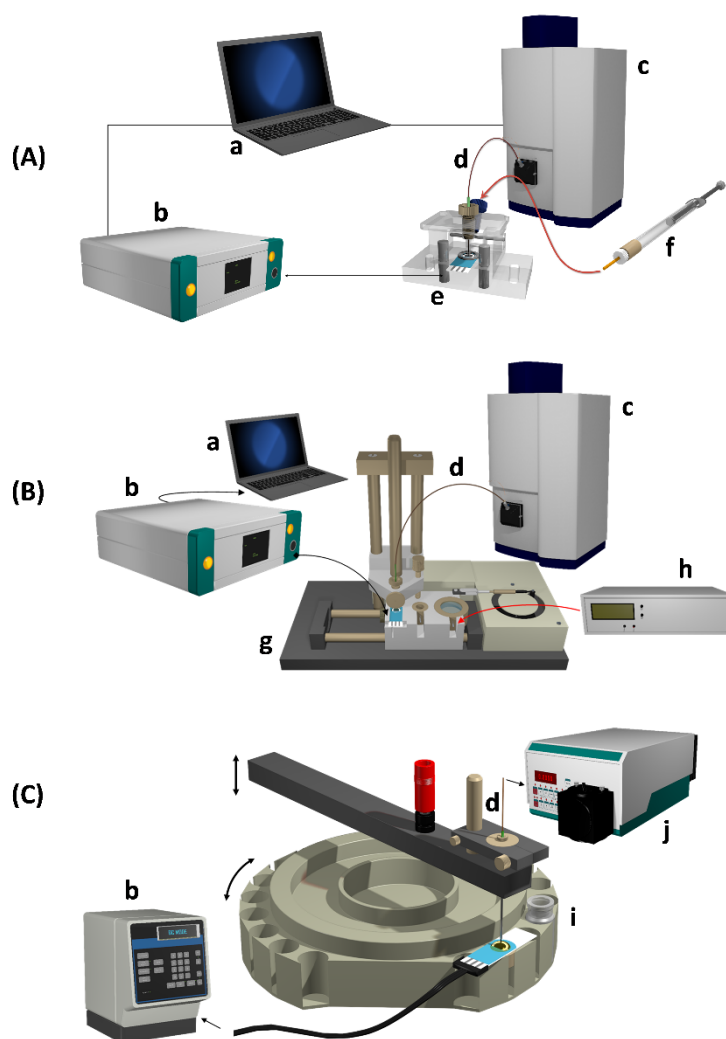


Figure 5.4.1 Schematic overviews of used setups: (A) EC-MS, (B) EC-CE-MS, and (C) EC-CE-UV/VIS. (a) Computer, (b) potentiostat, (c) time-of-flight mass spectrometer, (d) fused silica capillary, (e) flow cell with integrated SPCE, (f) syringe pump, (g) XZ-table with SPCE and buffer reservoirs, (h) HV source, (i) autosampler with SPCE and buffer reservoir, (j) UV detector.

5.4.3 Results and discussion

EC-MS measurements

Thymine was oxidizable on screen-printed carbon electrodes and showed an oxidation signal at about 1.1 V in static solution as depicted in the cyclic voltammogram in Figure 5.4.2A. Thus, EC-MS measurements were conducted for a real-time investigation of oxidation products within a short time scale, which was possible as the transfer time between electrochemical cell and mass spectrometer was only 1-2 s. In a linear potential scan from 0.5 to 2 V at a scan rate of 10 mV s^{-1} , the intensity of the

thymine mass trace (m/z 127.05, $[M+H]^+$, $C_5H_7N_2O_2$) started to decrease at around 1 V (potential shift due to transfer time neglectable for moderate scan rates), revealing a beginning consumption due to oxidation as can be seen in the mass voltammograms depicted in Figures 5.4.2B + 5.4.2C.

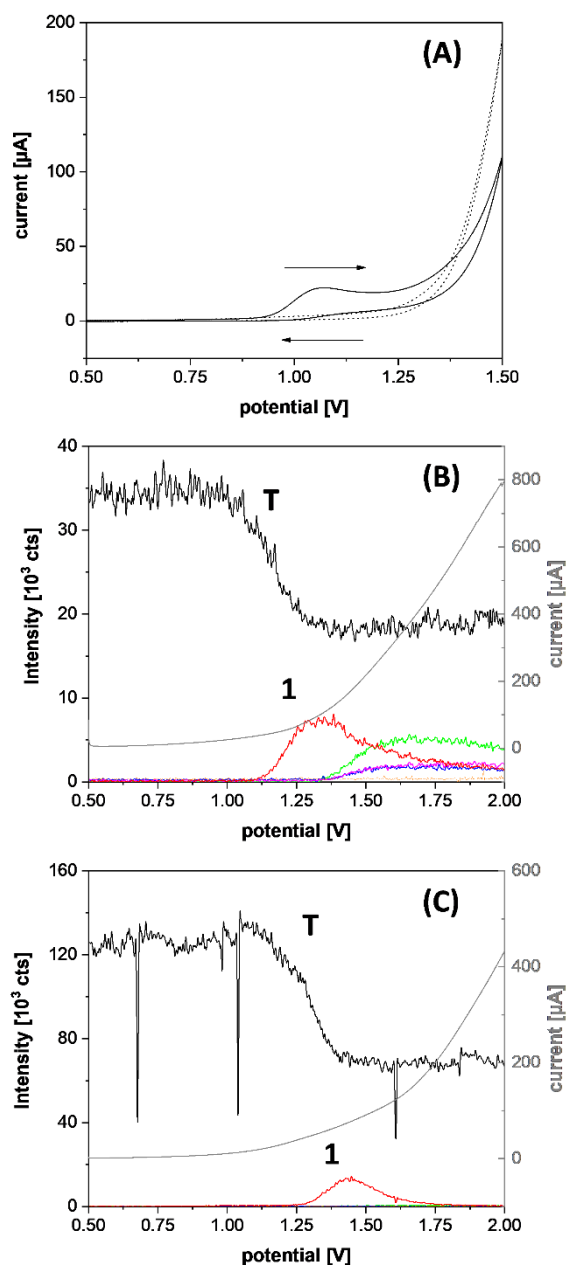


Figure 5.4.2 (A) Cyclic voltammogram of a 50 μ L droplet of 1 mM thymine (T) in 50 mM NH_4OAc on a SPCE at a scan rate of 50 $mV s^{-1}$ (dotted line electrolyte, solid line T in electrolyte), (B) EC-MS measurement of 0.1 mM T in 50 mM NH_4OAc and (C) EC-MS measurement of 0.1 mM T in 50 mM NH_4HCO_3 . Potential scans from 0.5 to 2 V at a scan rate of 10 $mV s^{-1}$. Flow rate 16 $\mu L min^{-1}$. Extracted mass traces m/z 127.05 (T, black), m/z 173.05 (green), m/z 190.08 (blue), m/z 191.07 (magenta), m/z 251.08 (product 1, red), and m/z 269.09 (orange). The current is plotted in gray. Transfer capillary 50 $\mu m \times 21$ cm.

A dimeric species with m/z 251.08 (1, $[M+H]^+$, $C_{10}H_{11}N_4O_4$) was the main product formed under the present conditions. The signal of this mass trace started to increase at around 1.1 V in NH_4OAc

electrolyte and around 1.25 V in NH_4HCO_3 electrolyte and decreased at potentials higher than 1.5 V in both cases indicating either a decomposition of the dimer or competing processes hindering the formation of this species. At higher potentials, additional products (m/z 173.05, m/z 190.08, m/z 191.07) were detected in NH_4OAc electrolyte (Figure 5.4.2B). Analogous to cytosine oxidation [31], these were most likely a result of the reaction of reactive intermediates with the electrolyte, as they were not detected if the oxidation was carried out in NH_4HCO_3 instead of NH_4OAc . MS data indicating the formation of acetoxy groups supported this suggestion. However, in both electrolytes the same main product (**1**) was detected in ESI-MS. In the time scale of EC-MS measurements, no significant amount of dimer hydrate species (m/z 269.09) could be detected, despite being proposed as final products in literature [3,30]. The mass voltammograms showed that EC-MS is a useful technique to characterize the electrochemical activity of analytes. Even if, in contrast to the cyclic voltammogram in static solution (Figure 5.4.2A), no clear oxidative wave was visible in the hydrodynamic potential scans depicted in Figure 5.4.2B and 5.4.2C, the oxidation of thymine was nevertheless visible in the MS signals. It can be assumed that adsorbed thymine contributes to the voltammetric signal and gets oxidized earlier in static solutions.

Separation behavior and product stability

Evaluating the migration behavior in CE, structural properties of the individual species were investigated based on protonation and deprotonation characteristics. MS detection allowed for identification of peaks by the corresponding molecular formulas. Neither thymine nor the oxidation products detected in this study were protonated in solution under the investigated conditions, as all were migrating with the EOF using NH_4OAc (pH 7.0) or HOAc (pH 3.0) as electrolyte for separation. Corresponding electropherograms are depicted in Figure 5.4.3A and 5.4.3B. Consequently, the structures exhibited no basic groups which would have resulted in cationic migration behavior in CE. In a CE measurement under alkaline conditions (NH_4HCO_3 , pH 10.0), a separation of thymine and its main oxidation product **1** with m/z 251.08 was possible. The measurements revealed that two isobaric species (**1a**, **1b**) with the same molecular formula ($\text{C}_{10}\text{H}_{11}\text{N}_4\text{O}_4$, $[\text{M}+\text{H}]^+$) but slightly different migration times were present (Figure 5.4.3C). These could not be distinguished in EC-MS measurements, as no separation step was included.

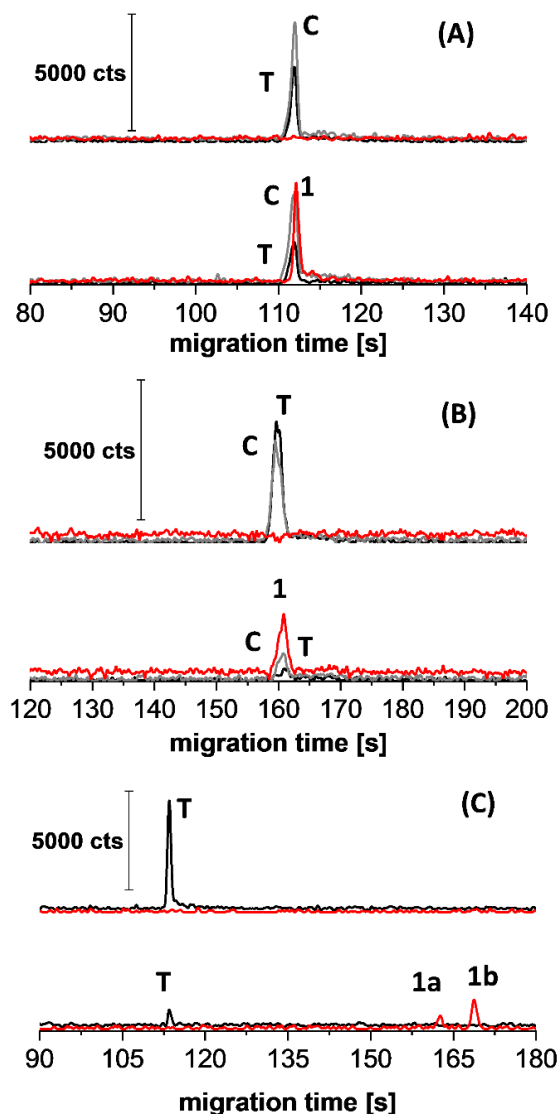


Figure 5.4.3 CE-MS measurements of 1 mM thymine (**T**) in 50 mM NH_4OAc in different electrolytes: 50 mM NH_4OAc at pH 7.0 (A), 50 mM HOAc at pH 3.0 (B), and 50 mM NH_4HCO_3 at pH 10.0 (C). The respective electropherograms at the top were recorded without oxidation and the electropherograms at the bottom were recorded after oxidation on an SPCE at 1.2 V for 15 s. Capillary 25 μm x 35 cm, separation voltage 18 kV, 10 s hydrodynamic injection. Extracted ion electropherograms of **T** (m/z 127.05, black), caffeine (**C**, m/z 195.09, gray), and product **1** (m/z 251.08, red).

In order to obtain additional structural information about the product isomers by collision induced dissociation (CID) measurements, HPLC-MS separations were carried out. Both product isomers could as well be separated by HPLC using a C18 column (Figure 5.4.4). However, due to the offline approach (oxidation on SPCE for 180 s followed by transfer into sample vial and HPLC-MS analysis) the obtained signal intensities of the products **1a** and **1b** were significantly lower compared to the thymine signal. Additionally, two peaks with m/z 269.09 (**2a** + **2b**, $\text{C}_{10}\text{H}_{13}\text{N}_4\text{O}_5$, $[\text{M}+\text{H}]^+$) were detected corresponding to the hydrated species of **1a** and **1b** as could be concluded from the mass difference of m/z 18 and the molecular formulas. The formation of such dimer hydrates is already known for quite a long time [33,34].

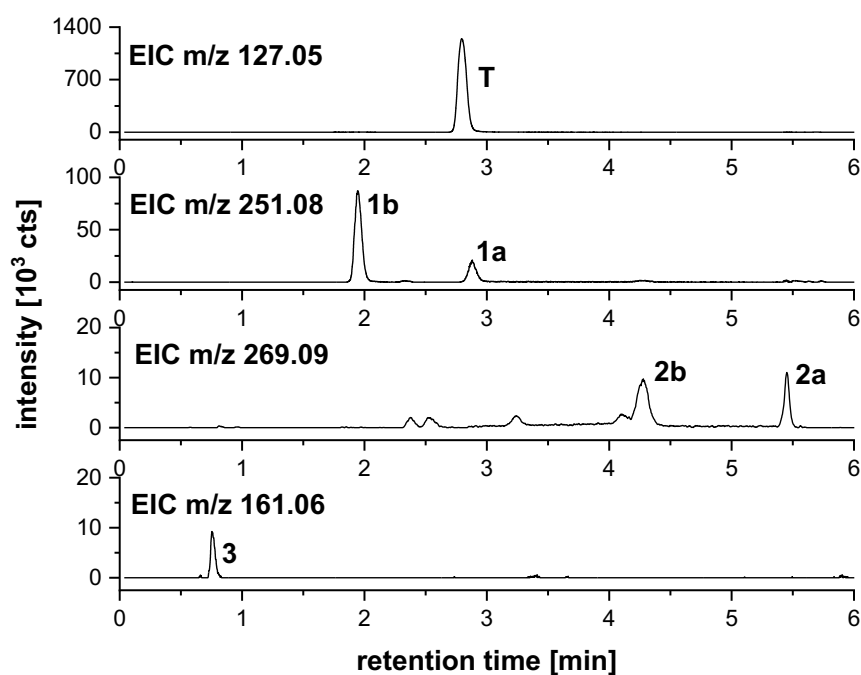
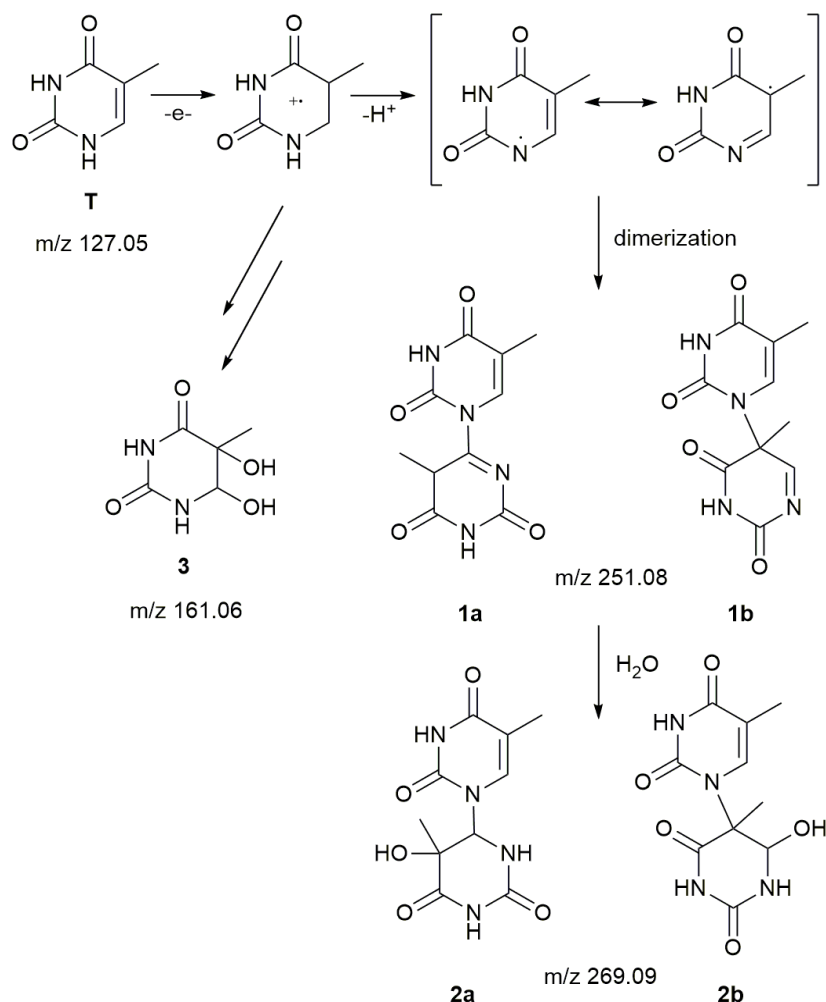


Figure 5.4.4 HPLC-MS of an electrochemically oxidized thymine solution (1.2 V, 180 s). Extracted ion chromatograms of thymine (**T**, EIC m/z 127.05), the dimeric products **1a** and **1b** (EIC m/z 251.08), the hydrated species **2a** and **2b** (EIC m/z 269.09), and the monomeric product **3** (EIC m/z 161.06). Separation on a C18 column.

CID measurements of all four compounds corresponding to the separated chromatographic peaks were carried out at collision energies of 10 and 20 eV (Figures 5.4.S1 and 5.4.S2). In all CID spectra a thymine fragment (m/z 127.05) was present. According to Chandran et al [3] this shows that the dimers were connected by C-N cross-links. A C-C cross-link could be ruled out, as in this case no thymine fragment and no dehydration to a fragment with m/z 251.08 would have been detected [3]. The occurrence of the corresponding dehydration fragments in CID supports the conclusion that **1a** and **1b** were direct precursors of **2a** and **2b**. Proposed structures of the different products are shown in Scheme 5.4.1 [3,30]. Comparing the collision spectra and the elution order of **2a** and **2b** to literature data, the structures could be assigned to the corresponding N(1)-C(5') (**2b**) and N(1)-C(6') linked species (**2a**) [3,30]. **2b** was more stable against CID as a much lower amount of fragments was obtained compared to **2a**, which already showed significant fragmentation at 10 eV (Figure 5.4.S2). Similar to **2b**, **1b** was more stable than **1a** where already significant fragmentation occurred at 10 eV (Figure 5.4.S1). By comparing the elution order, the relative signal intensities and the stability toward fragmentation, **1a** and **1b** were assigned to the corresponding N(1)-C(6') and N(1)-C(5') precursors of **2a** and **2b**. However, it has to be stated that further structural validation for example by preparative HPLC and NMR analysis is needed to fully confirm this, if the stability of the precursors is high enough to allow for this. This has to be tested in further measurements. As a side product of the electrochemical oxidation, a product most likely corresponding to thymine glycol (**3**, m/z 161.06, $C_5H_9N_2O_4$, $[M+H]^+$) could be detected based on measured mass and isotopic pattern.



Scheme 5.4.1 Proposed structures of the detected species and corresponding measured m/z values of $[M+H]^+$.

The product composition differed from previous studies found in literature where various additional monomeric products have been described [5,6,23]. This is probably due to the different kind of oxidation and sampling in this study (electrochemical oxidation instead of irradiation or radical mediated processes, short electrolysis time of 180 s on a carbon electrode instead of 5 h at 5 mA [34] or 150 min at 5 mA on a platinum electrode [30]). Due to the rather large surface area of the electrode compared to the small oxidized sample volume of 50 μL and the missing convection during oxidation, a high density of thymine radicals can be expected at the electrode surface so that radical coupling of thymine radicals to dimeric species was probably more favored than hydroxylation and subsequent reactions. However, as the time scale of oxidative sample preparation and analysis was quite short, the reaction intermediates **1a** and **1b** could be detected and characterized. CE-MS measurements with different time intervals between oxidation and separation showed a decrease of the intensity of m/z 251.08 and an increase of the intensity of m/z 269.09. This also verified that the primary oxidation products underwent hydration over time to the corresponding dimer hydrates **2a** and **2b**. A plot of the corresponding peak areas normalized to the thymine peak versus the time interval between start of the separation and the end of oxidation is shown in Figure 5.4.5. Due to low signal intensity in NH_4HCO_3 , these measurements had to be carried out in NH_4OAc so that only the cumulative information on both isomers could be obtained.

However, the general trend of hydration could be observed. To further characterize the intermediates **1a** and **1b**, the pH-dependent migration behavior was investigated using UV/VIS detection due to better reproducibility of migration times and higher flexibility in choice of separation buffer compared to MS detection.

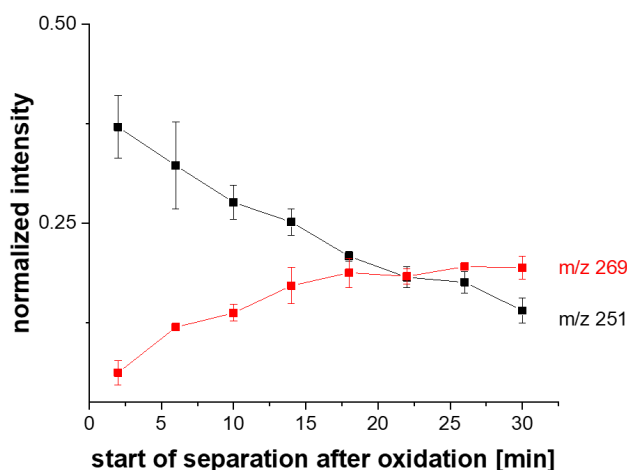


Figure 5.4.5 Development of the peak areas of products m/z 251.08 and m/z 269.09 depending on the time difference between end of oxidation (1 mM T in 50 mM NH₄OAc) and start of separation (50 mM NH₄OAc, pH 7.0). Oxidation on SPCE at 1.2 V for 600 s. Capillary 25 μ m x 35 cm, separation voltage 18 kV, 10 s hydrodynamic injection.

Characterization of oxidation products by EC-CE-UV/VIS measurements

For the characterization of the migration behavior of thymine and its main oxidation products **1a** and **1b**, two buffer systems (NaH₂PO₄/Na₂HPO₄ for pH 6-9 and NaHCO₃/Na₂CO₃ for pH 9-11) were used. The electrophoretic current was kept at 30 ± 5 μ A for all separations to avoid excessive Joule heating which would lead to irreproducible migration times. All measurements were carried out at a room temperature of 25 °C. The migration behavior relative to the EOF marker caffeine was evaluated and the electrophoretic mobility was calculated based on Caliaro and Herbots [22]. Figure 5.4.6 shows some representative electropherograms. First a measurement of caffeine was made to determine the EOF, followed by measurements of thymine solution without oxidation and after oxidation. Each set of measurements was carried out three times. With increasing pH values, the migration times of thymine and **1a** as well as **1b** increased relative to the EOF, showing an increasing rate of deprotonation. As expected, a plot of the electrophoretic mobilities versus pH showed a sigmoidal curve for thymine (Figure 5.4.7A) meaning that thymine exhibited one deprotonation step. A sigmoidal fit of the data based on Caliaro and Herbots [22] resulted in a calculated pK_a value of 9.80 ± 0.02 (Figure 5.4.S3), which is in reasonable accordance to literature where a pK_a value of 9.94 is reported [35]. The plots obtained for **1a** and **1b** (Figures 5.4.7B and 5.4.7C) showed two sigmoidal ranges, leading to the conclusion that, in contrast to thymine, two possible deprotonation sites were present due to the dimeric structure. Sigmoidal fits of the respective ranges of the experimental data revealed pK_a values of 7.9 ± 0.1 and 10.1 ± 0.4 for **1a** and 7.77 ± 0.03 and 10.45 ± 0.06 for **1b** (Figures 5.4.S4 and 5.4.S5). The

measurements demonstrated that varying the separation conditions in capillary electrophoresis is an attractive method to obtain molecular information like pK_a values of electrogenerated species. Oxidized samples can be analyzed without the need for quantitative generation and tedious sample preparation. Combined with MS data evaluating the migration behavior thus is a powerful method for the characterization of oxidation products.

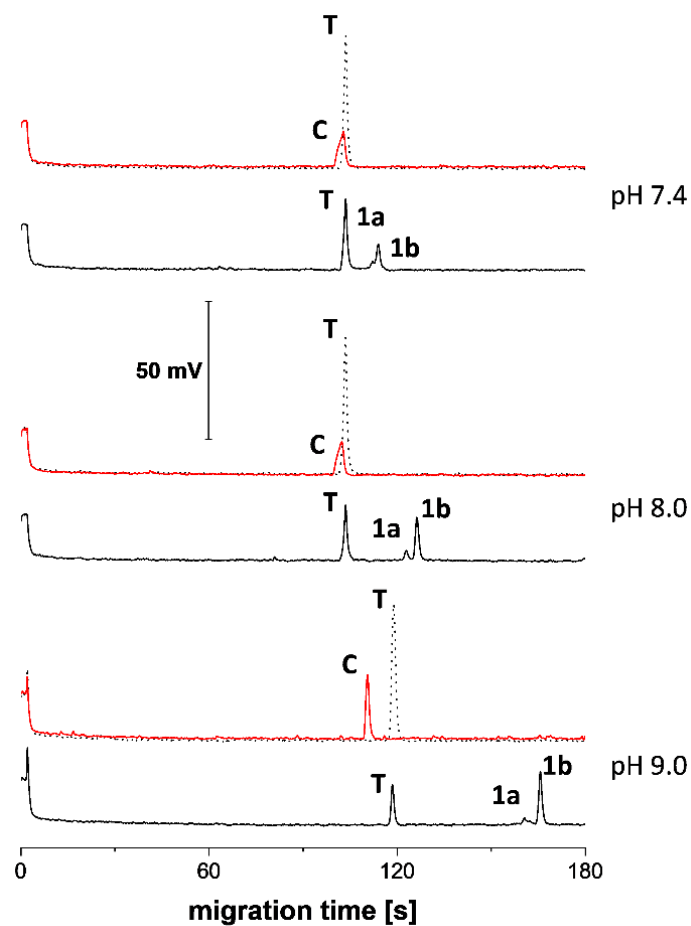


Figure 5.4.6 (A) Representative electropherograms at different pH of separation buffers showing the migration behavior of thymine (**T**), caffeine (**C**), and both isobaric products **1a** and **1b**. Capillary $50\ \mu\text{m} \times 50\ \text{cm}$, $L_{\text{eff}}\ 35\ \text{cm}$, $18\ \text{kV}$, $15\ \text{s}$ hydrodynamic injection, UV detection at $250\ \text{nm}$. Measurements of **C** (red) and **T** without oxidation (black, dotted) and **T** after oxidation at $1.2\ \text{V}$ for $60\ \text{s}$ (black).

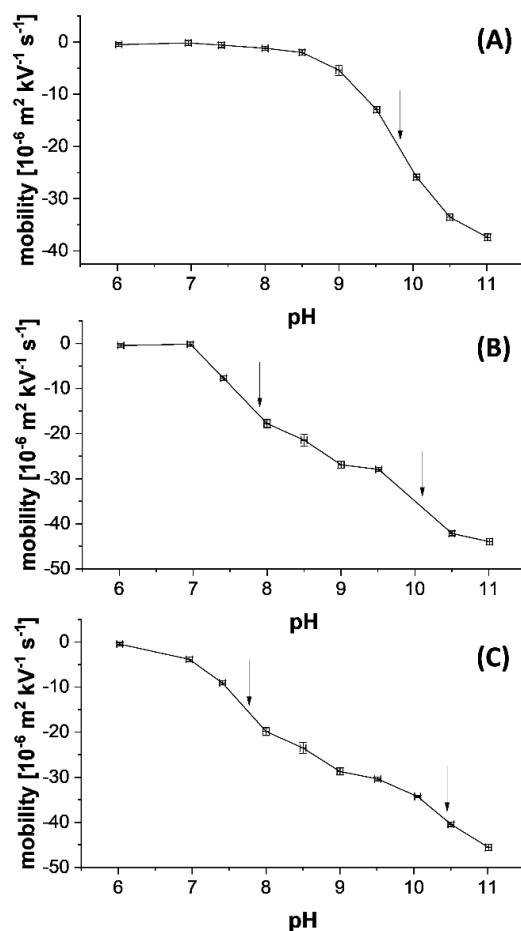


Figure 5.4.7 Evaluation of electrophoretic mobilities vs. pH for **T** (A), product **1a** (B), and product **1b** (C). Calculation of electrophoretic mobilities based on literature [22]. The pK_a values calculated by fitting the experimental data are marked by arrows (Fit data are shown in Figures 5.4.S3 – 5.4.S5).

5.4.4 Conclusion

Thymine was found oxidizable on commercial screen-printed carbon electrodes. A range of different methods were applied to investigate the thymine oxidation products generated on this electrode material. EC-MS measurements using electrochemical flow cells allowed for real-time characterization of the redox properties of thymine and showed that dimeric species were the main products that were formed upon electrochemical oxidation. Product generation started, depending on the electrolyte, at 1.1 to 1.2 V as could be seen by recording the real-time MS signals in parallel to potential scans. CE-MS measurements revealed that the primary dimeric product of thymine oxidation was present in two different isomers as two isobaric compounds could be separated under alkaline separation conditions. Further characterization of these products by CE-MS measurements with increasing time intervals between end of oxidation and start of separation showed that the primary products were precursors of stable dimer hydrates as already described in literature. EC-CE-UV/VIS measurements at different pH of separation showed that both precursor isomers exhibited two deprotonation steps and the corresponding pK_a values were determined based on the experimental data. This demonstrated the capability of EC-CE to analyze in-situ generated products which is very advantageous if the compounds

are not stable enough to be isolated and to be investigated by classical titration methods. To obtain further information, offline EC-HPLC-MS/MS measurements were carried out. By combining all results and comparing to literature, it could be concluded that thymine was forming N(1)-C(5') and N(1)-C(6') linked dimer hydrates induced by electrochemical oxidation on screen-printed carbon electrodes. Due to the short time scale of electrochemical sample preparation and subsequent analysis, the characterization of reaction intermediates could be achieved. Further studies might deal with cross-coupling reactions of oxidized thymine with other nucleobases or biologically relevant molecules such as pharmaceutical compounds. The results show that the presented complementary methods EC-MS, EC-CE-MS, EC-CE-UV/VIS, and EC-HPLC-MS/MS are an attractive approach for the characterization of electrogenerated species. They offer the advantages of high flexibility, low consumption of samples and solutions, fast analysis, and low sample preparation. Products can be characterized on different time scales and mass spectrometric data can be combined with the migration behavior in CE and retention behavior in HPLC, delivering a large range of valuable information. Considering the proceeding progress in computational techniques, the obtained experimental data (e.g. pK values) might be combined with simulations to verify proposed structures in nontargeted analysis and mechanisms in future applications.

Acknowledgements

J. Kiermaier of the MS department of the University of Regensburg is acknowledged for his support with MS/MS measurements.

References

- [1] G.S. Madugundu, J. Cadet, J.R. Wagner, Hydroxyl-radical-induced oxidation of 5-methylcytosine in isolated and cellular DNA, *Nucleic Acids Res.* 42 (2014) 7450–7460.
- [2] J. Ma, J.-L. Marignier, P. Pernot, C. Houée-Levin, A. Kumar, M.D. Sevilla, A. Adhikary, M. Mostafavi, Direct observation of the oxidation of DNA bases by phosphate radicals formed under radiation: a model of the backbone-to-base hole transfer, *Phys. Chem. Chem. Phys.* 20 (2018) 14927–14937.
- [3] J. Chandran, N.R. Vishnu, U.K. Aravind, C.T. Aravindakumar, ESI-CID spectral characterization and differentiation of the cross links of thymine formed by one electron oxidation with $\text{SO}_4^{\cdot-}$, *Int. J. Mass Spectrom.* 443 (2019) 53–60.
- [4] M. Gomez-Mendoza, A. Banyasz, T. Douki, D. Markovitsi, J.-L. Ravanat, Direct Oxidative Damage of Naked DNA Generated upon Absorption of UV Radiation by Nucleobases, *J. Phys. Chem. Lett.* 7 (2016) 3945–3948.
- [5] J. Cadet, J.R. Wagner, V. Shafirovich, N.E. Geacintov, One-electron oxidation reactions of purine and pyrimidine bases in cellular DNA, *Int. J. Radiat. Biol.* 90 (2014) 423–432.
- [6] J. Cadet, K.J.A. Davies, M.H. Medeiros, P. Di Mascio, J.R. Wagner, Formation and repair of oxidatively generated damage in cellular DNA, *Free Radic. Biol. Med.* 107 (2017) 13–34.
- [7] J.P. Hart, *Electroanalysis of Biologically Important Compounds*, Ellis Horwood Limited, Chichester, 1990.
- [8] A.M. Oliveira Brett, F.-M. Matysik, Voltammetric and sonovoltammetric studies on the oxidation of thymine and cytosine at a glassy carbon electrode, *J. Electroanal. Chem.* 429 (1997) 95–99.
- [9] R.N. Goyal, G. Dryhurst, Redox chemistry of guanine and 8-oxyguanine and a comparison of the peroxidase-catalyzed and electrochemical oxidation of 8-oxyguanine, *J. Electroanal. Chem. Interfacial Electrochem.* 135 (1982) 75–91.
- [10] M. Hocek, M. Fojta, Nucleobase modification as redox DNA labelling for electrochemical detection, *Chem. Soc. Rev.* 40 (2011) 5802–5814.
- [11] A. Brotons, F.J. Vidal-Iglesias, J. Solla-Gullón, J. Iniesta, Carbon materials for the electrooxidation of nucleobases, nucleosides and nucleotides toward cytosine methylation detection: A review, *Anal. Methods* 8 (2016) 702–715.
- [12] H. Li, X. Wang, Z. Wang, W. Zhao, Simultaneous determination of guanine, adenine, thymine and cytosine with a simple electrochemical method, *J. Solid State Electrochem.* 20 (2016) 2223–2230.
- [13] J. Jankowska-Śliwińska, M. Dawgul, J. Kruk, D.G. Pijanowska, Comparison of electrochemical determination of purines and pyrimidines by means of carbon, graphite and gold paste electrodes, *Int. J. Electrochem. Sci.* 12 (2017) 2329–2343.
- [14] A. Brotons, L.A. Mas, J.P. Metters, C.E. Banks, J. Iniesta, Voltammetric behaviour of free DNA bases, methylcytosine and oligonucleotides at disposable screen printed graphite electrode platforms., *Analyst* 138 (2013) 5239–49.
- [15] A. Brotons, I. Sanjuan, C.E. Banks, F.J. Vidal-Iglesias, J. Solla-Gullón, J. Iniesta, Voltammetric Behaviour of 7-Methylguanine Using Screen-printed Graphite Electrodes: Towards a Guanine Methylation Electrochemical Sensor, *Electroanalysis* 27 (2015) 2766–2772.
- [16] L. Portychová, K.A. Schug, Instrumentation and applications of electrochemistry coupled to mass spectrometry for studying xenobiotic metabolism: A review, *Anal. Chim. Acta* 993 (2017) 1–21.
- [17] P. Khanipour, M. Löffler, A.M. Reichert, F.T. Haase, K.J.J. Mayrhofer, I. Katsounaros, Electrochemical Real-Time Mass Spectrometry (EC-RTMS): Monitoring Electrochemical Reaction Products in Real Time, *Angew. Chemie Int. Ed.* 58 (2019) 7273–7277.

- [18] T. Herl, F.-M. Matysik, Characterization of electrochemical flow cell configurations with implemented disposable electrodes for the direct coupling to mass spectrometry, *Tech. Mess.* 84 (2017) 672–682.
- [19] H. Faber, D. Melles, C. Brauckmann, C.A. Wehe, K. Wentker, U. Karst, Simulation of the oxidative metabolism of diclofenac by electrochemistry/(liquid chromatography)/mass spectrometry, *Anal. Bioanal. Chem.* 403 (2012) 345–354.
- [20] P. Palatzky, F.-M. Matysik, Development and characterization of a novel semiautomated arrangement for electrochemically assisted injection in combination with capillary electrophoresis time-of-flight mass spectrometry, *Electrophoresis* 33 (2012) 2689–2694.
- [21] P. Palatzky, A. Zöpfl, T. Hirsch, F.-M. Matysik, Electrochemically Assisted Injection in Combination with Capillary Electrophoresis-Mass Spectrometry (EAI-CE-MS) - Mechanistic and Quantitative Studies of the Reduction of 4-Nitrotoluene at Various Carbon-Based Screen-Printed Electrodes, *Electroanalysis* 25 (2013) 117–122.
- [22] G.A. Caliaro, C.A. Herbots, Determination of pKa values of basic new drug substances by CE, *J. Pharm. Biomed. Anal.* 26 (2001) 427–434.
- [23] J. Cadet, J. Richard Wagner, DNA base damage by reactive oxygen species, oxidizing agents, and UV radiation, *Cold Spring Harb. Perspect. Biol.* 5 (2013).
- [24] T. Douki, M. Court, S. Sauvaigo, F. Odin, J. Cadet, Formation of the Main UV-induced Thymine Dimeric Lesions within Isolated and Cellular DNA as Measured by High Performance Liquid Chromatography-Tandem Mass Spectrometry, *J. Biol. Chem.* 275 (2000) 11678–11685.
- [25] K. Haiser, B.P. Fingerhut, K. Heil, A. Glas, T.T. Herzog, B.M. Pilles, W.J. Schreier, W. Zinth, R. de Vivie-Riedle, T. Carell, Mechanism of UV-Induced Formation of Dewar Lesions in DNA, *Angew. Chemie Int. Ed.* 51 (2012) 408–411.
- [26] B. Durbeej, L.A. Eriksson, Reaction mechanism of thymine dimer formation in DNA induced by UV light, *J. Photochem. Photobiol. A Chem.* 152 (2002) 95–101.
- [27] I. Conti, L. Martínez-Fernández, L. Esposito, S. Hofinger, A. Nenov, M. Garavelli, R. Improta, Multiple Electronic and Structural Factors Control Cyclobutane Pyrimidine Dimer and 6-4 Thymine-Thymine Photodimerization in a DNA Duplex, *Chem. - A Eur. J.* 23 (2017) 15177–15188.
- [28] M.D. Shetlar, V.J. Basus, The Photochemistry of Thymine in Frozen Aqueous Solution: Trimeric and Minor Dimeric Products, *Photochem. Photobiol.* 89 (2013) 631–639.
- [29] T. Douki, M. Court, J. Cadet, Electrospray-mass spectrometry characterization and measurement of far-UV-induced thymine photoproducts, *J. Photochem. Photobiol. B Biol.* 54 (2000) 145–154.
- [30] H. Hatta, L. Zhou, M. Mori, S. Teshima, S. Nishimoto, N(1)-C(5′)-Linked Dimer Hydrates of 5-Substituted Uracils Produced by Anodic Oxidation in Aqueous Solution, *J. Org. Chem.* 66 (2001) 2232–2239.
- [31] T. Herl, L. Taraba, D. Böhm, F.-M. Matysik, Electrooxidation of cytosine on bare screen-printed carbon electrodes studied by online electrochemistry-capillary electrophoresis-mass spectrometry, *Electrochem. Commun.* 99 (2019) 41–45.
- [32] J.J.P. Mark, P. Piccinelli, F.-M. Matysik, Very fast capillary electrophoresis with electrochemical detection for high-throughput analysis using short, vertically aligned capillaries, *Anal. Bioanal. Chem.* 406 (2014) 6069–6073.
- [33] J.R. Wagner, J. Cadet, G.J. Fisher, Photo-oxidation of thymine sensitized by 2-methyl-1,4-naphthoquinone: analysis of products including three novel photo-dimers, *Photochem. Photobiol.* 40 (1984) 589–597.

- [34] S. Nishimoto, H. Hatta, H. Ueshima, T. Kagiya, 1-(5'-Fluoro-6'-hydroxy-5',6'-dihydrouracil-5'-yl)-5-fluorouracil, a novel N(1)-C(5)-linked dimer that releases 5-fluorouracil by radiation activation under hypoxic conditions, *J. Med. Chem.* 35 (1992) 2711–2712.
- [35] S. Budavari, M.J. O'Neil, A. Smith, P.E. Heckelman, J.F. Kinneary, eds., *The Merck Index*, 12th editi, Merck Research Laboratories Division, New York, 1996.

5.4.5 Supporting information

The Supporting Information contains:

- Figure 5.4.S1 (CID spectra of oxidation products **1a** and **1b**)
- Figure 5.4.S2 (CID spectra of oxidation products **2a** and **2b**)
- Figure 5.4.S3 (fit data for the calculation of the pK_a of thymine)
- Figure 5.4.S4 (fit data for the calculation of the pK_a values of **1a**)
- Figure 5.4.S5 (fit data for the calculation of the pK_a values of **1b**)

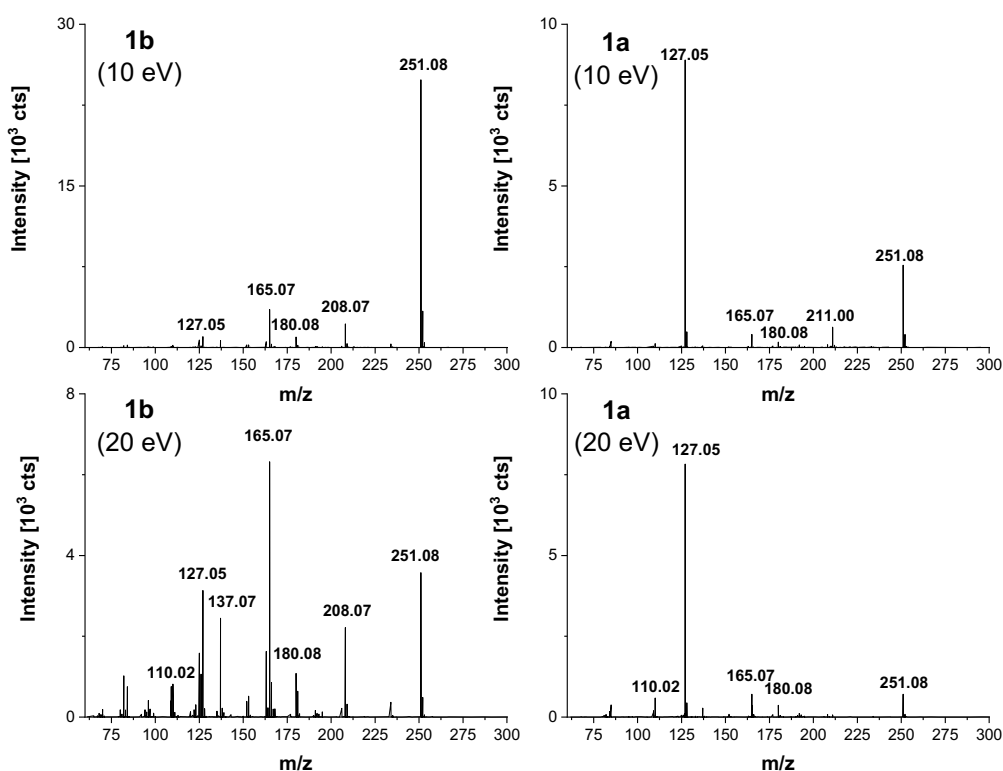


Figure 5.4.S1 CID spectra of **1b** at collision energies of 10 eV and 20 eV (left column) and CID spectra of **1a** at collision energies of 10 eV and 20 eV (right column).

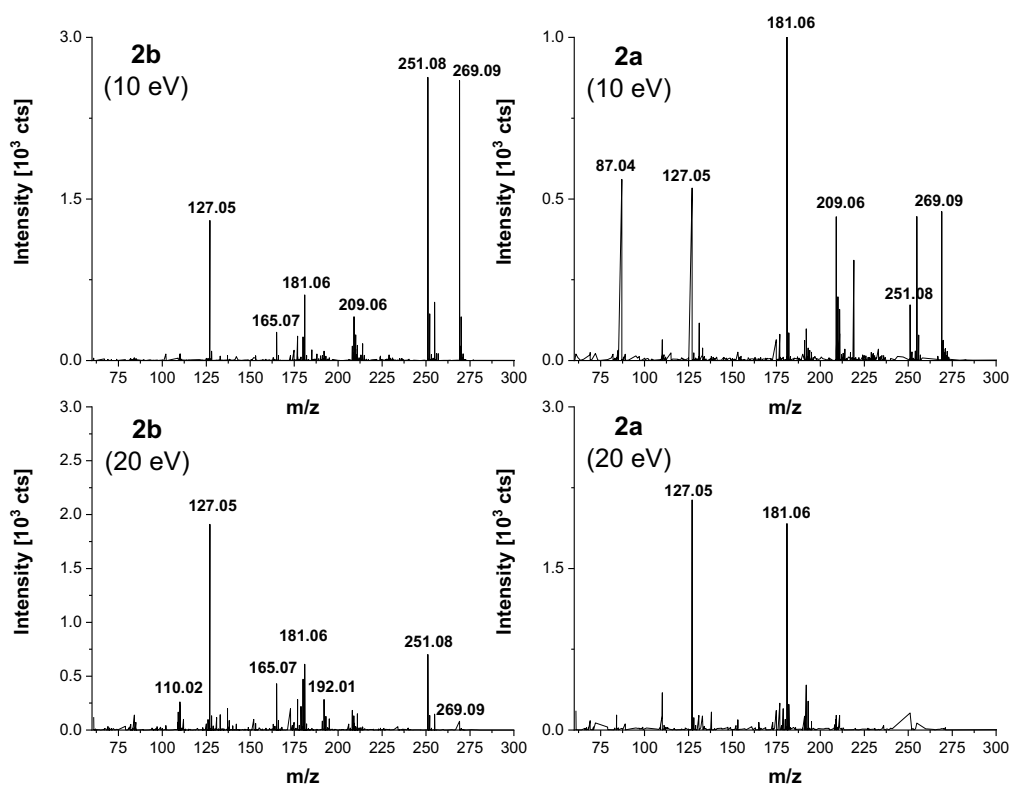


Figure 5.4.S2 CID spectra of **2b** at collision energies of 10 eV and 20 eV (left column) and CID spectra of **2a** at collision energies of 10 eV and 20 eV (right column).

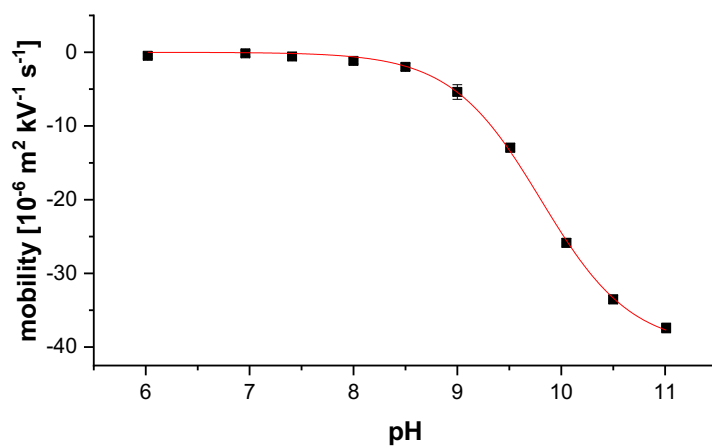


Figure 5.4.S3 Fit data for the calculation of the pK_a value of thymine. Fit by $M_e = M_a / (10^{(pK_a - pH)} + 1)$ with $M_a = -4.01 \cdot 10^{-5} \pm 0.06 \cdot 10^{-5} \text{ m}^2 \text{ kV}^{-1} \text{ s}^{-1}$ and $pK_a 9.80 \pm 0.02$.

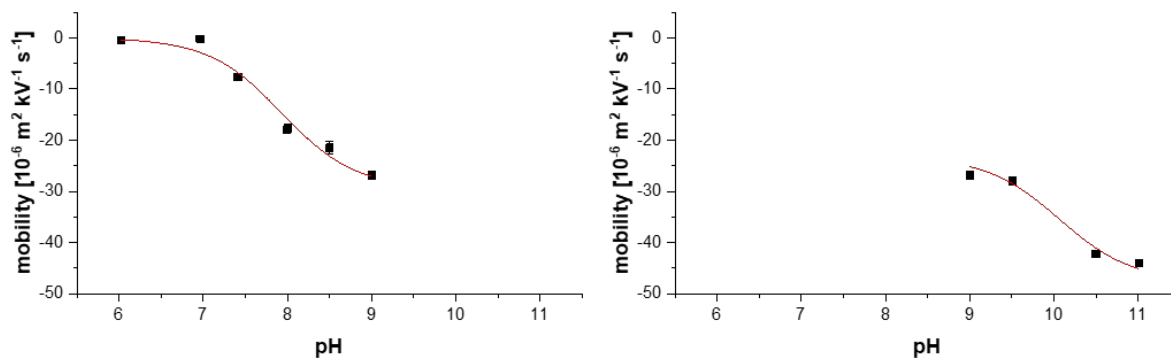


Figure 5.4.S4 Fit data for the calculation of the pK_a values of **1a**. Fit by $M_e = M_a/(10^{(pK_a-pH)}+1)$ with $M_a = -2.9 \cdot 10^{-5} \pm 0.3 \cdot 10^{-5} \text{ m}^2 \text{ kV}^{-1} \text{ s}^{-1}$ and $pK_a 7.9 \pm 0.1$ (left) and $M_e = M_a/(10^{(pK_a-pH)}+1)+C$ with $M_a = -2.4 \cdot 10^{-5} \pm 0.3 \cdot 10^{-5} \text{ m}^2 \text{ kV}^{-1} \text{ s}^{-1}$, $pK_a 10.1 \pm 0.4$ and $C -2.3 \cdot 10^{-5} \pm 0.4 \cdot 10^{-5} \text{ m}^2 \text{ kV}^{-1} \text{ s}^{-1}$ (right).

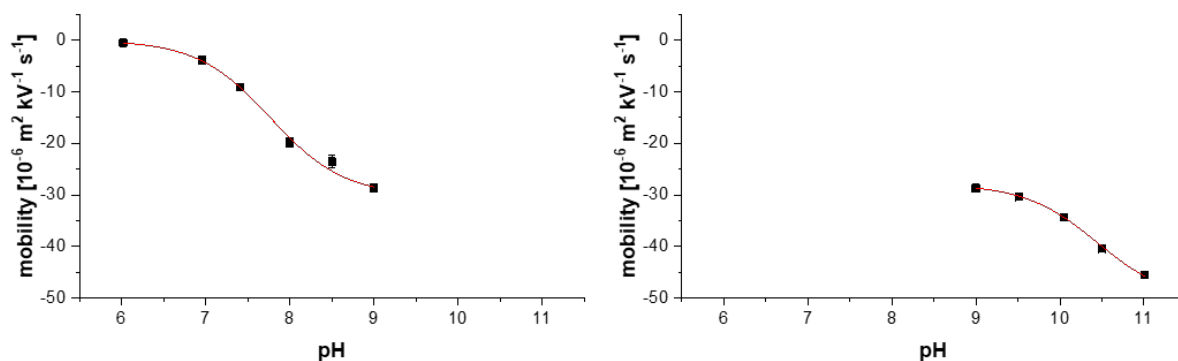


Figure 5.4.S5 Fit data for the calculation of the pK_a values of **1b**. Fit by $M_e = M_a/(10^{(pK_a-pH)}+1)$ with $M_a = -3.01 \cdot 10^{-5} \pm 0.08 \cdot 10^{-5} \text{ m}^2 \text{ kV}^{-1} \text{ s}^{-1}$ and $pK_a 7.77 \pm 0.03$ (left) and $M_e = M_a/(10^{(pK_a-pH)}+1)+C$ with $M_a = -2.3 \cdot 10^{-5} \pm 0.1 \cdot 10^{-5} \text{ m}^2 \text{ kV}^{-1} \text{ s}^{-1}$, $pK_a 10.45 \pm 0.06$ and $C -2.79 \cdot 10^{-5} \pm 0.04 \cdot 10^{-5} \text{ m}^2 \text{ kV}^{-1} \text{ s}^{-1}$ (right).

6. Summary

Hyphenation of electrochemistry and mass spectrometry is a very versatile method for different kinds of applications such as

- electrochemical online sample pretreatment for enhanced detectability of analytes and separation performance
- elucidation of oxidation and reduction mechanisms by identification of intermediates and products
- electrochemical simulation of oxidative processes of relevant biomolecules.

To meet the demands of the high diversity of different kinds of samples, flexibility of solutions and materials is very important. Because of that a novel injection cell for EC-CE-MS consisting of solvent-resistant materials and equipped with solvent-resistant thin-film electrodes was developed and characterized. EC-CE-MS could be applied to non-aqueous solutions and a mixture of ferrocene derivatives was analyzed as model system. After oxidation, the cations of ferrocenemethanol, decamethylferrocene and ferrocene could be separated with capillary electrophoresis and detected with mass spectrometry. This was not possible without oxidation as neutral ferrocene is not detectable in ESI-MS and neutral ferrocenemethanol can only be detected with very low intensity. Besides that, both would comigrate in CE due to the lack of charge. However, decamethylferrocene was separated and detected without electrochemical oxidation as it was easily oxidized by dissolved oxygen. In conclusion, it was shown that electrochemistry could be used to enhance the separation performance in CE and the detection performance in MS by generation of charged species. The applicability of online EC-CE-MS based on disposable electrode materials could be expanded to non-aqueous solvents, which was not possible before due to limitations of screen-printed electrode materials.

For optimization of oxidation procedures in the context of electrochemical sensing it is important to understand the processes that take place on an electrode surface. Different primary bile acids were shown to be suitable for direct electrochemical oxidation after an acid-induced dehydration step. CE-MS measurements revealed the dehydration and addition of an acetamide group to chenodeoxycholic acid, which could be confirmed by the migration behavior in CE and the identification of the molecular formulas of the corresponding species in MS. Hence, CE-MS could contribute to the elucidation of different reaction steps in the context of anodic oxidation of bile acids.

Nucleobases are essential for life due to their function as building blocks of DNA. In order to understand oxidative damage on DNA or to detect modified nucleobases electrochemically it is important to investigate the mechanisms of nucleobase oxidation. Online EC-MS, EC-CE-MS, EC-HPLC-MS and tandem MS were applied to investigate anodic oxidation of cytosine and thymine in aqueous solutions on screen-printed carbon electrodes. EC-MS based on electrochemical flow cells allowed for a fast and direct detection of oxidation products and thus for a screening of electrochemical activity and reactive

intermediates or instable species. By variation of the separation conditions in CE, the presence of acidic or basic functional groups could be investigated based on the migration behavior. Due to short analysis times, conclusions on product stability could be drawn by evaluating the development of the analyte signals in consecutive measurements. MS detection allowed for the identification of oxidation products. EC-HPLC-MS and tandem MS measurements added additional information due to the orthogonality of the separation methods and fragmentation patterns obtained in collision induced dissociation. Cytosine and thymine showed different kinds of products at the applied conditions. While in the case of cytosine monomeric oxidation products exhibiting hydroxy and hydroperoxy groups were detected as main products, thymine predominantly showed dimerization induced by electrochemical oxidation. The oxidation products of cytosine could be separated under acidic conditions while a separation of the oxidation products of thymine could only be achieved under alkaline conditions in capillary electrophoresis. Thus, both analytes behaved completely different despite using similar oxidation conditions.

All results mentioned above show that EC-MS based on disposable electrodes is a powerful and versatile instrumental approach to different analytical challenges. By combination of electrochemical oxidation with separation methods and MS detection a large amount of information can be obtained such as the nature of functional groups based on the migration behavior in CE and retention behavior in HPLC, the product stability, and the mechanisms of electrochemical reactions by identification of products and intermediates. Easy-to-use and virtually maintenance-free disposable electrode materials as well as short separation times make this method interesting for high-throughput measurements. Thus, EC-MS might be of rising interest for applications in medical or pharmaceutical industry in the future.

7. Zusammenfassung in deutscher Sprache

Die Kopplung von Elektrochemie mit der Massenspektrometrie ist eine sehr vielseitige Methode mit verschiedenen Anwendungsmöglichkeiten wie beispielsweise der

- elektrochemischen online-Probenvorbereitung zur verbesserten Detektierbarkeit von Analyten und Erhöhung der Trennperformance
- Aufdeckung von Oxidations- oder Reduktionsmechanismen über die Identifizierung auftretender Spezies
- elektrochemischen Simulation oxidativer Prozesse relevanter Biomoleküle.

Um den Anforderungen unterschiedlichster Proben gerecht zu werden ist eine hohe Flexibilität bezüglich verwendeter Lösungen und Materialien unabdingbar. Deshalb wurde eine neuartige Injektionszelle für die EC-CE-MS Kopplung entwickelt und charakterisiert, die aus lösemittelbeständigen Materialien bestand und mit lösemittelbeständigen Dünnschichtelektroden bestückt war. Die EC-CE-MS Methodik konnte somit auf nichtwässrige Systeme angewandt werden und eine Mischung von Ferrocenderivaten wurde als Modellsystem analysiert. Nach der Oxidation konnten die Kationen von Ferrocenmethanol, Decamethylferrocen und Ferrocen mittels Kapillarelektrophorese getrennt und mit Massenspektrometrie detektiert werden. Dies war ohne vorherige Oxidation nicht möglich, da neutrales Ferrocen mit ESI-MS nicht und neutrales Ferrocenmethanol nur sehr schlecht detektierbar ist. Außerdem würden beide im ungeladenen Zustand in der Kapillarelektrophorese komigrieren. Decamethylferrocen konnte auch ohne elektrochemische Oxidation als Kation detektiert werden, da es sehr leicht durch gelösten Sauerstoff oxidiert wird. Zusammenfassend konnte die Elektrochemie hier genutzt werden, um die Trennleistung in der Kapillarelektrophorese sowie die Detektierbarkeit in der Massenspektrometrie durch die Erzeugung geladener Spezies zu verbessern. Es wurde demonstriert, dass die Anwendbarkeit von EC-CE-MS auf der Basis von Einwegelektroden auf nichtwässrige Systeme erweitert werden konnte, was zuvor aufgrund der Limitierungen von Siebdruckelektroden nicht möglich war.

Für die Optimierung von Oxidationsprozessen im Kontext elektrochemischer Sensorik ist es wichtig, die Prozesse zu verstehen, die auf einer Elektrodenoberfläche stattfinden. Verschiedene primäre Gallensäuren erwiesen sich nach einem Säure-induzierten Dehydrationsschritt als für eine direkte elektrochemische Oxidation geeignet. Durch CE-MS Messungen konnte die Dehydratisierung und die Addition einer Acetamid Gruppe an Chenodeoxycholsäure aufgedeckt werden, was durch das Migrationsverhalten in der CE und die Identifikation der entsprechenden Summenformeln in der MS bestätigt wurde. So konnte die CE-MS Analyse zur Aufdeckung verschiedener Reaktionsschritte im Kontext der anodischen Oxidation von Gallensäuren beitragen.

Durch ihre Funktion als DNA-Bausteine sind Nukleobasen essenziell für das Leben. Um oxidative DNA-Schäden zu verstehen oder modifizierte Basen elektrochemisch zu detektieren ist es wichtig, die

Mechanismen der Oxidation von Nukleobasen nachzuvollziehen. Online EC-MS, EC-CE-MS, EC-HPLC-MS und Tandem-MS wurden zur Untersuchung der anodischen Oxidation von Cytosin und Thymin in wässriger Lösung auf Kohlenstoff-Siebdruck Elektroden angewandt. Die direkte EC-MS-Kopplung über elektrochemische Fließzellen ermöglichte eine schnelle und direkte Detektion von Oxidationsprodukten und eignete sich somit für einen schnellen Überblick über elektrochemische Aktivität und die Detektion reaktiver Intermediate oder instabiler Spezies. Durch eine Variation der Trennbedingungen in der CE konnte die Anwesenheit bestimmter funktioneller Gruppen über das Migrationsverhalten untersucht werden. Durch kurze Analysezeiten konnten über das Verfolgen der Signalintensitäten bei konsekutiven Messungen Rückschlüsse auf die Stabilität von Produkten gezogen werden. Die Detektion mittels MS ermöglichte die Identifikation von Oxidationsprodukten. EC-HPLC-MS und Tandem-MS Messungen lieferten zusätzliche Informationen durch die Orthogonalität der Trennmethoden und die Fragmentationsmuster, die in Kollisions-induzierter Dissoziation erhalten wurden. Unter den vorliegenden Bedingungen zeigten Cytosin und Thymin verschiedenartige Oxidationsprodukte. Während im Falle des Cytosins monomere Spezies als Hauptoxidationsprodukte detektiert wurden, welche Hydroxy- oder Hydroperoxygruppen aufwiesen, zeigten sich für Thymin dimere Oxidationsprodukte, die durch elektrochemische Oxidation induziert wurden. Die Oxidationsprodukte des Cytosins konnten in der Kapillarelektrophorese unter sauren Bedingungen getrennt werden, wohingegen eine Trennung der Produkte des Thymins nur unter alkalischen Bedingungen erfolgreich war. Somit zeigte sich, dass sich die beiden Substanzen trotz Anwendung ähnlicher Oxidationsbedingungen komplett unterschiedlich verhielten.

Alle oben dargestellten Ergebnisse zeigen, dass die EC-MS Kopplung auf Basis von Einwegelektroden eine leistungsstarke und vielseitige instrumentelle Methode ist, die für verschiedene analytische Herausforderungen eingesetzt werden kann. Durch die Kombination elektrochemischer Oxidation mit Trennsystemen sowie massenspektrometrischer Detektion kann ein hoher Informationsgehalt erzielt werden, wie etwa die Art vorhandener funktioneller Gruppen basierend auf dem Migrationsverhalten in der CE und dem Retentionsverhalten in der HPLC, die Produktstabilität, sowie die Mechanismen elektrochemischer Reaktionen über die Identifikation von Produkten. Der Einsatz einfach anwendbarer und durch die leichte Austauschbarkeit quasi wartungsfreier Elektrodenmaterialien sowie die schnellen Analysezeiten machen diesen Ansatz für Hochdurchsatzanwendungen interessant. So könnte die EC-MS Methodik für den Einsatz in der medizinischen oder pharmazeutischen Industrie zunehmend Aufmerksamkeit erlangen.

8. Appendix

List of abbreviations

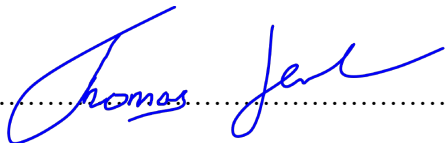
In the following list, the most important abbreviations used in this thesis are given.

AE	Auxiliary electrode
CE	Counter electrode, capillary electrophoresis
CID	Collision-induced dissociation
CV	Cyclic voltammetry
CZE	Capillary zone electrophoresis
DEMS	Differential electrochemistry mass spectrometry
E	Potential
EC-MS	Electrochemistry-mass spectrometry
ESI	Electrospray ionization
GC	Gas chromatography
HPLC	High-performance liquid chromatography
HV	High voltage
ID	Inner diameter
L	Length
LC	Liquid chromatography
LSV	Linear-sweep voltammetry
MS	Mass spectrometry
OD	Outer Diameter
PEEK	Polyether ether ketone
PMMA	Polymethyl methacrylate
PTFE	Polytetrafluoroethylene
RE	Reference electrode
SPCE	Screen-printed carbon electrode
SPE	Screen-printed electrode
WE	Working electrode

Eidesstattliche Erklärung

Ich habe die vorliegende Arbeit selbstständig verfasst, keine anderen als die angegebenen Quellen und Hilfsmittel benutzt und bisher keiner anderen Prüfungsbehörde vorgelegt. Von den in §27 Abs. 5 vorgesehenen Rechtsfolgen habe ich Kenntnis genommen.

Regensburg, den 12. Mai 2020



Thomas Herl